ANL-5916

ARGONNE NATIONAL LABORATORY
P. O. Box 299
Lemont, Illinois

BIOLOGICAL AND MEDICAL RESEARCH DIVISION SEMIANNUAL REPORT

January through June, 1958

September 1958

Preceding Report:
ANL-5841 - July through December, 1957

Operated by The University of Chicago
under
Contract W-31-109-eng-38
with the
United States Atomic Energy Commission

DISCLAIMER

Errata

Argonne National Laboratory Biological and Medical Research Division
Semiannual Report, January through June, 1958, ANL-5916

p. 93 Legend for Fig. 25 should read "Injury remaining 10 days after a first exposure to fission neutrons . . . . . ."

pp. 96 and 102 Figures 28 and 29 are transposed.

TABLE OF CONTENTS

TABLE OF CONTENTS

TABLE OF CONTENTS

TABLE OF CONTENTS

TABLE OF CONTENTS

PROGRESS REPORT: PRELIMINARY STUDIES ON HEMOLYSIN FORMATION IN RABBITS DURING LOW-LEVEL Co^{60} GAMMA IRRADIATION

Laurence R. Draper

The ability of rabbits to produce antibody has been shown to be markedly suppressed and delayed by a single, large dose of whole-body X-radiation given one or two days before the injection of antigen.(1) Taliaferro et al.(2) have reported that the effect of fractionated doses of X-rays over a period of two weeks prior to antigen injection is the same but to a lesser degree than if the same total dose had been given as a single exposure. Using the secondary tetanus antitoxin response in mice, Stoner and Hale(3) have reported that the tenth-day antibody titers are depressed following exposure to as little as 48 rep of Co^{60} γ-radiation given at a rate of 4 rep per hour. With greater doses given at the same rate, the depression was more marked.

In the present work the hemolysin system in γ-irradiated rabbits was used for the study of the qualitative as well as the quantitative characteristics of the response.

Methods

Albino rabbits received approximately 11 r per 16-hr day and were immunized in groups that had received accumulative doses that ranged from 77 r to 1637 r by the time of antigen injection. A group of nonirradiated rabbits served as controls. Exposure to the γ-radiation was continued throughout the immunization course which usually ended five weeks after the injection of antigen, so that, presumably, recovery and/or injury factors would be constant.

The antigen, heated sheep red cell stromata, was administered intravenously in a single dose equivalent to 1.6×10^9 cells/kg rabbit. Serum samples were obtained frequently (2 to 5 samples per week) and were titrated for hemolysin activity using the colorimetric techniques described by Taliaferro and Taliaferro*.(2) The curves yielded measurements of peak titer, the lengths of the induction period and of the rapid rise of antibody in days, the day of peak titer, the rates of rise to peak titer and the apparent half-life of the antibody as measured as a function of the slope of the decline after peak titer.

---

*The author is deeply indebted to Professor W. H. Taliaferro and his laboratory for carrying out these titrations.

Results and Discussion

Certain modifications of the hemolysin response were observed in rabbits which had received substantial doses of γ-radiation. The curves exhibit what appear to be bimodal and sometimes trimodal characteristics. Antibody curves of rabbits that had been exposed to approximately 1000 r or more at the time of immunization indicate some suppression of the early phase of antibody formation (i.e., during the first two weeks of the response) without a suppression of the later titers (three to four weeks after immunization). Thus actual peak titer occurred some 20 days following antigen injection in many cases among the more heavily irradiated rabbits.

In most cases the maximum antibody levels attained by these irradiated rabbits, disregarding the time of occurrence, are not significantly different from those of the controls. These results are not necessarily contradictory to those of Stoner and Hale[3] who, by titrating serums obtained on a given day following antigen injection, observed an apparent depression of peak antibody titer.

This delay of peak titer does not seem to be a result of a general delay of the response, since there is no observable lengthening of the induction period (the length of time between antigen injection and the start of the rise of serum antibody titer). In addition, the first crisis, although lower, is approached at rates as rapid as those observed in nonirradiated controls.

It is suggested that the nature of the hemolysin response in rabbits immunized after 1000 r or more of γ-irradiation (at 11 r/day) is similar to the response that might be expected to follow partial splenectomy. Since the early rapid response is probably the result of the activity of splenic and spleen-like antibody-forming sites, the suppressed early phase of antibody synthesis in the majority of the rabbits that received 1000 r or more appears to be a partial inhibition of splenic activity. The later response (the third-week peak) bears a resemblance to that formed by nonsplenic sites. Whether this later activity is due to the relative radioresistance of nonsplenic sites or to a general recovery of mechanisms of antibody synthesis even with continuing irradiation remains to be investigated.

References

1. Taliaferro, W. H., and L. G. Taliaferro. Further studies on the radiosensitive stages in hemolysin formation. J. Infectious Diseases 95:134-141 (1954).

2. Taliaferro, W. H., and L. G. Taliaferro. The effect of repeated doses of X rays on the hemolysin response in rabbits. J. Infectious Diseases 101:85-99 (1957).

3. Stoner, R. D., and W. M. Hale. The depressant effect of continuous cobalt-60 radiation on the secondary tetanus antitoxin response in mice. Radiation Research 8:375-387 (1958), pp. 438-448.

PROGRESS REPORT: THE USE OF IBM EQUIPMENT TO ANALYZE BIOLOGICAL DATA

Joan M. Gurian

The rectangular approximation to the solute distribution (C/C_0) in a sector-shaped cell yields the following equation(1,2)

$$\frac{C}{C_0} = \frac{e^{\frac{y}{\alpha}}}{\alpha\left(e^{\frac{1}{\alpha}} - 1\right)} + e^{\frac{y}{2\alpha}} \sum_{m=1}^{\infty} \left[C_m(\tau)\right] \left[\sin m\pi y + 2m\pi \cos m\pi y\right]$$

where

$$C_m(\tau) = \frac{16\,\alpha^2 m\pi e^{-\left(\alpha m^2\pi^2 + \frac{1}{4\alpha}\right)\gamma\tau}\left[1 - (-1)^m e^{-\frac{1}{2\alpha}}\right]}{(1 + 4\pi^2 m^2 \alpha^2)^2}$$

and its derivative:

$$\frac{\partial\left(\frac{C}{C_0}\right)}{\partial y} = \frac{e^{\frac{y}{\alpha}}}{\alpha^2\left(e^{\frac{1}{\alpha}} - 1\right)} + e^{\frac{y}{2\alpha}} \sum_{m=1}^{\infty} \frac{C_m \tau}{2\alpha} \left[(1 - 4\pi^2 m^2 \alpha^2) \sin m\pi y + 4\pi m\alpha \cos m\pi y\right]$$

A program for the IBM Type 650 computer has been devised to evaluate C/C_0 and its derivative for any given value of α, τ, and y. The problem was broken up into several sections:

1. Calculation of quantities dependent only on α: $f(\alpha)$.
2. Calculation of quantities dependent on α and τ: $g(\alpha,\tau)$.
3. Calculation of quantities dependent on α, τ and y: $h(\alpha,\tau,y)$.

The largest necessary value of m was determined by the convergence of the summation to a preset ϵ. By judicious packaging of combination of α, τ and y, frequent repetition of evaluation of the same quantity for the same constants could thus be avoided. A condensed scheme of the program is shown in Figure 1.

The program was written using the IBM Symbolic Optimal Assembly Program (SOAP) and the SOAP Interpretative Routine (SIR).

The problem was suggested by D. Yphantis.

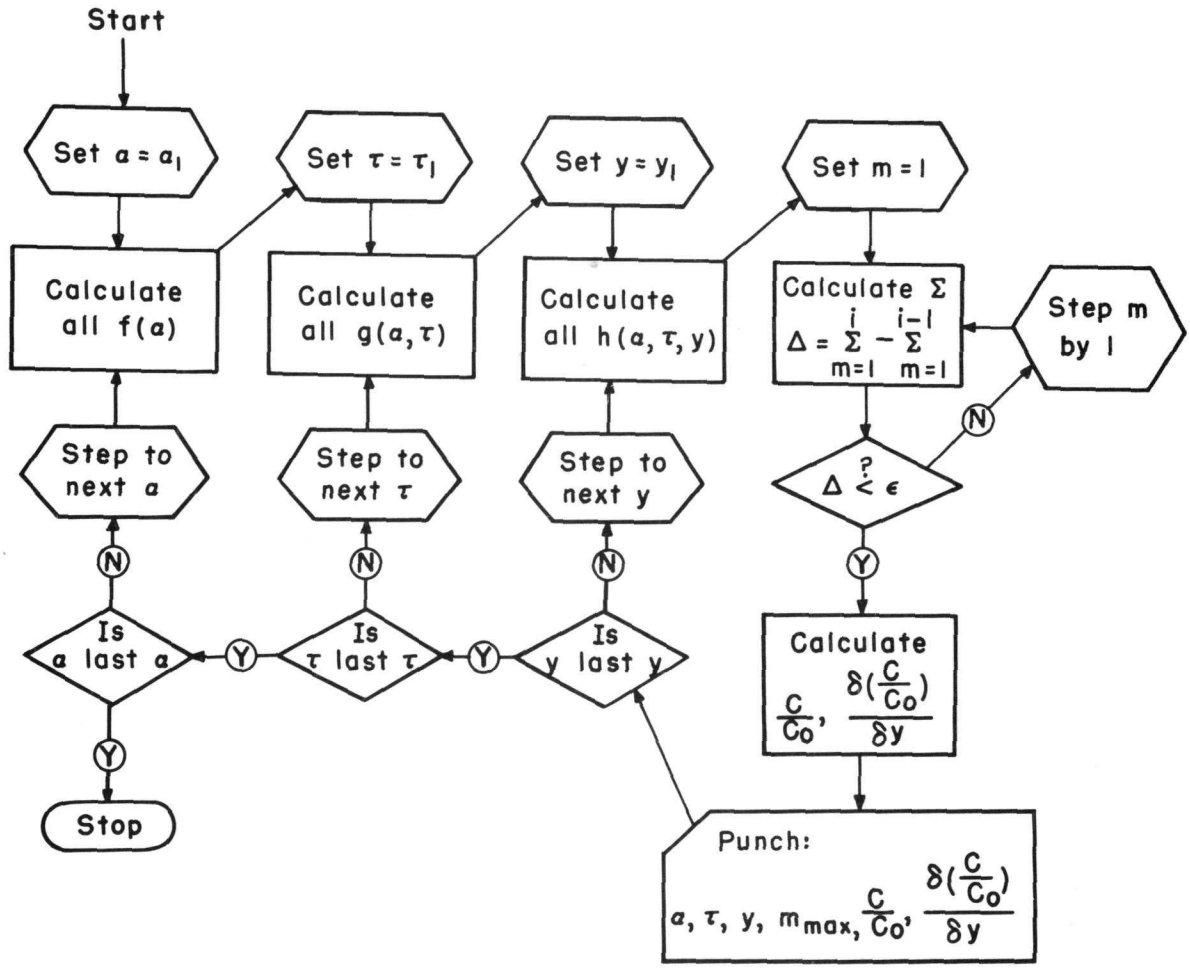

Figure 1. Flow Chart.

References

1. Mason, M. and W. Weaver. The settling of small particles in a fluid. Phys. Rev. 23:412-426 (1924).

2. Yphantis, D. A. and D. F. Waugh. Ultracentrifugal characterization by direct measurement of activity. I. Theoretical. J. Phys. Chem. 60:623-629 (1956).

CYTOLOGICAL STUDY OF TARTARY BUCKWHEAT (FAGOPYRUM TATARICUM (L.) GAERTN.) GROWN IN C^{14} CARBON DIOXIDE

Miguel Mota*

A few plants of Fagopyrum tataricum (L.) Gaertn. that had been cultivated in a sealed chamber containing C^{14}-labeled CO_2 were studied in order to find cytological abnormalities induced by β-radiation absorbed internally. One plant grown in a similar chamber but exposed only to normal C^{12} CO_2 was also studied as a control. The plants were studied at the age of 41 days.

A few normal mitoses were found in young leaves and somatic tissues of the anthers of the control plant. No divisions were found in about 30 preparations made of similar tissues of treated plants. No meiosis could be found in any of the buds, fixed in Carnoy fluid, of all plants studied.

It seemed that flower buds of treated plants were physiologically more advanced than those of the control plant, possibly a consequence of the "aging effect" of radiation.

Pollen grains were found in both treated and control plants, generally healthy looking, although somewhat irregular in size. As the first slides made gave the impression that there was some difference between size of treated and untreated pollen grains, it was decided to measure the larger diameter in a sufficient number of pollen grains in treated and control material. This proved to be fruitful, as the statistical distribution of that diameter is different in the two samples.

Five hundred and thirty six pollen grains from control plants and 312 pollen grains from treated plants were measured. The measurements were made on photographs obtained by projecting the image from the microscope directly on bromide paper. The larger diameter was measured and the results are described in Figure 2. There is a clear shift of the curve of frequencies of treated plants to the right, which means a higher proportion of pollen grains of larger diameter. The shape of the two curves is also different.

As meiosis could not be studied there is no information as to the causes of these differences. It is assumed, however, that larger grains are the result of higher than normal chromosome numbers. This may be a consequence of heteroploidy caused by radiation. If polyploidy (or other forms of heteroploidy) was induced early enough this would easily

*Resident Research Associate from Estação Agonómica Nacional, Sacavem, Portugal.

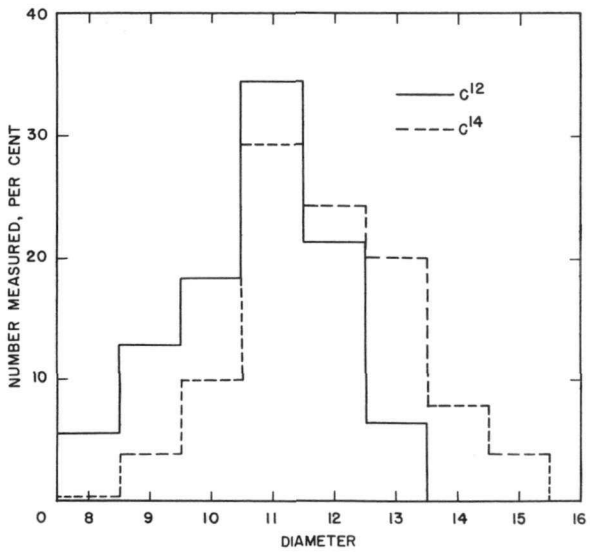

Figure 2. Frequency distribution of diameter of pollen grains of Fagopyrum tataricum (L.) Gaertn.

account for the reduced number of pollen grains of small diameter. Cells with chromosomes numbers lower than normal were probably nonviable and did not reach meiosis.

It seems also that treated plants formed far fewer pollen grains than the control plant, although no figures were recorded. It is, however, also an expected consequence of radiation.

In further experiments it seems advisable to attempt to study mitosis and meiosis in younger plants. Fagopyrum, however, is not a favorable plant for such a study because its chromosomes are small and do not stain very easily. Plants with larger chromosomes would probably be more suitable for the study of cytological abnormalities induced in the conditions of the experiment.

ELECTRON MICROSCOPIC OBSERVATIONS ON NUCLEI IN THE OVOTESTIS OF A PULMONATE SNAIL

L. E. Roth

The numerous problems in spermatogenesis and yolk formation have been studied intensively by light microscopists, but it is only recently that the electron microscope has been utilized in an effort to understand the profound nuclear and cytoplasmic changes which take place. Pulmonate snails offer choice material for such an electron microscope study. Ovotestes were dissected from the snail Otala vermiculata, fixed in buffered osmium tetroxide with saline, embedded, and thin-sectioned for observation in the RCA EMU 3A electron microscope.

Nuclei of spermatocytes in meiotic prophase and metaphase have chromosomal cores composed of one small fibril (13 mμ in diameter) equidistant from two larger fibrils (30 mμ in diameter) (C in Figure 3A); these fibrils thus form a ribbon-like structure about 175 mμ wide which is surrounded by chromatin masses containing smaller filaments with a tubular cross section 3 to 5 mμ in diameter. In some prophase stages, the cores are attached to darkened areas of the nuclear membrane. In the late spermatid when the chromatin has a more regular arrangement, 3- to 5-mμ filaments or sheets with a less dense material surrounding them are observable.

The nurse cell nucleus (N in Figure 3B) typically has large chromatin masses many of which contact the infolded nuclear membrane; the nucleoplasm is composed of fine, filamentous material with occasional clumps of material of higher electron density than the chromosomes. A large yolk nucleus (Figure 3C) is present at the time of appearance of early yolk granules (Y in Figures 3C and D). Five structural components are present in the yolk nucleus and show modifications correlated with the progress of yolk granule formation: large vesicles up to 1.5 μ in diameter (V in Figures 3C and D), dense homogeneous granules up to 0.3 μ in diameter (G in Figures 3C and D), a homogeneous fibrillar component about 16 mμ in diameter, a finer fibrillar component forming a rather coarse network (A in Figure 3C) at certain stages, and a filament which measures 30 mμ in diameter and which has a tubular cross section and a ladder-like appearance in longitudinal sections (T in Figure 3D). The sequence of events in yolk granules in the cytoplasm proceeds from spherical vesicles (Y in Figures 3C and D) to a more densely packed vesicle to a very dense vesicle to, finally, the breakdown into small units localized in regions of developing germ cells or young yolk cells (S in Figure 3B) which have absorbed the mature yolk granules.

Further observations will be directed toward correlating yolk granule changes with yolk synthesis, studying the cytochemistry of the yolk nucleus and granules, and extending these observations to other pulmonate snail species.

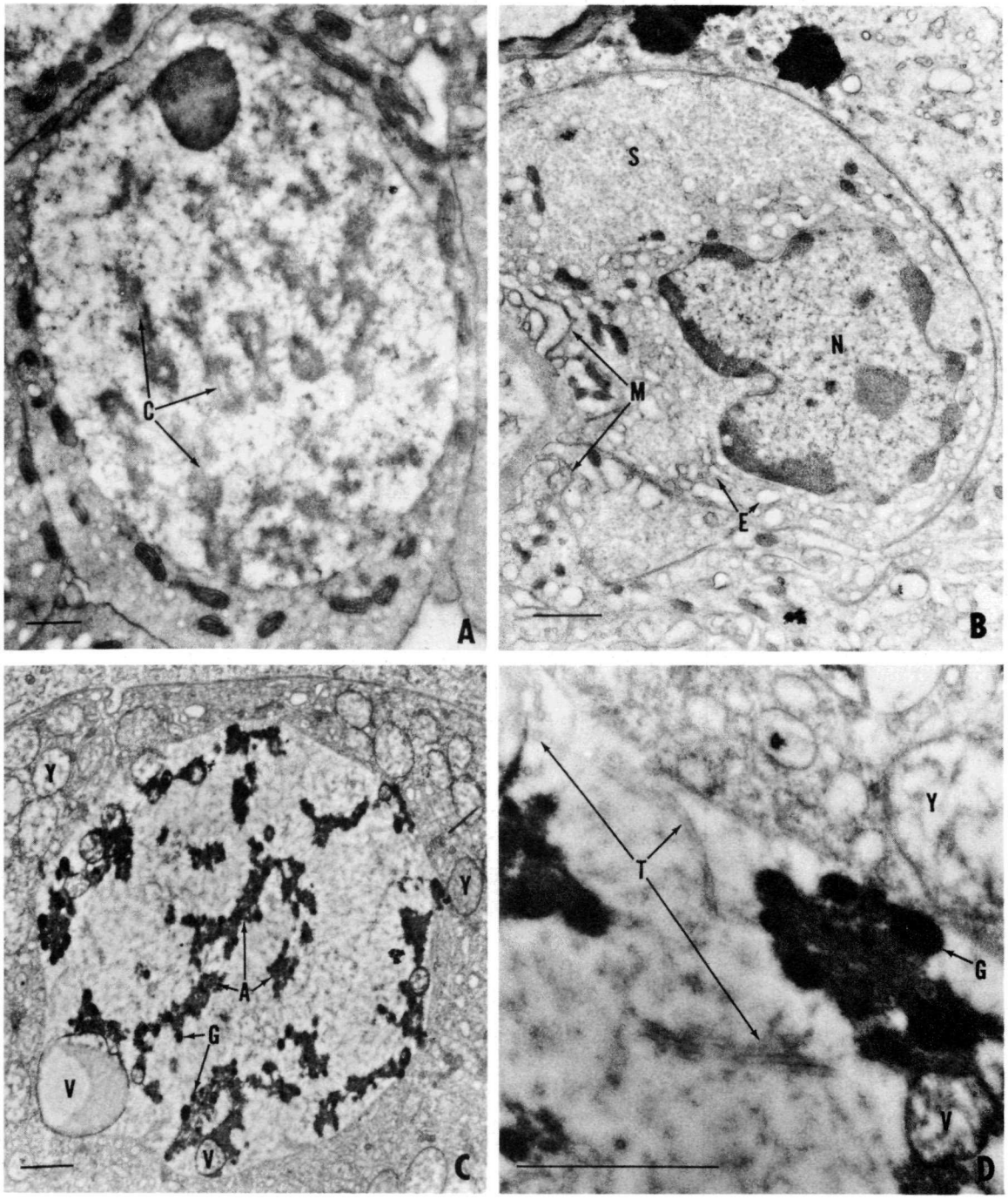

Scale markers on figures represent 1 μ.

Figure 3A. Spermatocyte in meiotic prophase.
B. Early yolk cell.
C. Yolk cell showing yolk nucleus and young yolk granules.
D. Higher magnification of yolk nucleus and young yolk granules.

ELECTRON MICROSCOPE OBSERVATIONS OF AMICRONUCLEATE TETRAHYMENA PYRIFORMIS

L. E. Roth and O. T. Minick

The unique position in ciliate nuclear phenomena occupied by the amicronucleate strains of Tetrahymena has not been investigated cytologically; despite this, a voluminous literature has accumulated on studies utulizing these organisms for a variety of investigations. The following report is a beginning toward improving our knowledge and describes macronuclear as well as cytoplasmic changes which may be related to stages in the division cycle.

Organisms of strain W from axenic cultures in active growth were fixed in buffered 1% osmium tetroxide, embedded in methacrylate, and sectioned at 1/40 μ for observation in the electron microscope.

In some of the organisms, the macronucleus is composed of numerous dense bodies 0.3 to 0.5 μ in diameter which are probably nucleoli (N in Figure 4A) and smaller bodies of lower electron density (C in Figure 4A) embedded in a nucleoplasm of finely granular and filamentous material; a double-layered membrane is present. In the cytoplasm of these organisms, the mitochondria are usually densely packed with tubules (M in Figure 4A); little endoplasmic reticulum is observed.

However, in many other organisms, the lower-density nuclear material is aggregated into an irregular network (C in Figure 4B) surrounded by a clear nucleoplasm; the nuclear membrane remains continuous though it may be separated from the network by a wide space. Numerous small dense granules about 50 mμ in diameter are interspersed in the network (G in Figure 4B). The nucleolus-like bodies remain (N in Figure 4B) but frequently are observed grouped in localized regions of the macronucleus. In these organisms the mitochondria (M in Figure 4B) are characterized by clear spaces separating the tubules and by dense irregular central masses (MM in Figure 4B); mitochondrion-like bodies are also seen which lack the typical tubules (ML in Figure 4B). In addition, endoplasmic reticulum with attached granules is observed (E in Figure 4B) in larger amounts.

Further studies will correlate these observations with the events of mitosis and relate them to similar ones in micronucleate strains.

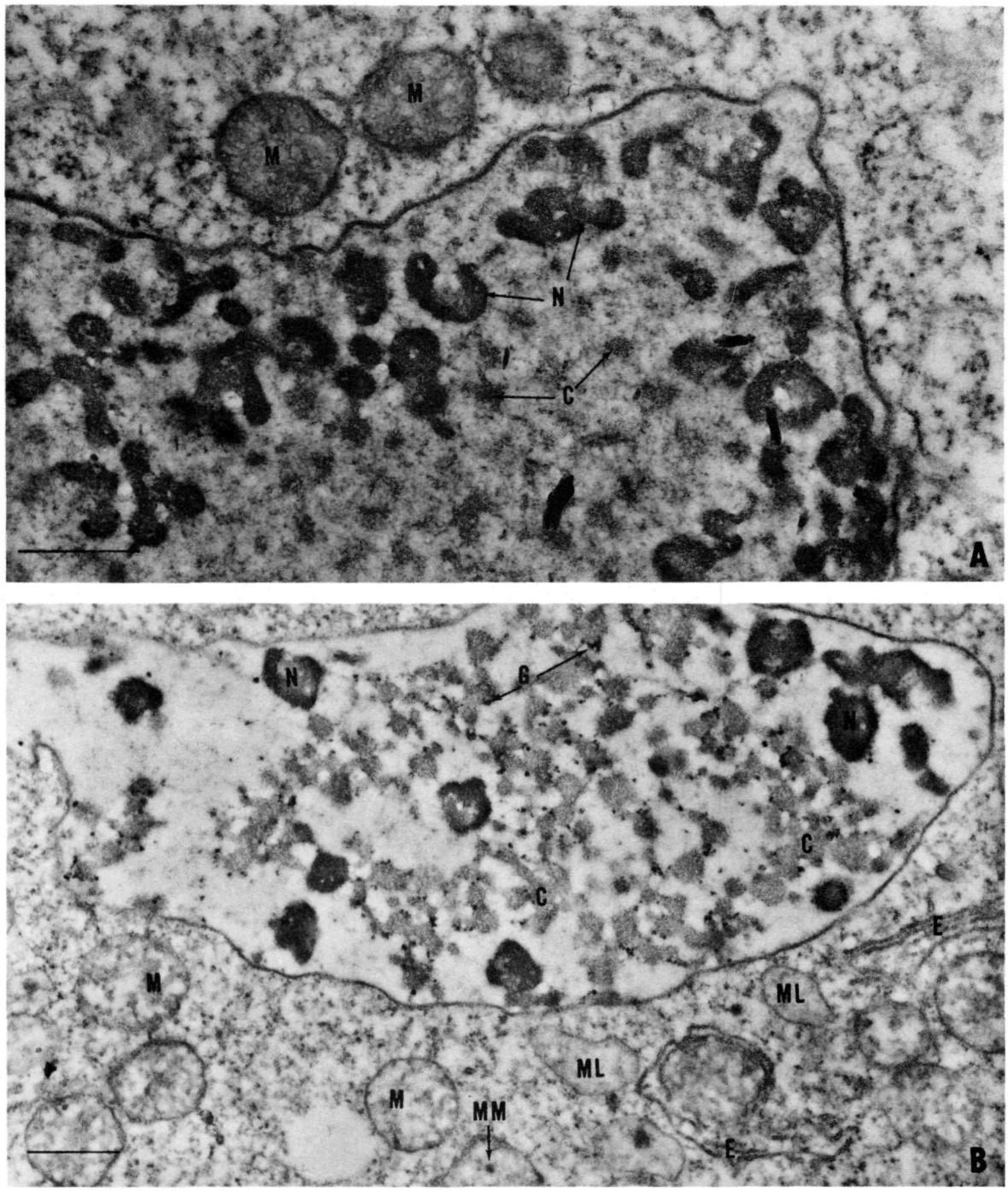

Scale markers on the figures represent 1 μ.

Figure 4. A. Section of a portion of the macronucleus of Tetrahymena pyriformis strain W including a small amount of cytoplasm.
B. Section of another organism from the same preparation, illustrating alterations in macronuclear morphology and cytoplasmic components.

COMPARATIVE CARCINOGENICITY OF Ra^{226}, Sr^{90}, AND Ca^{45} IN MICE

Miriam P. Finkel and Birute O. Biskis

The carcinogenic potency of a radioisotope is dependent upon its physical and biochemical characteristics. For example, α-rays are more effective than β-rays, and materials with a long biological half-time are more effective than those that decay rapidly or are quickly excreted.(1) Many of the factors responsible for the actual dose that elicits the neoplastic response cannot be investigated independently because isotopes with the necessary characteristics do not exist. However, certain comparative studies are possible with those that are available. Ra^{226}, Sr^{90}, and Ca^{45} were selected for study because they are similar chemically while some of their physical properties differ substantially. Their excretion rates are much the same, and that part that is retained by the body is fixed primarily in bone crystal. However, radium is an α-emitter, and the other two nuclides are β-emitters. Ca^{45} has a relatively weak β-ray and a relatively short half-life (Table 1). Sr^{90} has a much longer half-life, and its Y^{90} daughter decays in a very short time with the emission of a strong β-ray.

TABLE 1

Physical characteristics

Isotope	Energy and type of emission	Half-life	Subsequent radiation
Ra^{226}	4.18 mev α	1620 years	5.49 mev α from radon (3.8-day half-life) followed by 2 more α-emitters in several minutes.
Sr^{90}	0.54 mev β	28 years	2.18 mev β from Y^{90} (64 hr half-life)
Ca^{45}	0.25 mev β	155 days	None

Procedure

CF No. 1 female mice received a single, intravenous injection of an isotonic solution of $Ra^{226}Cl_2$, $Sr^{90}Cl_2$, or $Ca^{45}Cl_2$ when they were approximately 70 days old. The Sr^{90} was in equilibrium with Y^{90}. The experimental design is given in Table 2. The animals were permitted to live until moribund, when they were killed with sodium pentobarbital and examined

for gross and microscopic evidence of disease. Specimens of spine and long bones, as well as any abnormal areas detected on roentgenographic examination of the skeleton, were taken for histologic study. The data presented here include only osteogenic sarcomas.

TABLE 2

Dosage and number of animals

Ra^{266}		Sr^{90}		Ca^{45}		Total number of animals
Dose, c/kg	Number of animals	Dose, c/kg	Number of animals	Dose, c/kg	Number of animals	
4170	13	9330	15	49,600	10	
2080	15	7000	30	25,000	15	
1040	30	4500	45	12,100	10	
762	30	2200	30	11,200	26	
521	30	880	45	5,600	42	
288	45	440	45	1,100	45	
100	45	200	60	560	60	
50	45	88	75	110	75	
28.8	60	44	90	55	75	
12	75	8.9	105	16	90	
6	90	4.5	120			
3	90	1.3	150			
1.2	105					
0.6	120					
Total	793		810		448	2051
		Radium controls				210
		Strontium and calcium controls				150
				Total		2411

Tumor Production

Malignant bone tumors began to appear about 6 months after injection, and in a few dosage groups all of the animals had died with such neoplasms by 10 months. Many mice had more than one tumor. Since it has been determined that tumors produced by radiostrontium are distributed at random among the animals exposed to similar risk,[2,3] the tumor rather than the tumor-bearing mouse has been used as the statistical unit.

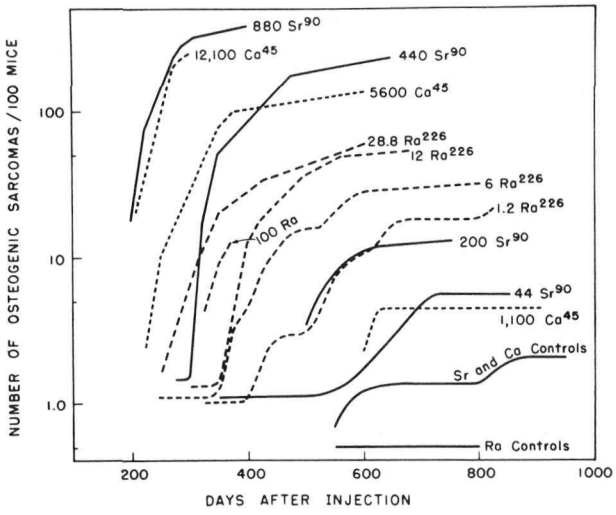

Figure 5. Cumulative incidence of osteogenic sarcomas at representative isotope doses (μc/kg) as a function of time after injection.

Figure 5 presents the cumulative tumor incidence of representative dosage groups as the logarithm of the number of osteogenic sarcomas per 100 mice. A few curves of the high and intermediate dose levels, as well as most of those within the control range, have been omitted for the sake of clarity. Noteworthy features are that Sr^{90} and Ca^{45} produced many more tumors than radium, that much more calcium than strontium was required for comparable results, and that in the range where radium was effective, its carcinogenic potency per μc greatly exceeded that of strontium.

The relationship between carcinogenicity and isotope dose can be presented by plotting the likelihood that an animal at each dose will die with an osteogenic sarcoma against the days it has already lived after injection. Tumor expectancy is calculated by dividing the number of tumors still to appear in a dose group by the number of animals still alive. This was done at 25-day intervals from 150 days after injection until less than three animals remained alive. The results of most of these calculations are presented in Figure 6; some data were omitted to prevent crowding of the curves. It is interesting that two of the curves, 5600 μc/kg Ca^{45} and 200 μc/kg Sr^{90}, did not show an increase in tumor expectancy with increasing time whereas the others do suggest such a progression. This is particularly true of all of the radium levels. Since, the total integrated dose to the animals that received radium or strontium was constantly increasing during this period because of the long half-lives and low excretion rates of these materials, it would be anticipated that tumor expectancy would increase with increasing time. However, this trend is counterbalanced by the fact that at each successive interval the surviving population had 25 fewer days to live, and, consequently, 25 fewer days in which to develop an osteogenic sarcoma.

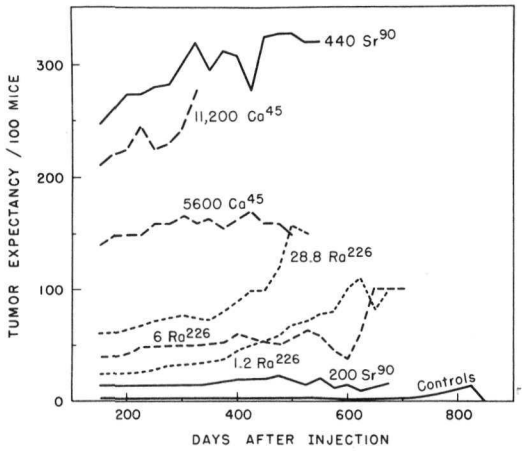

Figure 6. Tumor expectancy as a function of survival time after injection.

In order to compare the carcinogenicity of one isotope with that of another it is necessary to express each isotope-dose by a single value so that the individual materials can be represented by one curve rather than by a family of curves. This can be done by averaging the tumor expectancies at 25-day intervals that were presented in Figure 6. Such averages for all the dose levels have been plotted against the logarithm of the dose in Figure 7. The control value is indicated by the shaded area; average tumor expectancy was 3/100 among the strontium and calcium control population and 0.6/100 among the radium control population. From the point of view of the amount of material required to produce tumors, radium was much more efficient than Sr^{90} or Ca^{45}. Maximum tumor expectancy was reached with 28.8 μc/kg Ra^{226}, 880 μc/kg Sr^{90}, and 24,800 μc/kg Ca^{45}. These give ratios of 1:30:860. However, strontium and calcium produced five and three times as many tumors, respectively, at these levels as radium. With each material the optimum carcinogenic dose was exceeded, and many animals that lived long enough to develop tumors nevertheless did not do so.

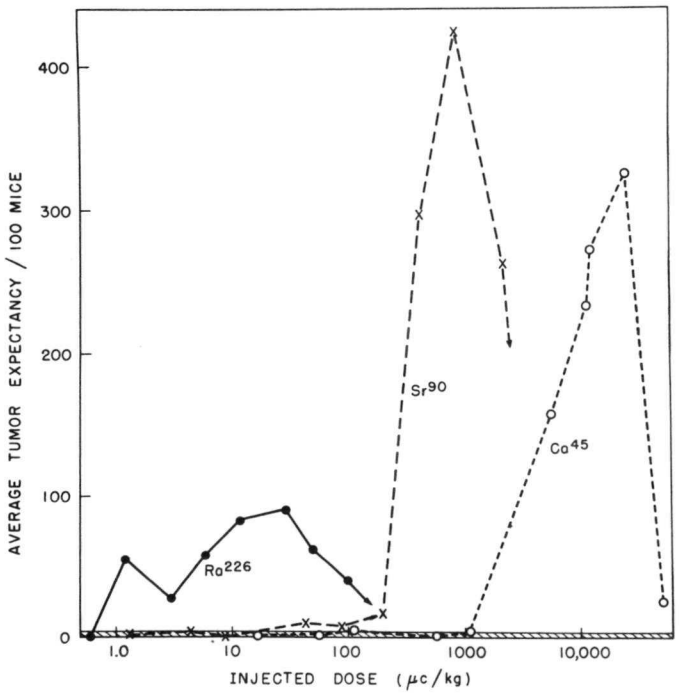

Figure 7. Average tumor expectancy from 150 days after injection as a function of dose.

Another measure of tumor production is tumor rate. This is calculated by dividing the number of tumors appearing among animals dying during a specific interval by the number of animals alive at the beginning of the interval. In general, the rate for any isotope dose increases with time, and the rate of increase is directly proportional to the dose. A single statistic for each tumor rate curve is the slope of the curve. These values can be plotted for each dose of an isotope, and the resulting dose-response curve can then be compared with similar curves for other isotopes. Tumor rates per 100 mice at 50-day intervals were so calculated, and the slopes of their least squares lines were determined. The logarithm of these slopes are plotted against the logarithm of the dose in Figure 8. The value for the combined control populations was 0.003. This means that there was a mean increase of 0.003 tumors per 50 days per 100 control mice. The radium data show a reasonably smooth trend from 1.2 through 100 μc/kg; 0.6 μc/kg, which did not result in a statistically significant

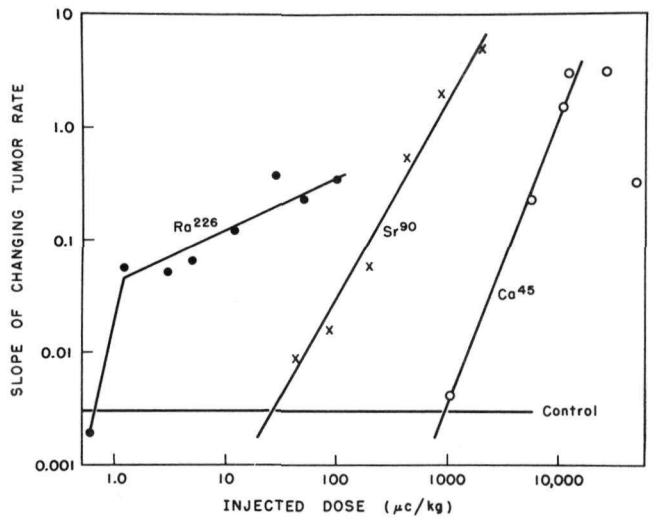

Figure 8. Slope of tumor rate increase with time as a function of dose.

increase in osteogenic sarcomas, deviated sharply from this trend. The Sr^{90} data show no marked departures from a straight line. The next lower dosage group, which received 8.9 μc/kg, had no malignant bone tumors. Except for the two highest dose levels, the Ca^{45} values also fall along a straight line. The slope at the next lower point on the calcium curve, 560 μc/kg, was -0.003. The slopes of the strontium and calcium lines in Figure 8 are quite similar. There is a factor of 10 between the dosages that increased tumor rate by 3 per 50 days per 100 mice and a factor of 35 at dosages that increased the rate by 0.003 per 50 days per 100 mice. The slope of the radium line is very much lower, so that the difference in carcinogenicity between radium and the beta emitters becomes greater as the dose, and, consequently, the effect, decreases. As a result, estimations of the human hazard from internal emitters based upon radium toxicity as the common denominator between animal and man will vary according to the magnitude of the response under consideration.

Latent Period

The length of time between injection of a mouse with a radioisotope and its death with an osteogenic sarcoma can be very long in relation to the normal life span of this species. In our experience it has never been shorter than 150 days. This minimum latent period is 25% of the average post-injection life expectancy of the strontium and calcium control population and 15% of the life span of the longest survivor. The present data were examined for evidence of a relationship between latent period and isotope. The time of death of each tumor-bearing mouse is indicated in Figure 9. The first radium tumor death occurred 230 days after injection. The first strontium and calcium tumor deaths were at 160 and 190 days after injection, respectively. The mode of the frequency distribution was 390 days for radium, 200-260 days for strontium, and 260 days for calcium. The median was 420 days for radium, 320 days for strontium, and 290 days for calcium. The frequency distribution pattern of the radium tumors suggests that either they result primarily from the constant irradiation by the retained material or they appear only after recovery from the initial insult. The shape of the frequency distribution for calcium tumors indicates that these tumors result primarily from the initial dose that immediately follows

injection. This interpretation is consistent with the relatively short physical half-life of Ca^{45}. The Sr^{90} data suggest that both the initial high dose and the retained dose are important in the production of osteogenic sarcomas. Many tumor-bearing mice died within 100 days after the end of the latent period, but the frequency was not insignificant even beyond 600 days after injection.

Figure 9 indicates by symbols the dose level group to which each animal belonged so that relationships between latent period and dose are apparent. In general, the animals at the higher levels died with tumors earlier than those at lower levels, but there are many exceptions to this trend of increasing latent period with decreasing dose. It has been shown in Figure 8 that the slopes of the tumor rate curves increase with increasing dose.

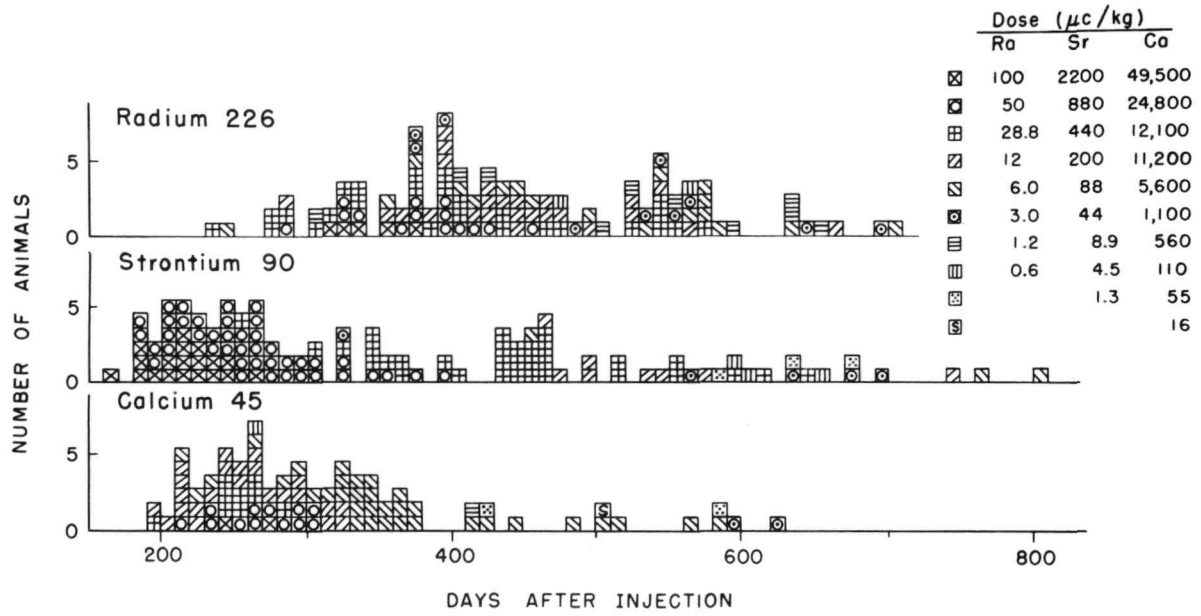

Figure 9. Frequency distribution of animals dying with osteogenic sarcomas at 10-day intervals after injection.

Consequently, the probability of dying with a tumor at any particular day increases with increasing dose. This explanation for the observation that tumors in general appear earlier among animals receiving higher doses does not suffer from the necessity of overlooking the occasional early tumors among animals in intermediate and low dosage groups. Therefore, it would seem that the latent period is independent of the dose and that the apparent dependence is due to the fact that the daily tumor expectancy increases with increasing dose.

References

1. Finkel, M. P. Induction of tumors with internally administered isotopes. In Radiation Biology and Cancer, University of Texas (1958). In press.

2. Finkel, M. P., H. Lisco, and A. M. Brues. Toxicity of Sr^{89} in mice. Malignant bone tumors. Quarterly Report of Biological and Medical Research Division, Argonne National Laboratory. ANL-5378, pp. 106-117 (1955).

3. Finkel, M. P., B. O. Biskis, and G. M. Scribner. Toxicity of Sr^{90} and of Ca^{45} in mice. III. Effect of Sr^{90} upon life span and neoplasms of bone and the blood-forming tissues. Semiannual Report of Biological and Medical Research Division, Argonne National Laboratory. ANL-5841, pp. 51-59 (1958).

THE DEATH OF BACTERIA IN GROWING CULTURE

Arthur L. Koch*

In an actively growing culture of Escherichia coli, the breakdown of proteins within growing cells cannot be detected.[1,2,3] The limit of detection of the most sensitive technique[1] is such as to suggest that "turnover" per se is not occurring. There are a number of other processes that may or may not occur in a population of growing cells which might with justification be called "turnover." One such process is that in which the cells incorporate a constituent of the growth medium into some material which is then liberated into the environment and may or may not be subsequently reutilized. An example of this process has been shown to occur in the incorporation of glycine or serine into an extracellular peptide-like material.[4] Furthermore, the released material was shown to be produced as an offshoot of synthetic activities and not as a result of the degradation of cellular macromolecules.

Another process, which we will refer to here as "cellular turnover," is that in which a proportion of the cells in the population die and subsequently liberate some of their contents into the medium. Some components may then be reutilized by other cells in the population that are growing and metabolizing.

The first portion of this paper is devoted to a description of the sequelae of cell death as measured by various tracer compounds. It was subsequently found that the death in these studies was not natural, but caused by centrifugation and by chilling the culture. However, from a knowledge of consequence of death, it was possible to design a tracer experiment which shows that under conditions of constant temperature and in the absence of centrifugation, cell death in growing populations occurs very rarely.

Experimental Procedure

The experimental techniques were those previously reported.[1,4] The bulk of the experiments were carried out in the following manner. A sub-inoculum from a suitable medium was introduced into a medium containing the tracer and allowed to grow with aeration. The choice of the growth medium was determined by the nature of the tracer and the cellular component it was desired to label (see Table 3). The cells were harvested, washed three times by centrifugation in the cold, resuspended in the unlabeled medium, and aerated for one hour. Then the cells were harvested

*Present address: Department of Biochemistry, College of Medicine, University of Florida, Gainesville, Florida.

by centrifugation, resuspended in unlabeled medium, and aerated for a second hour. This process was repeated, a third and occasionally a fourth time. During the growth period, aliquots of bacteria were taken and the radioactivity of the aliquot was determined in a gas flow proportional counter. The supernatant collected at the end of the hour aeration periods was passed through a "millipore" filter to remove any intact bacterial cells not eliminated by centrifugation. An aliquot of this ultrafiltrate was also assayed for radioactivity. From the time period, the activity of aliquots of bacteria, and the supernatant at the end of the period, the net rate of release is calculated in per cent per hour. Sometimes in the first regrowth period, the rate of release was higher than the values obtained in subsequent periods by not more than a factor of two. Since this could result from inadequacies in the washing procedures, or the "turnover" or loss to the cells of components of small molecular weight, these first-hour values were discarded. The reported values in Table 3 are averages of the succeeding periods. Although the centrifugations and resuspension in fresh medium took about 10 minutes, most of this time the temperature of the cells was 5° C; consequently, this period of time was omitted in carrying out the above calculation.

TABLE 3

The release of isotope from cells labeled and maintained at 37° C, but washed by centrifuge in the cold

Radioactive tracer used to label cells	Major high-molecular-weight cellular component labeled	Growth medium		Rate of release of isotope, %/hr
		Labeling medium	Regrowth medium	
Glycine-2-C^{14}	Protein*	M-9 + Purines	M-9	5.0
DL-Lysine-2-C^{14}	Protein	M-9	M-9	5.0
Mixed, uniformly labeled amino acid-C^{14}**	Protein	M-9	M-9	5.2
				3.7
			M-9 + 0.08% nutrient broth	3.6
				3.7
				3.8
Adenine-8-C^{14}	Nucleic acids	M-9	M-9	0.2
		M-9	M-9 + Bacterial extract†	4.9
Phosphate-P^{32}	Nucleic acids	"g"‡	M-9 + 0.08% nutrient broth	3
				7
				3.6

*Adenine + guanine were present in the labeling medium and thus prevented entry of glycine into the nucleic acid purine.

**The mixture of uniformly labeled amino acids was prepared from uniformly labeled soybean leaves obtained through the kindness of Dr. N. J. Scully. The hydrolyzed protein fraction was absorbed on a column of Dowex-50; it was then eluted with NH_4OH in order to eliminate contaminating carbohydrate materials.

† See text.

‡ "g" medium is a low phosphate medium[5] which is used to obtain efficient incorporation of the P^{32}.

Results and Discussion

The Rate of Release of Various Tracers from the Growing Culture: Centrifuged in the Cold Periodically

The rate at which the radioactive tracer appears in the growth medium is a "net" release and must be equal to the difference between the rate at which it is actually liberated by cells, and the rate at which it is taken back up by the bacterial cells. The rate of reutilization would be expected to depend on the nature of the medium and various physiological factors, as well as the chemical nature of the material that had been secreted into the growth medium. In the case of adenine, reutilization of tracer could be greatly decreased by modifying the medium to include unlabeled nucleic acid fragments (see below).

In Table 3 the rate of release of radioactivity from cells labeled with a variety of isotopic compounds is given. It is seen that except for the adenine-labeled cells grown in a medium not containing a nonlabeled purine source, the rate of release is in the range 3 to 7% per hour. This is evidence for the conclusion that, with the exception noted, the rate of reutilization is much smaller than the rate of release of the isotope-labeled materials, and that at the same time a variety of different chemical substances are released to the medium all in substantially the same proportion. This suggests that under the conditions of these experiments, a certain fraction of the cells are liberating the bulk of their cellular constituents into the medium, and the remainder are producing a very much smaller amount, if they produce any at all. This circumstance would occur if cells were dying and subsequently lysing and liberating material into the medium.

Of the cellular components that would be produced by lysis of the cell, the cell wall is the only one that might be expected to be retained by the ultrafilter. This represents only a small fraction of the cellular material and may be fragmented to a size that passes through the filter. The rate of release of isotope should be substantially equal to the rate of lysis of the bacterial cells.

If a period of time intervenes between the death of a cell and its lysis, the rate of lysis may or may not be equal to the death rate of bacteria. It can be shown, however, that equality of these two rates obtains, after the culture has been maintained in a condition of growth in which the death rate has been maintained constant for a period of time which is longer than the period of time required for lysis. The observed rate of lysis is made up of contributions ensuing from the death of cells in previous time intervals which are only now lysing, and under the conditions mentioned equals the sum of the contributions resulting from cell death in a previous interval. For example, if half of the cells lyse the second hour after death and

the other half the third hour, then in the fourth hour of an experiment of the kind described here, the observed percentage release of isotope results from equal contributions from the second and third hour period of the experiment. Each contribution amounts to half of the death rate and the sum is numerically equal to the death rate per hour, which is assumed constant during the entire experiment.

The equality of death rate and lysis rate can be shown to hold no matter what time course the lysis reaction exhibits as long as lysis is complete in less time than the duration of the experiment. It also holds for the case in which some anabolic processes occur subsequent to the death of the cell, if these processes do not lead to a cell division in which one daughter cell continues to grow and does not lyse.

Glycine-2-C^{14}. In the present experiments the equality of the rate of death of cells and observed lysis must be equal because of the constancy of the observed release of isotope in the experiment of Table 4. It can be concluded that the interval between death and disintegration probably must be less than an hour.

TABLE 4

Constancy of the release of isotope from labeled cells. Experimental conditions were as described in the first line of Table 3 for glycine-2-C^{14}

Time interval, hr	Release per hr, %
0-1	4.9
1-2.08	4.85
2.08-3.3	4.6
3.3-4.4	5.6

Two other conclusions may be drawn from this experiment. First, the rate of release of isotope does not diminish with time or as the amount of isotope present in the bacteria decreases. At the end of the experiment 79% of the isotope remained. If half of the activity had been incorporated into a form which was not released into the medium, the apparent rate should then have halved by the end of the fourth experimental period. It therefore follows that the bulk of the protein in the bacteria is susceptible to release from the cell.

The second conclusion follows from the fact that during this experiment the bacterial protoplasmic mass increased by 1600%; four divisions occurred. Therefore, the release of isotope can not be associated with cell division, for if it were, the release in the final period should be one-fourth to one-sixteenth the initial rate, depending on the type of mechanism envisioned.

Adenine-8-C^{14}. As mentioned above, in synthetic medium adenine-labeled cells release isotope to a very small extent. This observation is in confirmation of that which had been made previously[6] using the same experimental procedure. As this result was not in line with the other experiments, the possibility existed that material was released and secondarily reincorporated into growing cells of the populations. To minimize this reutilization, a nonradioactive extract of bacteria was added to the growth medium. The extract was prepared by grinding alumina in the same way as used for the preparation of enzymatically active extracts.[7] In the experiment shown in Table 3 the regrowth medium was made 10% in bacterial extract. The extract contains a great deal of nucleic acid materials, and these effectively dilute out the radioactive materials as they are released so that reincorporation is greatly reduced.

Recently,[8] it has been shown that chloramphenicol-inhibited cells produce RNA, which is broken down when the drug is removed from the medium. The fragments so produced are excreted into the medium, but subsequently are reutilized to a high degree by the new bacterial growth. Thus, this case is similar to the reutilization of the purine-labeled nucleic acid fragments produced by the death of cells resulting from cold shock.

Uniformly C^{14}-labeled amino acid mixture. The values obtained in Table 3 indicate that the bulk of the cellular amino acids are treated similarly in regard to the process under study. In addition to the experiments shown in Table 3, experiments were conducted with 10 times increased levels of amino acids in the labeling medium. Although a much higher radioactivity was obtained per bacterial cell, the observed rate of release of isotope to the medium was somewhat lower: 1.9 and 2.2% per hour in two different experiments. At first it was thought that this might result from a diversion of the amino acid C^{14} when present at high level to nonprotein constituents of the cell which might be "turning over," and then be reutilized. This possibility was rendered much less likely by the discovery that very little radioactivity is released (less than 0.10%) in the form of $C^{14}O_2$, which would be the main degradation product of most conceivable turnover processes.

The low values observed after labeling at high levels of amino acid are probably attributable to the fact that the cells grown in this medium were thrown into lag upon being returned to the synthetic M-9 medium containing no supplement. As indicated below, nongrowing conditions seem to decrease the rate of release of isotope from killed cells.

Podolsky[9] has studied the decrease in activity of bacterial cells tagged with uniformly labeled arginine, during growth and during the stationary phase in various media. His method is relatively insensitive and mainly concerns phenomena in the stationary phase, but also concerns the process under study here, since he did wash his cells by centrifugation in the cold.

Contrary to our findings, he observed slightly larger release in cells labeled in complex media, but in agreement with our expectation he observed a several-fold decrease in the release associated with partial anaerobiosis.

During the active growth phase, his observed releases were less than those indicated from our experiments. This is probably due to extensive reutilization enhanced in his experiments by the failure to remove the media from the cells periodically. Support is lent to this supposition because, in this case the observed release was less in simple medium than in media supplemented with broth or amino acids.

DL-Lysine-2-C^{14}. The L form of this isotopic compound is used by the cell in the synthesis of lysine moiety of the protein, and is not metabolized to other cellular constituents.(10) Therefore, this tracer compound was convenient for study of the released proteinaceous materials. An experiment was carried out to assess the role of an energy source. Labeled bacteria were divided into two aliquots. One portion was added to complete M-9 medium, and the other to medium lacking glucose, the carbon and energy source. In the former, the rate of release was 3.7% per hour and in the latter, 0.89% per hour. This result can either be interpreted as indicating decrease in the release in the absence of energy source, or that under these conditions the released material is rapidly reassimilated. Similar results have recently been reported by Mandelstam.(11)

Using lysine as a tracer, an attempt was made to measure the temperature coefficient of the release process. It was found that the rate of release was less at lower temperatures, and that, if the centrifuge used in washing the cells was brought to the temperature of growth, the rate of release was greatly diminished from about 5% per hour to about 0.8% per hour. This finding was the clue that the phenomenon that had been under study was the lysis of cells killed by the experimental conditions employed, namely, the "cold shock" of chilling the cells during the centrifugation procedure.

The lethal action of cold had been studied by Hegarty and Weeks(12) who had found the effect to be most potent on cells in the logarithmic phase of growth. This work has in the main been disregarded, and it is routine procedure in many laboratories to chill and centrifuge cells for many purposes particularly in phage work.

The observation that a constant fraction of the cells are caused to lyse under the present experimental conditions suggests that in growing culture only in a certain phase of the division cycle are the organisms being killed by "cold shock."

Experiments in which the Cells are not Centrifuged and the Temperature is Maintained Constant

The experiments described above indicate that shortly after death caused by "cold shock," the susceptible cells lyse and liberate their contents into the medium. The important question remains as to the rate of death of cells in young actively growing cultures in the absence of external destructive forces such as "cold shock" or centrifugation. It was indicated that in the absence of "cold shock" the rate of release is less than 1% per hour, but it is possible that the observed value is the result of death caused by the packing of cells during centrifugation, even though no temperature change is involved.

With these considerations in mind, the following experiment was devised. A small volume of cells were grown in a medium consisting of M-9 plus a supplement of 50 μM glycine-2-C^{14} and 150 μM adenine. The amount of glycine was chosen so that free glycine would be completely removed from the medium before the adenine was utilized.(4) Then a portion of the culture was taken for analysis and another small portion diluted into fresh M-9 medium and allowed to grow for 8.5 hours. The data for this experiment are given in Table 5. Initially 26.7% of the activity remains in the growth medium. It has been shown(4) That this material is formed by the bacteria and is reutilized at a negligibly slow rate. A small amount of activity is found in the nucleic acids. In previous experiments, it has been seen that the activity resides in the purine - mainly in the guanine. The amount of activity located in the nucleic acids could have been reduced by increasing the purine content of the initial medium,(1) but then the bacteria could not have eliminated the purines from the growth medium, and consequently washing procedures would have been necessary.

TABLE 5

Absence of redistribution of protein glycine label after extensive growth

	Total distribution of radioactivity, %	
	initial	After 8.5 hr growth
Medium	26.2	22.8
Nucleic acid	4.4	3.7
Protein	69.4	73.6
	100.0	99.1

It is seen that no significant redistribution of activity occurs after 8.5 hours of exponential growth. If any deaths had occurred then the subsequent lysis should have increased the medium radioactivity. If, in addition,

growing cells in the population incorporated some of this material, then it would be probable that this material would be broken down (digested) to the point where it would serve as a precursor of the purine rings of the nucleic acids, which are necessarily being synthesized de novo after the consumption of the adenine supplement. It, therefore, appears quite probable that cell death in growing cultures is very small and probably considerably less than 1% per hour in synthetic medium at 37° C.

The problem of bacterial death is an old one. The experiments of Wilson[13] are widely quoted in the textbooks of bacteriology. He found that the viable count and the cell count differed and concluded that a high proportion (20%) of the bacteria were nonviable. Actually, in four out of twelve experiments, equality between the two measurements was observed. Probably the main source of deviation of the two measures is not in the measurement procedures, but may be attributed to the fact that he used standing cultures with no aeration. Mitchell[14] reaches similar conclusions, based on data obtained under conditions in which the bacterial culture was not growing exponentially. On the other hand, Kelley and Rahn[15] microscopically observed the growth of Aerobacter aerogenes at 30° C. They noted that if a cell divided, cell division would proceed at least to the fourth generation with no daughter cells failing to divide. As the observation was made repeatedly, it would appear that cell death is not frequent in Aerogenes.

Summary and Conclusions

In growing cultures of bacteria, intracellular protein degradation[1,2,3] and nucleic acid degradation[1, 16,17] are not observed. Under normal conditions in which the cells are not subject to stress, cell death is a rare occurrence. Therefore, cellular turnover is also a minimal process.

In the stationary phase of growth, protein degradation most certainly occurs,[9] but at the present time, it is impossible to assess the relative roles of cellular death with intracellular breakdown of the macromolecules inside of living cells. In resting cell suspensions, the physiological situation is much different from that obtained in the stationary cultures and in the growing culture. Degradation and an equal resynthesis have been shown both for bacteria[11,18] and for yeast.[19] The authors of these experiments have considered this degradation to be an intracellular process. This conclusion follows from the observed conservation of an adapted enzyme within the cells of the resting suspensions and from two assumptions. The first is that any released adaptive enzyme would not be inactivated or degraded subsequent to its release. The second assumption is that no enzyme synthesis occurs in the remaining cells of the population. In view of the recent findings in two laboratories[18,20] that RNA isolated from adapted cells can cause the formation of adaptive enzyme in recipient cells, this assumption is suspect.

The phenomenon of cold shock is of considerable interest. Hegarty and Weeks[12] found that the phase of growth determined to a large extent whether death would or would not occur. The cells were most sensitive during early exponential growth. Because of the widespread use of cells in late exponential growth phase, this observation may explain why more investigations have not been complicated by the death of cells. In this phase of growth, many changes in the cells are occurring: the cells are growing smaller, there are fewer nuclear bodies, the RNA content is decreasing, the susceptibility to virus infection is decreasing, the growth rate is decreasing, etc. These changes may be thought to prepare the cells for the conditions that obtain in stationary cultures. Future work will be required to understand the relation of the probability of death resulting from cold shock with other physiological changes during the growth cycle.

References

1. Koch, A. L., and H. R. Levy. Protein turnover in growing cultures of Escherichia coli. J. Biol. Chem. 217: 947-957 (1955).

2. Rotman, B., and S. Spiegleman. On the origin of the carbon in the induced synthesis of β-galactosidase in Escherichia coli. J. Bacteriol. 68: 419-429 (1954).

3. Hogness, D. S., M. Cohn, and J. Monod. Studies on the induced synthesis of β-galactosidase in Escherichia coli: The kinetics and mechanism of sulfur incorporation, Biochem. Biophys. Acta 16: 99-116 (1955).

4. Koch, A. L. The kinetics of glycine incorporation by Escherichia coli. J. Biol. Chem. 217: 931-945 (1955).

5. Maale, O., and J. D. Watson. The transfer of radioactive phosphorous from parental to progeny phage. Proc. Nat. Acad. Sci. 37: 507-513 (1951).

6. Koch, A. L. Biochemical studies of virus reproduction. XI. Acid-soluble metabolism. J. Biol. Chem. 203: 227-237 (1953).

7. Koch, A. L., and W. A. Lamont. The metabolism of methylpurines by Escherichia coli. J. Biol. Chem. 219: 189-201 (1956).

8. Neidhardt, F. C., and F. Gros. Metabolic instability in the ribonucleic acid synthesized by E. coli in the presence of chloromycetin. Biochim. Biophys. Acta 25: 513-520 (1957).

References

9. Podolsky, R. J. Protein degradation in bacteria. Arch. Biochem. Biophys. 45: 327-340 (1953).

10. Siddiqi, M. S. H., L. M. Kozloff, F. W. Putnam, and E. A. Evans, Jr. Biochemical studies of virus reproduction. IX. Nature of the host cell contributions. J. Biol. Chem. 199: 165-176 (1952).

11. Mandelstam, J. Turnover of protein in growing and non-growing populations of Escherichia coli. Biochem. J. 69: 110-111 (1958).

12. Hegarty, C. P., and O. B. Weeks. Sensitivity of Escherichia coli to cold shock during the logarithmic growth phase. J. Bacteriol. 39: 475-484 (1940).

13. Wilson, G. S. The proportion of viable bacteria in young cultures with especial reference to the technique employed in counting. J. Bacteriol. 7: 405-445 (1922).

14. Mitchell, P. Physical factors affecting growth and death. In Bacterial Physiology (O. H. Werkman and P. W. Wilson, Eds.). Academic Press, New York. pp. 126-177 (1953).

15. Kelley, C. D., and O. Rahn. The growth rate of individual bacterial cells. J. Bacteriol. 23: 147-153 (1932).

16. Fujisawa, Y., and A. Sibatini. Is there a quantitative relationship between the synthesis and breakdown of nucleic acid in living cells? Experientia 10: 178-180 (1954).

17. Hershey, A. D. Conservation of nucleic acid during bacterial growth. J. Gen. Physiol. 38: 145-148 (1954-5).

18. Hunter, G. B., and J. A. V. Butler. Stimulation by ribonucleic acid of induced β-galactosidase formation in Bacillus megaterium. Biochim. Biophys. Acta 20: 405-406 (1956).

19. Halvorson, H. Intracellular protein and nucleic acid turnover in resting yeast. Biochim. Biophys. Acta, 27: 255-266 (1958).

20. Kramer, M., and F. B. Straub. Role of specific nucleic acid in induced enzyme synthesis. Biochim. Biophys. Acta 21: 401-402 (1956).

STUDIES ON THE DNA CONTENT OF KREBS-2 MOUSE ASCITES TUMOR CELLS AFTER IRRADIATION AND HETEROLOGOUS TRANSPLANTATION

Agnes N. Stroud, Austin M. Brues, and Beverly Richard

We have reported previously[1] on heterologous growth of a mouse ascites tumor in the rat. A brief summary of these findings is as follows: (1) Over a three-day period in the rat the tumor cells grow logarithmically and with a concentration of around 10^8 cells per ml of fluid. (2) There is a linear relationship between cell number and the volume of ascites fluid. (3) Cell and nuclear volumes during the growth period increase 3- or 4-fold. (4) There is evidence that their volume increase could be associated with an immunological response of the host against the heterologous cells.

In this report we examine the nature of these volume increases, and also of the cell and nuclear volume increases that follow X-irradiation of cells prior to inoculation.

The problem was first approached by determining whether increased volume was the result of chromosome duplication (polyploidy). Chromosome counts showed no significant increase over the model number of 75 in the controls. In irradiated cells, chromosome counts were more difficult because of stickiness and breaks in the chromosomes; therefore polyploidy could not be determined accurately.

The second approach was to estimate the DNA (deoxyribose nucleic acid) content of the cells. This would determine polyploidy and give information about the synthesis of DNA. The method of Schneider[2] was used, and DNA was determined by the diphenylamine reaction. All cells used for the determination were stored free of ascitic fluid in liquid nitrogen at -320° F.

The results of two experiments are shown in Table 6, where the data include DNA in $\mu\mu$g/cell and the calculated DNA/1000 μ^3. The cell population is represented as well as the mitotic index for the tumor population.

The data for DNA per cell for both controls and irradiated groups show no change over the 3-day period, nor is there any difference between the control and the irradiated groups for any one day. During this time cell and nuclear volumes are increasing progressively in both nonirradiated and irradiated cells. The increase in the irradiated groups is almost three times that in the nonirradiated group. The calculated DNA per unit nuclear volume shows a sharp decrease in the irradiated group, whereas,

TABLE 6

DNA per cell, concentration of DNA in cell nuclei, cell numbers, and mitoses in irradiated ascites tumor cells growing in rats

Irradiation dose to cells, r	Days after inoculation 0	1	2	3	Irradiation dose to cells, r	Days after inoculation 0	1	2	3
	DNA, $\mu\mu$g/cell (mean)*					Cells x 10^8 (mean)*			
0	2.6	2.5	2.0	2.8**	0	1.1	4.5	8.0	16.4
2000	2.7	2.4	2.8	2.6	2000	1.1	2.8	4.8	1.7
3000	2.8**	2.6	2.9	2.6**	3000	1.1	2.1	3.1	1.2
	DNA/1000 μ^3 (mean)†					% Mitosis (mean)‡			
0	2.4	1.8	1.2	1.8	0	2.4	4.6	3.5	3.6
2000	2.4	0.6	0.7	0.8	2000	2.2	5.4	3.2	1.5
3000	2.4	0.6	0.6	-	3000	2.4	3.8	2.8	0.7

*Each value represents the mean of 8 animals except as noted otherwise.
**Represents the mean of 4 animals.
†Calculated from nuclear volumes of 200 cells for each value.
‡Each value represents the mean of 2000 cells.

there is only a slight decrease in the controls. At the same time the cell population in the irradiated group increases for 48 hr. This is contrary to the findings of Forssberg[3] for the Ehrlich ascites tumor with homologous transfer and an irradiation dose of 1250 r.

Our data show that there is an inhibition of DNA synthesis in the irradiated group (heterologous transplant), which is contrary to what is seen when mice are inoculated with the donor cells (homologous transplant). Unreported results show an increase in DNA over a 4-day period. This suggests that the inhibition of DNA synthesis of the tumor cells in the rat is depressed because of the immunological response. There is a significant increase in cell population as well as in cell mass.* The increase in the per cent of mitosis over a 48-hr period is the result of partial mitotic inhibition (arrested metaphases), that is, the increased numbers of mitotic figures may result from increased duration of visible stages of mitosis. However, there are also cells in visible telophase, but the percentage is extremely low compared to the controls. It is true that by 48 hr most of the cells in mitosis are abnormal.

*Preliminary interference microscope determinations on cells show a progressive increase in cell mass 72 hr after irradiation.

References

1. Stroud, A. N., A. M. Brues, D. H. Chatterley, and M. Summers. Serial transplantation of Krebs-2 and Ehrlich ascites tumors to rats. Cancer Research 17:1102-1107 (1957).

2. Schneider, E. C. Phosphorous compounds in animal tissues. V. The precipitation of nucleoproteins from rat liver homogenates by calcium chloride. J. Biol. Chem. 166:595-601 (1946).

3. Forssberg, A. The influence of radiation on the metabolism of ascites tumor cells, in Ciba Foundation Symposium on Ionizing Radiation and Cell Metabolism, eds. G. E. W. Wolstenholme and D. M. O'Connor. London: J. and A. Churchill Ltd. (1956).

PARTITIONMENT OF THE RADIATION SYNDROME IN CHICK EMBRYOS FOLLOWING EXPOSURE TO Co^{60} GAMMA RAYS

S. Phyllis Stearner, Sylvanus A. Tyler, Margaret H. Sanderson and Emily J. Christian

Investigations of the acute radiation response in young chicks reveal an early mortality concentrated sufficiently at 1-2 days to be easily separated from the later mortality occurring between 3-12 days. Differences in the gross pathology observed among decedents support the separation of the observed mortality into two periods and suggest that at least two distinct modes of injury comprise the radiation effect.[1,2] From an analysis of the dose exposure-time relationships by equimortality groups for each mortality period, it can be inferred that at least two different and independent injury processes are operating within the acute period.[3] Since the appearance of a large number of radiation deaths on the first day after irradiation is unusual for moderate dosages, the behavior of the chick embryo under similar irradiation became of immediate interest. In an experiment involving 2500 embryos subjected to Co^{60} γ-irradiation, not only was a similar first effect observed, but at least two further indicators of injury mechanisms, distinct in time range of expression, were revealed.

Six-day chick embryos were exposed in ovo to doses ranging from 800 to 13,000 r, delivered over periods varying from 15 min to 24 hr. Temperature and humidity comparable to incubator conditions were maintained during all exposures. Survival during the 12-day postirradiation period was determined by transillumination of the eggs. Recognition of radiation deaths is impossible after 12 days. In the prehatching period (18-20 days of incubation) there is high control mortality associated with physiological changes that occur prior to hatching. Approximately 25 indicators of radiation damage were identified by gross observation in more than 1600 embryos autopsied at time of death. From these, 3 sets of indicators were selected, on the basis of their interrelationships and severity, as descriptive of independent injury processes. Normally much of the circulating blood volume of a 6- or 7-day chick embryo is extraembryonic and only a small part is present in the embryo (Figure 10A). The first characterizing radiation syndrome is distinguished by pooling of blood in the large veins (Figure 10B). This syndrome is almost entirely limited to deaths occurring with 24 hr after irradiation. Commonly associated with venous pooling are large diffuse hemorrhages over the brain and in the posterior appendages (Figure 10C). These effects contribute to circulatory collapse.

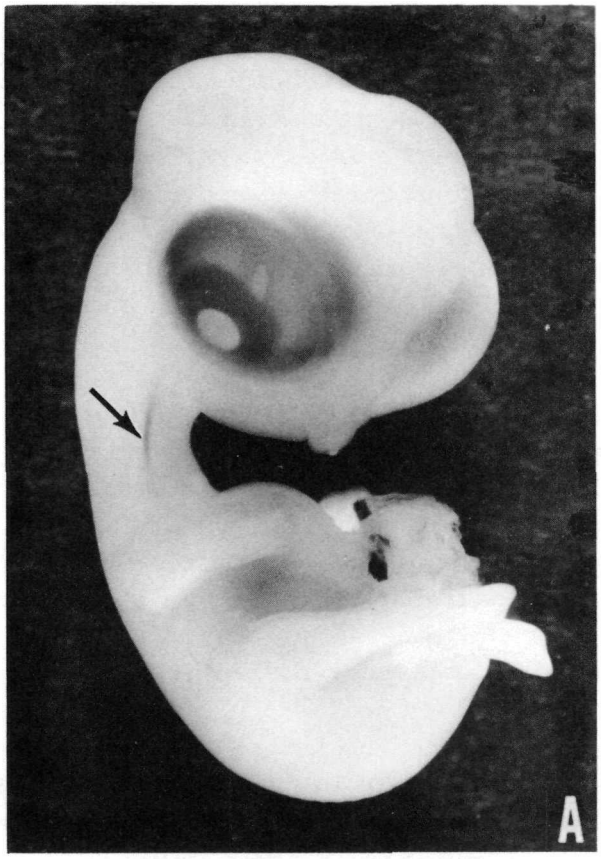

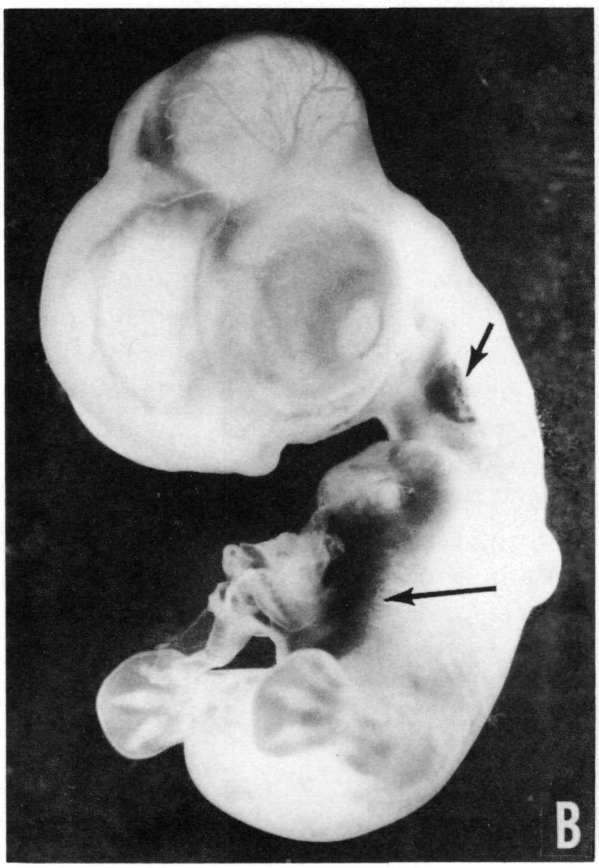

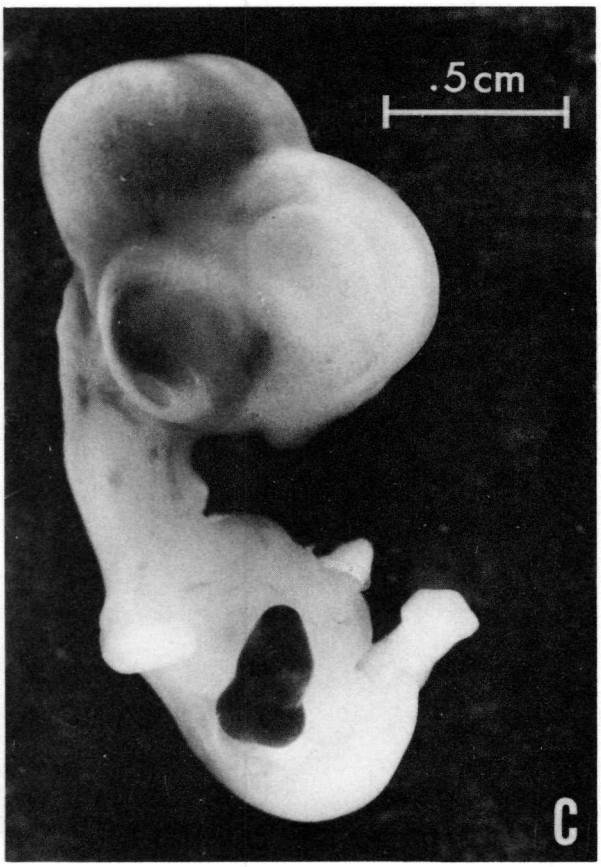

Figure 10. Lesions associated with the first radiation syndrome in 6-day chick embryos exposed to Co^{60} γ-rays.

A. Control embryo, 7 days of incubation.
B. Blood pooled in the large veins 6 hours after exposure to 1000 r, delivered in 15 min (cf, A).
C. Large diffuse hemorrhage over mesencephalon and massive hemorrhage in the right foot, present 24 hours after exposure to 1000 r.

Localization of fluid in the pericardial sac and in subcutaneous vesicles characterizes the second syndrome (Figure 11). Lymph channels begin to function on the seventh and eighth day of incubation (1 to 2 days after irradiation). The plexuses drain into the superior caval vein in the cervical region and into the coccygeal intersegmental vein in the region of the tail. Hemorrhagic lymph vessels are frequently seen in this period, and fluid accumulation may result from inadequate drainage from the lymphatics. This expression of injury is observed predominantly in the mortality occurring between 2 and 5 days postirradiation.

Extensive liver pathology is consistently present in decedents after 5 days. Abnormalities of the liver include large multiple necrotic areas, extensive hemorrhages and marked atrophy (compare Figs. 12A and 12B). This pathology is designated as the third radiation syndrome. In addition, evidence of typical "radiation disease" may be expressed in multiple petechiae in muscle, subcutaneous tissue and visceral surfaces. Other lesions occurring randomly throughout the 12-day period and less pronounced in severity were not used as indicators and are thought to be nonspecific accompanying effects.

In a preliminary report[4] the second syndrome was considered as roughly characterized by a generalized edema. This condition we now feel to be a nonspecific phenomenon occurring also in association with the second and third syndromes. Table 7 gives the daily frequency of deaths by syndrome. Few animals showed a combination of effects. In most cases those that possessed multiple syndromes can be assigned a single syndrome by using time of death as the criterion. The number of animals in which only edema was observed is significant, but for this discussion it is believed to be an accompanying effect. The daily frequency of deaths over the 12-day postirradiation period is given in Figure 13, based on the total number of embryos autopsied. The modal frequencies that appear at 1,3 and 8 days are again seen in Figure 14, in which are plotted the daily mortality rates for each of the three syndromes previously described. From Figure 14, the time distribution of the three syndromes seems to be sufficiently distinct in time to allow each to be described on the basis of time of death. Use of such a criterion makes possible a unique classification of all decedents. This approach has permitted description of the dose exposure-time relations by syndrome, and the determination of constants which characterize injury processes operating in the irradiated embryo.

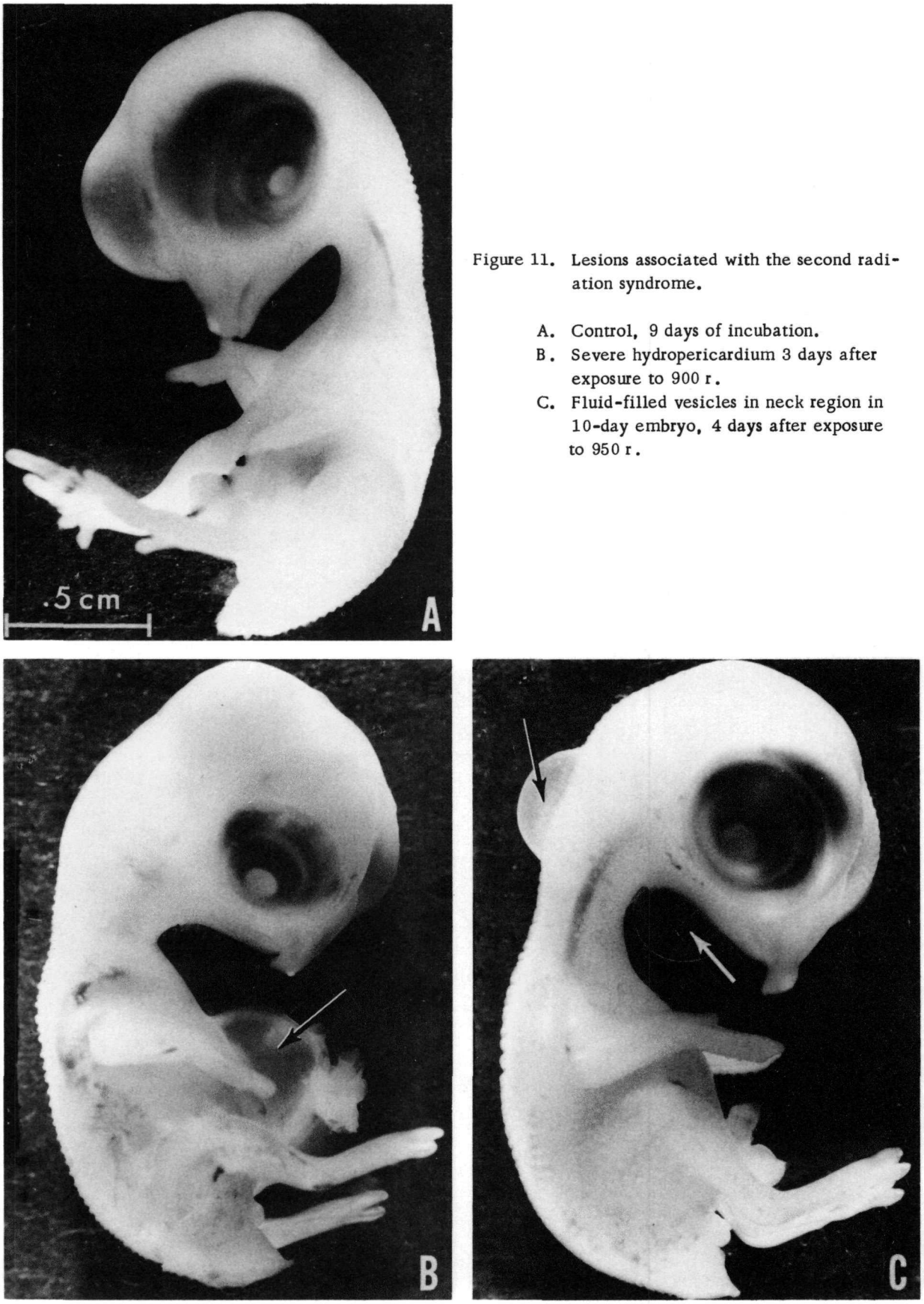

Figure 11. Lesions associated with the second radiation syndrome.

A. Control, 9 days of incubation.
B. Severe hydropericardium 3 days after exposure to 900 r.
C. Fluid-filled vesicles in neck region in 10-day embryo, 4 days after exposure to 950 r.

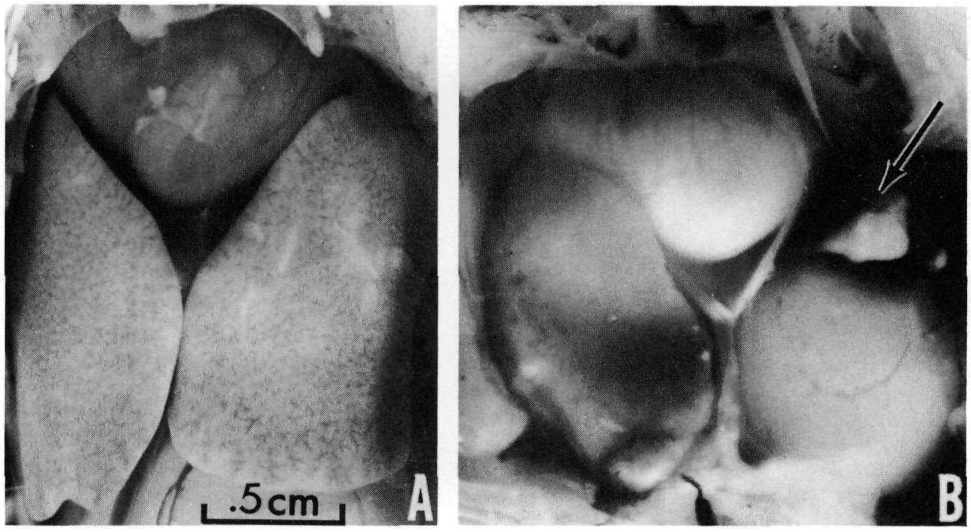

Figure 12. Hepatic lesions characterizing the third radiation syndrome.

A. Liver of control embryo, 15 days' incubation.
B. Nine days after exposure to 1000 r; left lobe shows severe atrophy, with necrotic and hemorrhagic areas. Necrotic lesions and biliary obstruction are present in right lobe.

TABLE 7

Frequency of characterizing syndromes by day of death after irradiation

Syndrome*	Days after irradiation												Total
	1	2	3	4	5	6	7	8	9	10	11	12	
1	386	16	9	7	4								422
2		87	136	37	10					2			272
3		1	9	5	2	25	63	129	55	58	17	24	388
1,2	2	45	12	1									60
1,3				2			1	1			2		6
2,3				9	3			2	13	14	8	11	60
1,2,3			2							1			3
Edema		2	61	44	71	47	53	21	15	6	15		335
None	44	16	12	4	16		3		15				110
Total	432	167	241	109	106	72	120	153	98	81	42	35	1656

*1, venous pooling; 2, localized fluid accumulation; 3, hepatic lesions.

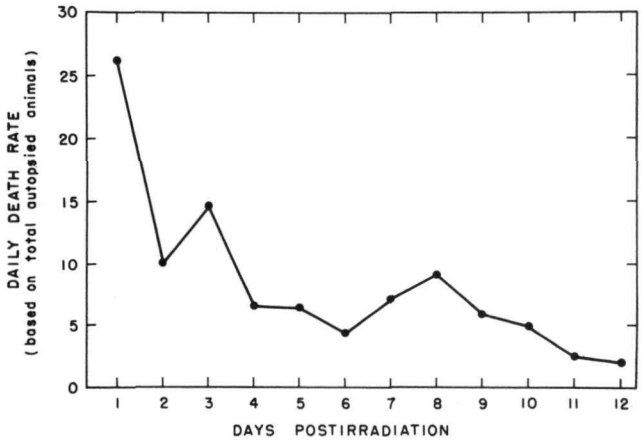

Figure 13

Daily frequency of death following γ-irradiation of 6-day chick embryos, based on total number autopsied.

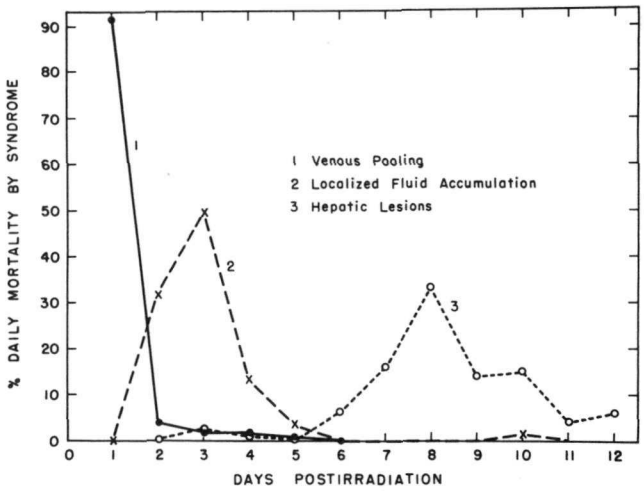

Figure 14

Distribution of daily mortality rates by syndrome.

References

1. Stearner, S. P. The effect of variation in dosage rate of roentgen rays on survival in young birds. Am. J. Roentgenol. 65:265-71 (1951).

2. Stearner, S. P., A. M. Brues, M. Sanderson, and E. J. Christian. Role of hypotension in the initial response of X-irradiated chicks. Am. J. Physiol. 182:407-410 (1955).

3. Stearner, S. P., and S. A. Tyler. An analysis of the role of dose and dosage rate in the early radiation mortality of the chick. Radiation Research 7:253-266 (1957).

4. Stearner, S. P., and S. A. Tyler. Recognition of modes of death in the analysis of acute radiation mortality. Semiannual Report of Biological and Medical Research Division, Argonne National Laboratory. ANL-5732, pp. 98-101 (1957).

PHYSICOCHEMICAL CHARACTERIZATION OF GLUTAMIC-ASPARTIC TRANSAMINASE

David A. Yphantis

Samples of porcine glutamic-aspartic transaminase prepared by Dr. W. T. Jenkins at Massachusetts Institute of Technology have been characterized using the ultracentrifuge. Using a separation cell technique[1] the enzymatic activity has been identified with the main component of the preparations. Sedimentation analyses showed the preparations to be 81 ± 3% pure. The active component had an apparent diffusion coefficient, $D^{app}_{20,w} = 4.6 \pm 0.1 \times 10^{-7}$ cm^2 sec^{-1} and a sedimentation coefficient, $s_{20,w} = 5.24 \times 10^{-13}$ sec at a concentration of 12.6 mg/ml in 0.15 M Tris - HCl buffer at pH 8.0. The molecular weight calculated from these, on assumption of a partial specific volume of 0.745, is 108,000 ± 3000.

A molecular weight of 110,000 ± 11,000 was estimated for the active component from approach-to-equilibrium runs using modifications of the Archibald technique.[2,3,4]

The pyridoxal phosphate content of the preparations corresponds to a minimum molecular weight of 57,800 ± 3000; thus there are two molecules of pyridoxal phosphate per enzyme molecule of molecular weight 115,000 ± 6000.

References

1. Yphantis, D. A. and D. F. Waugh. Ultracentrifugal characterization by direct measurement of activity. I. Theoretical. II. Experimental. J. Phys. Chem. 60: 623-635 (1956).

2. Klainer, S. M. and G. Kegeles. Simultaneous determination of molecular weight and sedimentation constants. J. Phys. Chem. 59:952-955 (1955).

3. Ginsburg, A., P. Appel, and H. K. Schachman. Molecular-weight determination during the approach to sedimentation equilibrium. Arch. Biochem. Biophys. 65:545-566 (1956).

4. Ehrenberg, A. Determination of molecular weights and diffusion coefficients in the ultracentrifuge. Acta Chem. Scand. 11: 1257-1270 (1957).

ABSOLUTE MEASUREMENTS OF SPHERICAL PARTICLES OF SOME POLYSTYRENE LATEXES

Herbert E. Kubitschek and John F. Thomson

During the last decade polystyrene spheres have been used as standards for the measurement of sizes of cells and cell elements with electron microscopy. In the more recent work the polystyrene latexes have been replaced by replica gratings for greater accuracy. Nevertheless, these latexes can be very useful as standards in many other measurements, especially those made upon living matter in suspension. Because of their potential importance, we have attempted to measure the mean diameters of the spheres of several polystyrene latexes, obtained through the courtesy of Dr. J. Vanderhoff, Dow Chemical Company. Absolute measurements of mean diameters were made by phase contrast and electron microscopy, and by centrifugation in a sucrose gradient.

For the optical measurements a small volume (platinum loop) of the latex was added to a drop of microscope oil (Cargille's; density, 1.515) upon a microscope slide and mixed gently. The resulting emulsion, after being covered with a slip, often displayed single layers of the spheres in hexagonal array in the oil phase. Optical difficulties were avoided in measuring the length of a line of spheres in such an array by measuring between the points of contact between the outermost spheres and their neighbors. The ocular reticle used in these measurements was calibrated against a silicon replica grating of 30,000 lines per inch. Results are given in Table 8.

TABLE 8

Measurements of polystyrene spheres

Run or lot number	Diameter, listed values, μ	Measured diameter, μ		
		Phase contrast	Electron microscope	Sucrose gradient
15 N-8	0.511 ± 0.007	-	-	0.519 ± 0.007
LS-067-A	1.171 ± 0.0133	1.132 ± 0.002	1.198 ± 0.002	1.126 ± 0.016
L-3830-1	1.8	1.671 ± 0.003	1.708	1.669 ± 0.022
L-3830-19-E	3.0	3.186 ± 0.001	3.205	-

Electron micrographs were made of particles deposited upon carbon membranes deposited upon collodion-covered copper grids. Each set of four micrographs was monitored against the silicon replica grating. The inaccuracies of this method include the change in apparent cross section of the polystyrene spheres under electron impact and the nonlinearity of the images obtained.

For measurements in sucrose gradients, essentially linear gradients were prepared with sucrose concentrations ranging from 2 to 10%, and with uniform concentrations of 0.5% NaCl. Small volumes (0.05 to 0.10 ml) of latex suspensions were layered onto these gradients and centrifuged at 1°C. After centrifugation, the distances that the bands of particles had moved from the meniscus were measured (see Figure 15). The mean particle diameter was calculated from a derivation of Stokes' law containing empirical corrections for changes in the viscosity and density of the medium in terms of tube length.[1] The results of these measurements agree well with the optical measurements.

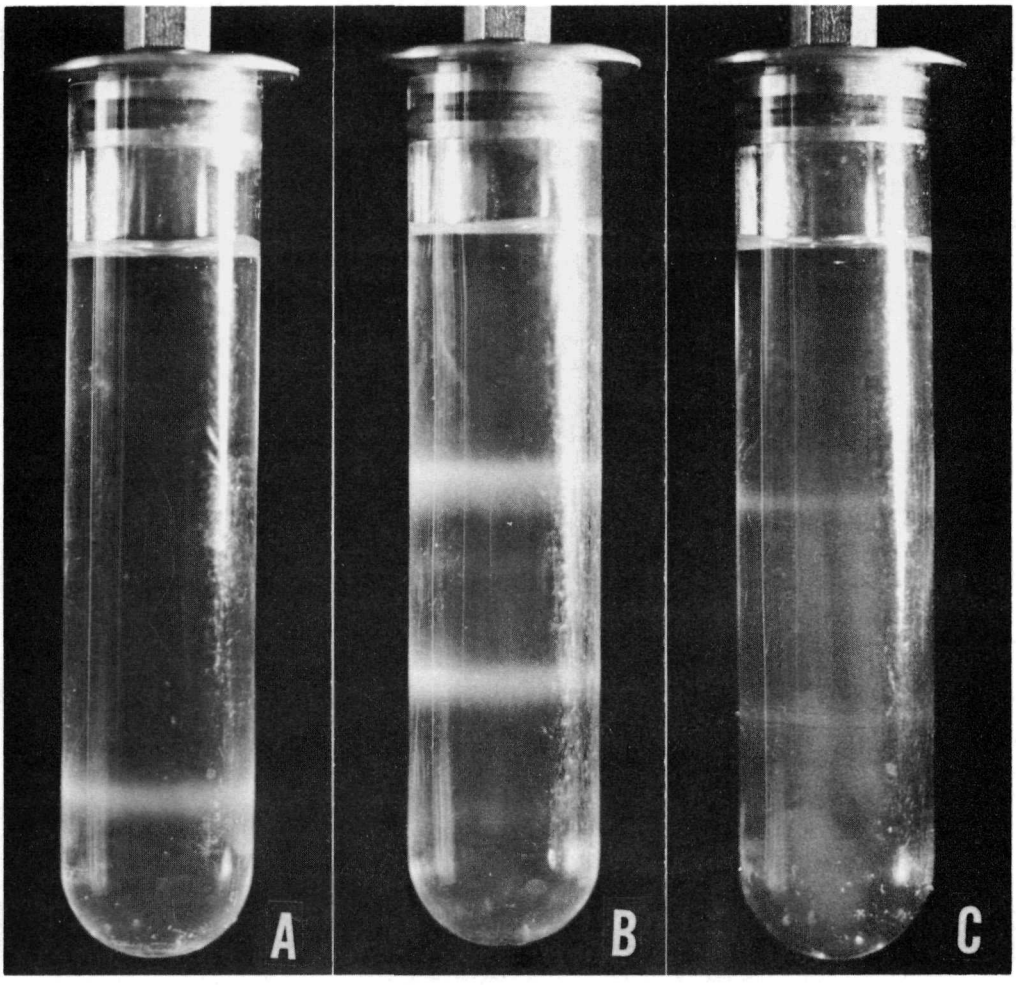

Figure 15. Separation of polystyrene latex spheres by density-gradient centrifugation. Runs A and B, 10^8 particles layered; Run C, 10^7 particles. Run A, $\omega^2 t = 4.054 \times 10^8$ sec^{-1}; Run B, 1.554×10^8 sec^{-1}; Run C, 1.589×10^8 sec^{-1}. In Run A, the band represents 1.13-μ particles; in Runs B and C, the upper bands are 1.13-μ particles, the lower bands 1.67-μ particles. In Run B, faint bands can be seen slightly below the principal ones; these represent "doublets" of the particles (i.e., apparent diameter of 1.43 μ and 2.10 μ).

Reference

1. Thomson, J. F., and E. T. Mikuta. Enzymatic activity of cytoplasmic particulates of rat liver isolated by gradient centrifugation. Arch. Biochem. Biophys. 51: 487-498 (1954).

3-AMINO-1,2,4-TRIAZOLE

IX. The heat-stable factor necessary for inhibition of catalase

Robert N. Feinstein

It has been demonstrated that in dilute solution 3-amino-1,2,4-triazole (AT) will, upon incubation, inhibit the catalase activity of tissue homogenates but not of purified catalase.[1] This suggests that crude tissues contain an additional factor which is necessary for the AT effect, and such a factor is indeed to be found in a variety of tissues.[1,2] It is stable to 20-min heating in boiling water over a pH range from 3 to 11, and so is referred to as the heat-stable factor (HSF). The HSF content of a variety of rat tissues is listed in Table 9.

TABLE 9

Heat-stable factor (HSF) content of rat tissues

Tissue	Half-inhibition concentration,* %
Whole blood	0.85
Testis	0.19
Brain	0.15
Spleen	0.13
Intestine	0.11
Kidney	0.09
Liver	0.05

*"Half-inhibition concentration" refers to the concentration (expressed as per cent of whole fresh tissue) of heat-stable supernatant fluid required to reduce the activity of a crystalline catalase preparation to half that obtaining in the absence of the HSF, after a standard 30-min, 37° C, incubation with AT. Preparation of the tissues consisted of homogenizing as 2% aqueous homogenates, heating for 10 min in a boiling water bath, rehomogenizing, centrifuging, filtering the supernatant fluids, and finally diluting the filtrates serially over the desired range. The amounts of catalase inhibition brought about by the various dilutions were plotted on semilog paper, and the 50% inhibition value was interpolated.

A commercial dehydrated beef kidney powder,** defatted with ethylene dichloride, has served as a convenient source of the heat-stable factor. Approximately 1 mg of this kidney powder gives a maximal response in the system used. In an attempt to obtain some information as to the chemical nature of the HSF, the supernatant solutions of heated, centrifuged suspensions of the kidney powder were extracted with peroxide-free ether

**VioBin Corporation, Monticello, Illinois.

containing small amounts of ethanol. The resulting aqueous phase was completely devoid of HSF activity. The ether phase, reduced to dryness and dissolved in water, was also free of such activity, as was combination of the aqueous phase and the reconstituted ether phase. Such loss of activity could also be brought about by mixing with ethanol and evaporating off the ethanol. The effect was not produced by corresponding treatment with chloroform, acetone, or alcohol-free ether, however, and thus is apparently an effect of the ethanol content of the ether used.

Not only does the alcohol treatment destroy HSF activity, but it apparently creates a new factor, which, when added in extremely small amounts to an incubated catalase-AT-HSF system, prevents the otherwise invariable inhibition of catalase activity. An indication of the effectiveness of this alcohol-treated material in preventing the inhibition is given in Table 10. In repeated experiments, excellent effects have been obtained from alcohol-treated HSF preparations containing less than one-third μg dry weight. Alcohol-treated HSF preparations which will thus prevent the usual inhibition will not reverse it.

TABLE 10

Prevention of AT-HSF inhibition of catalase by alcohol-treated HSF

Concentration of alcohol-treated HSF, μg/ml	Catalase activity, perborate units/ml		
	Initial	At 30 min	Decrease
0	2.12	0.56	1.56
0.256	2.32	0.71	1.61
1.28	2.31	1.02	1.29
6.4	2.30	2.16	0.14
32.0	2.36	2.16	0.20

Assay system: AT, 0.02 M; HSF, 0.5 mg-equivalents/ml; catalase, 0.5 μl commercial suspension/ml; incubation, 30 min at 37°C (mg-equivalent refers to the material resulting from the treatment of 1 mg original dehydrated beef kidney).

As noted above, HSF treated with peroxide-free, alcohol-containing ether will prevent catalase inhibition by an otherwise active AT-HSF system. If, however, active HSF is treated with alcohol-free, peroxide-containing ether, an increase HSF activity will be noted. This has been traced to the peroxide content of the ether. Peroxide-rich ether can be evaporated to dryness, leaving a thin, sometimes undetectable film of

(presumably) ether peroxides, and this residue, dissolved in water, serves effectively as an HSF source. It has been designated a "pseudo heat-stable factor" (PHSF), and its properties follow surprisingly closely those of the true HSF from liver, kidney, etc.

Among these properties are the following.

1. Combination with AT, either the true or the pseudo HSF will inhibit catalase.
2. Treatment with ethanol or ethanol-containing ether prevents catalase inhibition by an otherwise active system. Either the true or the pseudo HSF, after alcohol treatment, will abolish the effect of either one of the HSF's.
3. Either is absorbed on the anion exchanging resin Dowex 1.
4. Phosphate buffer will elute either HSF from Dowex 1.
5. Neither is adsorbed on the cation exchanger Dowex 50.
6. When treated with ethanol, neither is adsorbed on either Dowex 1 Dowex 50.

On the other hand, certain points of disparity exist between the two types of preparations.

1. Whereas doubling the concentration of the true HSF will double the effect on catalase (within the assayable range), it requires approximately a five-fold increase in PHSF concentration to double the effect on catalase.
2. The true HSF is relatively unstable; if incubated in neutral aqueous solution at 37° C. for 2 hr., it loses approximately 50% of its activity; during a second 2-hr period, 50% of the residual activity disappears. The PHSF, on the other hand, shows no diminution of activity under identical circumstances.
3. If the true HSF is incubated with AT preliminary to admixture with catalase, the decrease in HSF activity is greatly augmented; in 2 hr, 87% of the activity disappears; after 4 hr, only 9% of the initial activity remains. The PHSF preparation, however, loses no activity in an identical situation.

Two possible explanations suggest themselves with regard to the two latter points of disparity. First, the true and the pseudo HSF may actually be different molecules, the latter a more stable one. Second, the two may be identical, but the true HSF may be present in so complex a milieu that it reacts with some other component of the milieu and so becomes diminished in activity. This has been tested by examining systems containing the true

and the pseudo HSF, separately and together. In these systems it is found that although the initial level of HSF activity in the presence of both materials is approximately equal to the sum of the two individuals, after a period of incubation the combined activity has decreased to that of the PHSF alone. This is true in both the presence and the absence of AT. It thus appears probable that, despite their many similarities, the "true" HSF from animal tissues and the "pseudo" HSF from peroxide-containing ether are not identical. As additional evidence of the nonidentity of the two, there may be cited the fact that it has not been possible to detect peroxides in HSF preparations; however, the biological (i.e., catalase-inhibitory) effect is more sensitive than the chemical (ACS standards) test for peroxides by a factor of at least 25, thus requiring an HSF concentration near the maximal obtainable. When it becomes feasible to concentrate HSF activity beyond this point, the question of identity or nonidentity will be reinvestigated. To the present, all efforts at purification of the HSF have failed, chiefly due to the instability of the material, an instability which appears to be independent of pH, degree of oxygenation, or the removal of inactive material.

There have been recent suggestions in the literature[3,4] that the inhibition of catalase by AT and HSF may in reality be due to slow, continuous formation of hydrogen peroxide from the HSF by autoxidation, the H_2O_2 then destroying the catalase under the influence of the AT. Margoliash and Novogrodsky[3] have in fact demonstrated that if H_2O_2 is permitted to dialyze slowly into a mixture of catalase and AT, the catalase activity will be reduced; in the absence of the AT, or if the H_2O_2 is initially present in high concentration, such reduction in activity does not occur. The significance of these latter findings is not immediately apparent, nor are they necessarily the explanation of the findings reported above.

The effect of alcohol in preventing AT-HSF inhibition of catalase has been suggested[4-6] to be due to a coupled oxidation of the ethanol by formed H_2O_2, the catalase here acting as a peroxidase. The ethanol thus prevents the accumulation of inactive catalase-H_2O_2 complex II and so minimizes catalase inactivation. This seems an incomplete, if indeed at all accurate, explanation of the ethanol effect observed. It certainly does not account for the fact that ethanol-treated HSF, in the complete absence of catalase, is no longer retained on a Dowex-1 column, nor does it explain the observed irreversibility by ethanol of AT-HSF inactivation of catalase.

It thus appears essential to design experiments crucial to the point of whether there is actually a single molecular species accounting for the so-called HSF effect, or whether this is in fact an autoxidation of a variety of sulfhydryl and related compounds to yield H_2O_2 which, in the presence of AT, inactivates catalase. If the latter, there is then obviously no point in efforts to isolate and identify an active molecular species.

References

1. Feinstein, R. N., S. Berliner, and F. O. Green. Mechanism of inhibition of catalase by 3-amino-1,2,4-triazole. Arch. Biochem. Biophys. 76: 32-44 (1958).

2. Sugimura, T. The mechanism of liver catalase depression by 3-amino-1,2,4-triazole. Gann 47: 159-170 (1956).

3. Margoliash, E., and A. Novogrodsky. A study of the inhibition of catalase by 3-amino-1,2,4-triazole. Biochem. J. 68: 468-475 (1958).

4. Alexander, N. M. Catalase inhibition by normal and neoplastic tissues. J. Biol. Chem. 227: 975-985 (1957).

5. Nelson, G. H., F. W. Kinard, J. C. Aull, Jr., and M. G. Hay. Effect of aminotriazole on alcohol metabolism and hepatic enzyme activities in several species. Quart. J. Studies on Alcohol 18: 343-348 (1957).

6. Nelson, G. H. Ethanol protection against the catalase-depressing effect of 3-amino-1,2,4-triazole. Science 127: 520-521 (1958).

PROGRESS REPORT: THE ENZYMATIC DECOMPOSITION OF S-ADENOSYLMETHIONINE

Stanley K. Shapiro and Adaline N. Mather*

In the course of studies with S-adenosylmethionine as a methyl donor for the homocysteine-transmethylase system of bacterial and yeast cells,[1] it was apparent that the methyl donor is decomposed enzymatically. Preliminary observations concerning this enzymatic decomposition of S-adenosylmethionine have been reported previously from this laboratory.[2-4] In all the systems that have been investigated, the pattern of enzymatic destruction appears to be similar, but the speed of the reaction varies greatly. Cell-free extracts of Aerobacter aerogenes were selected for this study because the enzymes degrading S-adenosylmethionine are particularly active.

After incubation of S-adenosylmethionine with cell-free extracts of A. aerogenes, aliquots of the reaction mixtures were placed on paper chromatograms for analysis of the decomposition products. Adenine and much smaller amounts of hypoxanthine were the only purine compounds formed. The only sulfur-containing product was methylthioribose. Homoserine and α-amino-γ-butyrolactone were the only amino acid decomposition products.

Formation of α-amino-γ-butyrolactone. The isolation and identification of the lactone of homoserine as a product of the chemical hydrolysis of S-adenosylmethionine has been observed by Parks and Schlenk.[5] Homoserine lactone is formed from S-adenosylmethionine by extracts of A. aerogenes. Identical reaction mixtures with homoserine as substrate failed to yield detectable amounts of the lactone during a period of 5 hr. It appears that the enzymatic formation of the latter compound precedes the formation of homoserine. Furthermore, pure α-amino-γ-butyrolactone is converted to homoserine at virtually the same rate with or without the presence of a crude enzyme mixture. Consequently, the actual enzymatic product resulting from the four-carbon amino acid moiety of S-adenosylmethionine is apparently α-amino-γ-butyrolactone, which is converted to homoserine by a nonenzymatic process.

Decomposition of methylthioadenosine. Along with the formation of α-amino-γ-butyrolactone one would expect methylthioadenosine. However, only traces of this compound are found during the enzymatic decomposition of S-adenosyl-L-methionine, but adenine and methylthioribose accumulate. A comparison of the rate of formation of methylthioribose from S-adenosyl-L-methionine and methylthioadenosine is shown in Figure 16. It is obvious that methylthioadenosine is decomposed much more rapidly (about 6 times faster) than is S-adenosyl-L-methionine. Under identical conditions

---

*Resident Research Associate.

methylthioadenosine is converted quantitatively to methylthioribose in 2.5 hr, while only 25% of S-adenosyl-L-methionine is decomposed to the same product. Thus it is clear that methylthioadenosine is decomposed as rapidly as it is formed from S-adenosyl-L-methionine.

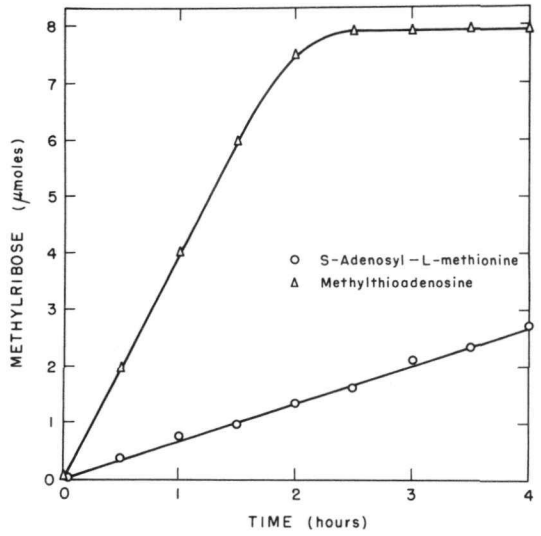

Figure 16. The formation of methylthioribose from S-adenosyl-L-methionine (o) and methylthioadenosine (Δ) as a function of time. Ten ml of each reaction mixture contained 80 μM substrate and 50 mg of protein of A. aerogenes extract, and were incubated at 35° in 0.1 M phosphate buffer, pH 6.8. One-ml samples were removed every 30 min for the determination of methylthioribose.

Comparison of the reactions. A comparison of the reaction products formed from S-adenosylmethionine, methylthioadenosine and adenosine is given in Table 11. The homoserine figure represents the value obtained from the combined eluates of α-amino-γ-butyrolactone and homoserine. It is interesting to note that methylthioadenosine is more rapidly decomposed than adenosine, suggesting that different nucleosidases are involved. It is again clear that methylthioadenosine is much more rapidly decomposed than S-adenosyl-L-methionine. Thus the enzymatic decomposition of S-adenosyl-L-methionine may be described as follows:

S-Adenosyl-L-methionine

I ↓

Methylthioadenosine + α-Amino-γ-butyrolactone

II ↓ III ↓ (nonenzymatic)

Adenine + Methylthioribose Homoserine

Under these conditions, homoserine, adenine, and methylthioribose are not metabolized and accumulate as end products of the reaction. With fresh preparations of enzyme, adenine is deaminated to hypoxanthine. Since reaction II proceeds much faster than reaction I, the concentration of methylthioribose may be used as a convenient measure of the rate of decomposition of S-adenosyl-L-methionine.

TABLE 11

Enzymatic decomposition of S-adenosylmethionine and methylthioadenosine*

	Quantity of substrate	Reaction products					
		S-Adenosylmethionine	Methylthioadenosine	Adenosine	Adenine	Methylthioribose	Homoserine
S-Adenosyl-L-methionine	9.4	7.5	0.1	0	2.0	1.9	2.0
S-Adenosyl-D-methionine	9.3	8.8	--**	--**	--**	0.4	--**
Methylthio-adenosine	8.1	0	0	0	8.2	8.0	0
Adenosine	8.3	0	0	5.8	2.6	0	0

*All quantities are expressed as μM per 2 ml of reaction mixture. The mixtures contained 10 mg protein of A. aerogenes extract and were incubated for 3 hr at 35°C in 0.1 M phosphate buffer, pH 6.8.

**Not determined; see text.

The reaction is stereospecific in that only S-adenosyl-L-methionine serves as a substrate. The amount of methylthioribose produced from S-adenosyl-D-methionine (Table 11) is equivalent to the amount of L-isomer present in the preparations of S-adenosyl-D-methionine.

Extracts of A. aerogenes that have been dialyzed for 24 hr against 0.01 M phosphate buffer, pH 6.8, retain full activity in the enzymatic decomposition of S-adenosyl-L-methionine and methylthioadenosine. Heating the crude extract for 5 min at 80° C results in inactivation of both enzymes. However, when this extract is heated at 70° C for 2 min, reaction II is decreased sufficiently so that methylthioadenosine can be identified qualitatively as a product of reaction I.

References

1. Shapiro, S. K. Adenosylmethionine-homocysteine transmethylase. Biochim. Biophys. Acta. 29: 405-409 (1958).

2. Shapiro, S. K. S-Adenosylmethionine-homocysteine transmethylase. Bacteriol. Proc., p. 116 (1957).

3. Shapiro, S. K. and A. N. Mather. The utilization of S-adenosylmethionine by microorganisms. Abstracts of 132nd American Chemical Society Meeting, New York, September, p. 21C (1957).

4. Schlenk, F., S. K. Shapiro, and L. W. Parks. Proceedings of the International Symposium on Enzyme Chemistry, Tokyo and Kyoto, Japan. In press. (1957).

5. Parks, L. W. and F. Schlenk. Formation of α-amino-γ-butyrolactone from S-adenosylmethionine. Arch. Biochem. Biophys. 75: 291-292 (1958).

PROGRESS REPORT: PROTEIN SYNTHESIS IN PANCREAS

V. Fractional Extraction and Precipitation of Pancreatic Enzymes

Anna Kane Laird and A. D. Barton

Previous studies of this series[1-5] have described the intracellular distribution of amylase in the pancreas and the changes observed in this distribution during the secretory cycle. The present report concerns the extraction of amylase and lipase from the secretory granules and microsomes by several ionic media, and the precipitability of these enzymes and of the RNA of the final supernatant fluid at pH 5.

Male Sprague-Dawley rats weighing 350-450 g were used for these experiments; they were fed ad libitum, with the exceptions noted below. They were killed in the morning, several hours after the completion of their nocturnal feeding; the pancreas tissue was, therefore, in the late recovery phase following the depletion of its enzymes by feeding. For the experiments with secretory granules and microsomes, the pancreases from 4 to 6 rats were homogenized in 0.88 M sucrose, and the secretory granules were isolated from this medium as described before.[5] The 20,000 x g supernatant fluid containing the microsomes and soluble proteins was then diluted 3.5-fold to reduce the sucrose concentration to 0.25 M; in this medium the microsome material is sedimented more nearly completely during the subsequent centrifugation at 105,000 x g for 65 min.[2,4] The secretory granule and microsome fractions from 3 to 5 g of pancreas were suspended in 10 cc of 1% sodium acetate at pH 6.8 (cf 6). The suspension was allowed to stand in the cold for 10 to 30 min and was then centrifuged at 20,000 x g for 10 min. Both extracts were clear; the secretory granule extract was colorless and that from the microsomes was pink. The sediment from the secretory granules was smaller and brownish gray in contrast to its original white color, while that from the microsomes was pink and opaque in contrast to its relative translucency when first isolated. These sediments were then extracted in 0.01 M phosphate buffer at pH 8.0 by a procedure identical to that used for the extraction with sodium acetate. The phosphate extracts and sediments were similar in appearance to those obtained with acetate. Finally the sediments were extracted in 0.06% sodium desoxycholate by the same procedure; the extracts were water-clear, and the sediments were not changed in appearance.

The supernatant fluid was prepared by two different procedures from animals starved overnight. In one case the pancreas was homogenized directly in 0.25 M sucrose and the homogenate centrifuged at 105,000 x g for 65 min. In the second, the supernatant fluid was obtained by a procedure similar to that described above for obtaining microsomes: the

20,000 x g supernatant fluid from a homogenate prepared in 0.88 M sucrose was diluted 3.5-fold and then centrifuged at 105,000 x g for 65 min. In both cases, after removal of samples for analysis, the supernatant fluid was brought to pH 5 by the addition of one drop of 1 N acetic acid. The cloudy suspension that resulted was centrifuged at 105,000 x g for 15 min.

The various fractions obtained were analyzed for protein by the method of Lowry et al.,[7] for amylase by a slight modification of the method of Meyer et al.,[6] and for lipase by the method of Seligman and Nachlas,[8] using sodium taurocholate in the medium. The RNA content of the supernatant fluid and its fractions was determined by Schneider's method.[9]

The protein, amylase and lipase contents of the three extracts and of the final sediments obtained from the secretory granules and microsomes are given in Tables 12 and 13. It is evident that under the conditions of these experiments: (1) the sodium acetate extracted about half the protein from both the secretory granules and the microsomes; (2) phosphate buffer at pH 8 extracted about half the remaining protein from both cell fractions; and (3) sodium desoxycholate extracted about 2/3 of the remaining protein from the secretory granules, but only about 1/4 of that from the microsomes. The distribution of the amylase and lipase in the extracts was quite different from that of the protein; about 80% of the amylase of the secretory granules was found in the acetate extract, and 80% of the remainder was extracted by phosphate buffer at pH 8, leaving an insignificant residue in the desoxycholate extract and the final sediment. Although about half the amylase of the microsomes was extracted by acetate, in rough proportion to the protein extracted, essentially all the remaining amylase was removed by phosphate buffer at pH 8. Very little or no lipase was extracted by the reagents used in these experiments; since the recovery was low, especially from the secretory granules, it is possible that some inactivation occurred also during these procedures.

The distribution of protein, RNA, amylase and lipase in the pH 5 fractions of the supernatant fluid is given in Table 14. It is evident that the method of preparation of the homogenate influences the results obtained (these differences have been obtained in several experiments; Table 14 gives results typical of those obtained). Homogenization of the pancreas in 0.25 M sucrose resulted in a much higher yield of soluble protein than did homogenization in 0.88 M sucrose followed later by dilution to 0.25 M, after removal of the larger particulate fractions. The additional protein was found mainly in the fraction not precipitated at pH 5. Although the total amounts of RNA and amylase in the supernatant fluid were similar in the two experiments, their responses at pH 5 differed considerably depending on the initial medium of homogenization. Relatively little of the RNA was precipitated when the homogenate had been prepared in 0.25 M sucrose, but more than half was precipitated when the homogenate had been made in 0.88 M sucrose.

TABLE 12

Distribution of protein, amylase, and lipase after extraction of secretory granules with sodium acetate, phosphate buffer (pH 8.0), and sodium desoxycholate

	Protein	Amylase		Lipase	
	Total E*	Total E*	E/protein E	Total E*	E/protein E
Original secretory granules	95.0	(76.8)**	(.81)**	8.2	0.086
Acetate supernatant	50.0	61.6	1.23	1.1	0.030
Acetate sediment	36.4	15.2	0.42	5.9	0.162
Phosphate supernatant	18.0	11.7	0.65	1.1	0.064
Phosphate sediment	15.8	0.2	0.01	2.3	0.145
Desoxycholate supernatant	10.0	0	0	0	0
Desoxycholate sediment	3.1	0	0	1.7	0.550

*E = optical density in colorimetric assay, according to method given in text.

**These values were not measured directly, but were calculated from the sum of the values for the acetate supernate and sediment.

TABLE 13

Distribution of protein, amylase, and lipase after extraction of microsomes with sodium acetate, phosphate buffer (pH 8.0), and sodium desoxycholate

	Protein	Amylase		Lipase	
	Total E*	Total E*	E/protein E	Total E*	E/protein E
Original microsomes	217	(80)**	(0.37)**	3.82	0.019
Acetate supernatant	90.0	46.7	0.52	0	0
Acetate sediment	96.7	33.4	0.35	3.75	0.039
Phosphate supernatant	42.0	30.0	0.71	0	0
Phosphate sediment	49.8	1.3	0.03	3.26	0.062
Desoxycholate supernatant	12.2	0.7	0.06	0	0
Desoxycholate sediment	38.1	0.8	0.02	2.31	0.067

*E = optical density in colorimetric assay, according to method given in text.

**These values were not measured directly, but were calculated from the sum of the values for the acetate supernate and sediment.

TABLE 14

Distribution of protein, RNA, amylase, and lipase after precipitation of 105,000 x g supernatant fluid at pH 5. Effect of method of preparation of homogenate

	Protein	RNA		Amylase		Lipase	
	Total E*	Total E*	E/protein E	Total E*	E/protein E	Total E*	E/protein E
		Homogenate prepared in 0.88 M sucrose**					
Orig. supernatant	51.7	8.46	0.16	480	9.3	54.0	1.05
pH 5 supernatant	31.6	3.58	0.11	190	6.0	42.3	1.34
pH 5 sediment	16.7	4.43	0.26	248	15	10.5	0.63
		Homogenate prepared in 0.25 M sucrose**					
Orig. supernatant	180	9.12	0.06	(301)†	(1.7)†	-	-
pH 5 supernatant	112	6.64	0.06	72.8	0.65	-	-
pH 5 sediment	26.8	2.32	0.09	228	8.5	-	-

*E = optical density in colorimetric assay, according to method given in text.

**In one experiment, the original homogenate was prepared in 0.88 M sucrose, with subsequent dilution to 0.25 M sucrose (after removal of nuclei, secretory granules, and mitochondria), and in the other the original homogenate was prepared directly in 0.25 M sucrose (see text).

† This value was not measured directly, but was calculated from the sum of the values for the pH 5 supernate and sediment.

The possibility of an association between the amylase and the RNA in the pH 5 sediment was investigated by paper electrophoresis. When electrophoresis was carried out using phosphate buffer at pH 7.4 ($\mu = 0.005$) or at pH 7.0 ($\mu = 0.005$), with or without the addition of sodium chloride to give $\mu = 0.05$, the RNA moved rapidly toward the positive pole, as expected. The amylase activity remained with a protein band that moved slightly toward the negative pole. Apparently its rate of migration was slightly less than the movement of the solvent due to endosmosis.

Preliminary investigation of the extracted sediments with the electron microscope indicates that the acetate removes the contents of the secretory granules and leaves only their outer membrane. The sediments appear to consist largely of various membrane structures. Since the lipase is not extracted from the secretory granule or microsome fractions by sodium acetate or phosphate buffer, it is probable that it is associated with the membranes.

The present results lend further support to our supposition that the amylase found in the microsome fraction is not simply amylase derived from the secretory granules, since the proportion of amylase extracted by sodium acetate and by phosphate buffer at pH 8 is quite different in the two fractions.

The finding that the precipitability of RNA, amylase and protein from the 105,000 x g supernatant fluid at pH 5 differs with the method of preparation, extends our previous demonstration[2,4] that homogenization of pancreas in isotonic (0.25 M) sucrose disrupts the ergastoplasmic complex, producing fragments of differing size and composition. Apparently a large amount of protein is also rendered soluble by homogenization in this medium; this protein is not a complex with RNA nor is it simply amylase. There was actually less amylase present under these conditions, especially in the pH 5 soluble fraction. The RNA is also less easily precipitated at pH 5 after homogenization in 0.25 M sucrose, suggesting a change toward smaller particles. The change in response to pH 5 is not due to depolymerization of the RNA, since the method used for its analysis measures only material insoluble in trichloroacetic acid. However, it is not clear in terms of the morphological components of the cell, just what redistribution of these components is produced by homogenization in isotonic sucrose.

In general, for a given procedure and physiological condition of the pancreas, the proportion of amylase to RNA in the pH 5 sediment has been constant, whereas this ratio has not been constant in the pH 5 soluble material. This fact suggested a physiological association between the amylase and the RNA that precipitated at pH 5. However, a strong binding seems unlikely because the two substances are separated easily by electrophoresis, and in other experiments not reported here, streptomycin has been shown to precipitate most of the RNA from the 105,000 x g supernatant fluid, but not any of the amylase.

In summary, 1% sodium acetate can be used to extract amylase of relatively high specific activity from microsomes and secretory granules, and offers a preliminary step in its purification for metabolic studies using labeled amino acids. Subsequent extraction with phosphate buffer at pH 8 yields another fraction, which also can be purified. Precipitation of the 105,000 x g supernatant fluid at pH 5 yields different fractions depending on the method of preparation of the homogenate; at present the significance of these differences is not clear.

References

1. Laird, A. K., and A. D. Barton. Protein synthesis in pancreas. Quarterly Report of Biological and Medical Research Division, Argonne National Laboratory. ANL-5426, pp. 110-113 (1955).

2. Laird, A. K., A. D. Barton. Progress report: Protein synthesis in pancreas. Intracellular localization of a pancreatic digestive enzyme. Quarterly Report of Biological and Medical Research Division, Argonne National Laboratory. ANL-5518, pp. 131-133 (1956).

3. Laird, A. K., and A. D. Barton. Progress report: Protein synthesis in pancreas. IV. Changes in the intracellular distribution of amylase during the secretory cycle. Semiannual Report of Biological and Medical Research Division, Argonne National Laboratory. ANL-5732, pp. 47-51 (1957).

4. Laird, A. K., and A. D. Barton. Protein synthesis in pancreas. I. Intracellular distribution of amylase. Biochim. et Biophys. Acta 25: 56-62 (1957).

5. Laird, A. K., and A. D. Barton. Protein synthesis in rat pancreas. II. Changes in the intracellular distribution of pancreatic amylase during the secretory cycle. Biochim. et Biophys. Acta, 27: 12-15 (1958).

6. Meyer, K. H., E. H. Fischer, and P. Bernfeld. Sur les enzymes amylolytiques. I. L'isolement de l'α-amylase de pancreas. Helv. Chim. Acta 30: 523-585 (1951).

7. Lowry, O. H., N. J. Rosebrough, A. L. Farr, and R. J. Randall. Protein measurement with the Folin phenol reagent. J. Biol. Chem. 193: 265-275 (1951).

8. Seligman, A. M., and M. M. Nachlas. The colorimetric determination of lipase and esterase in human serum. J. Clin. Invest. 29: 31-36 (1950).

9. Schneider, W. C. Phosphorus compounds in animal tissues. I. Extraction and estimation of desoxypentose nucleic acid and of pentose nucleic acid. J. Biol. Chem. 161: 293-303 (1945).

PROGRESS REPORT: PROTEIN SYNTHESIS IN PANCREAS

VI. Changes in the secretory granule fraction and the microsome fraction that accompany physiological changes in the pancreas

A. D. Barton and Anna Kane Laird

The secretory granule and microsome fractions were isolated[1] from the pancreas of rats starved overnight (resting pancreas), and from rats that had been starved overnight and then treated with pilocarpine 3 hr before sacrifice, (during early stages of resynthesis of digestive enzymes following the secretion induced by pilocarpine). Fifteen min before sacrifice, each animal received phenylalanine-2-C^{14} (10μc in 0.2 ml saline solution) by intraperitoneal injection. Each particulate fraction was extracted first with 1% sodium acetate at pH 6.8 and then with 0.01 M phosphate at pH 8.0.[2] Each acetate extract, phosphate extract, and phosphate residue was assayed for total protein,[3] total amylase[4] and total radioactivity. The values found are given in Tables 15 and 16.

Previous studies[1,5] indicated that the pancreatic secretion induced by pilocarpine results in a loss of secretory granule material from the pancreas. The present experiments show that the pilocarpine treatment causes a loss of protein from the acetate and phosphate extracts, but not from the phosphate residue of the secretory granule fraction. The pilocarpine treatment produced little change in the total protein of the microsome fraction, but did result in a decrease of protein in the acetate and phosphate extracts and an increase in the protein of the phosphate residue of the microsome fraction.

Treatment with pilocarpine produced a more extensive loss of amylase than of total protein, with the result that the amylase activity per unit of protein decreased in all of the fractions studied. This effect was least in the acetate extract from the microsome fraction.

In both cases, the total radioactivity in the secretory granule fraction was only about 2% of that found in the microsome fraction, and this small amount of radioactivity was confined to the phosphate extract. Preliminary studies with the electron microscope have shown that the extraction with acetate removes the contents of the secretory granules and leaves only their surface membranes. Since the acetate extract contained no radioactivity, it is evident that 15 min after administration of the phenylalanine-2-C^{14}, the contents of the secretory granules still were not labeled.

TABLE 15

Distribution of protein and amylase after extraction of the secretory granule fraction and the microsome fraction from rat pancreas with sodium acetate and with phosphate. Effect of pilocarpine treatment after starvation overnight

	Acetate extract			Phosphate extract			Phosphate residue		
	Protein*	Amylase**	Am/Pr	Protein	Amylase	Am/Pr	Protein	Amylase	Am/Pr
	Secretory granule fraction								
Starved	107	22.6	0.221	54	12.7	0.236	26	0.25	0.009
Pilocarpine-treated	37	3.15	0.084	37	3.95	0.108	29	0.11	0.004
	Microsome fraction								
Starved	91	7.62	0.084	155	7.79	0.050	181	5.85	0.032
Pilocarpine-treated	52	3.80	0.074	106	1.72	0.016	248	4.54	0.018

*Protein; total optical density as measured by the colorimetric method of Lowry et al. (3)

**Amylase activity; total optical density as measured by the colorimetric method of Meyer et al.(4)

TABLE 16

Distribution of protein and radioactivity after extraction of the secretory granule fraction and the microsome fraction from rat pancreas with sodium acetate and with phosphate. Effect of philocarpine treatment after starvation overnight

	Acetate extract			Phosphate extract			Phosphate residue		
	Protein*	Radio-activity**	Ra/Pr	Protein	Radio-activity	Ra/Pr	Protein	Radio-activity	Ra/Pr
	Secretory granule fraction								
Starved	107	0	0	54	1440	27	26	0	0
Pilocarpine-treated	37	0	0	37	2160	59	29	0	0
	Microsome fraction								
Starved	91	6,800	75	155	42,000	270	181	31,000	170
Pilocarpine-treated	52	31,000	590	106	19,000	180	248	45,000	190

*Total protein; total optical density as measured by the colorimetric method of Lowry et al.(3)

**Total radioactivity (total cpm).

In both cases, all subfractions of the microsome fraction were labeled. The subfraction showing the highest specific radioactivity was the acetate extract from the animals treated with pilocarpine. In these animals, the acetate extract was much more highly labeled than the phosphate extract. In the animals that were starved overnight, the phosphate extract was heavily labeled but the acetate extract contained relatively little label. The pilocarpine treatment produced little change in the labeling of the phosphate residue of the microsome fraction.

It is evident that extraction of the secretory granule fraction and the microsome fraction with acetate and phosphate yields subfractions which differ from one another in metabolic activity. Further study of these subfractions and of enzymes isolated from them is expected to yield information concerning the elaboration and secretion of digestive enzymes by the pancreas.

References

1. Laird, A. K., and A. D. Barton. Protein synthesis in rat pancreas II. Changes in the intracellular distribution of pancreatic amylase during the secretory cycle. Biochem. et Biophys. Acta 27: 12-15 (1958).

2. Laird, A. K., and A. D. Barton. Progress report: Protein synthesis in pancreas V. Fractional extraction and precipitation of pancreatic enzymes. This report, p. 55.

3. Lowry, O. H., N. J. Rosebrough, A. L. Farr, and R. J. Randall. Protein measurement with the Folin phenol reagent. J. Biol. Chem. 193: 265-275 (1951).

4. Meyer, K. H., E. H. Fischer, and P. Bernfeld. Sur les enzymes amylolytiques. I. L'isolement de l'α-amylase de pancreas. Helv. Chim. Acta 30: 523-585 (1951).

5. Laird, A. K., and A. D. Barton. Progress report: Protein synthesis in pancreas IV. Changes in the intracellular distribution of amylase during the secretory cycle. Semiannual Report of Biological and Medical Division, Argonne National Laboratory. ANL-5732, pp. 47-51 (1957).

AN ELECTRON MICROSCOPE STUDY OF MITOSIS IN THE PROTOZOAN HYPOTRICH STYLONYCHIA

L. E. Roth

The study of mitotic events by electron microscopy has been greatly retarded by inability to select dividing cells among the relatively much greater proportion of cells that are not in division. The protozoa, even though their micronuclear division is a specialized mitosis, offer the possibility of isolation and observation of selected cytological events and therefore provide choice material for such observations. In addition, dividing ciliate protozoa must also apportion their macronuclear contents nearly equally between daughters and also form a rather large number of cilia near the time of division. Therefore, dividing ciliates offer the possibility of study of the three events, micronuclear mitosis, macronuclear division, and ciliary formation.

The organism Stylonychia, which was chosen to begin this study, possesses two macronuclei in interphase (N in Figure 17 A) which are easily visible under 100 X enlargement; in preparation for division into two daughter organisms, these nuclei fuse, and divide once, and then a second time (N in Fig. 17 B). These easily recognizable events allow recognition and categorization of division stages. A mass culture of organisms was fixed by standard osmium tetroxide methods and embedded in methacrylate; single organisms were then selected, sectioned and observed under the electron microscope.

The macronucleus in interphase consists of an irregular network of chromatin (C in Figure 17 E) with interspersed nucleolar spheres (NL in Figure 17 E) except when the reorganization bands are present during deoxyribose nucleic acid synthesis. At mitosis, the macronucleus pinches in two, showing a passive alignment of chromatin (C in Figure 17 D) and the appearance of numerous, parallel, fine filaments at the point of division (F in Fig. 17 D). The nuclear membrane remains intact in all cases thus far observed.

The interphase micronucleus is characterized by 40- to 50-mμ chromatin fibers which are irregularly connected to a network. In mitosis, the membrane is reduced to disconnected remnants (M in Figure 17 E); the chromosomes are cylindrical masses which lack any chromosomal membranes and which are run together at many points (MC in Figure 17 E). Fine filaments with a low density center and a 3-to 4-mμ diameter are seen in most stages and probably represent deoxyribose nucleoprotein complexes.

Newly-formed ciliary groups may be detected by light microscope observations, so that such organisms may be chosen for sectioning (unlettered arrows in Figures 17 B and C). Newly-formed cilia usually possess two central (in addition to nine peripheral) fibrils in their bases while others do not. Numerous centriole-like structures are present in the cytoplasm in groups of four to six but are not necessarily close to other cilia; they often lack central fibrils and may also have missing peripheral fibrils (unlettered arrows in Figure 17 F).

These lines of study are being continued in this and other organisms.

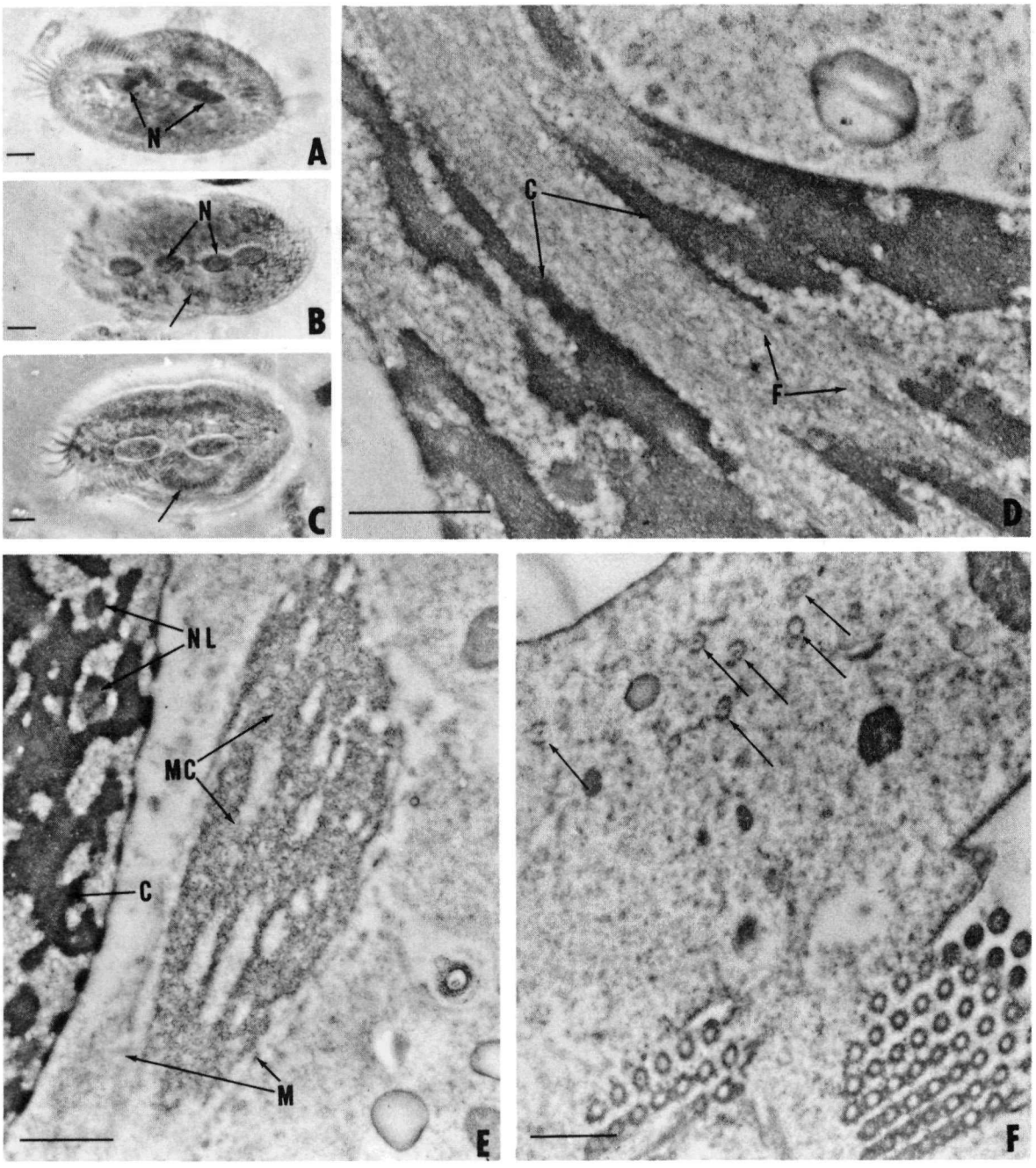

Figure 17. Scale markers on Figures 17 A through C represent 10 μ and on D through F represent 1μ.

A. Interphase organism.
B. Early division stage.
C. Earlier division stage.
D. Macronucleus at point of division.
E. Mitotic micronucleus with a small portion of the macronucleus which has the interphase morphology.
F. Ciliary groupings and centriole-like structures grouped in the cytoplasm.

ELECTRON MICROSCOPE STUDIES OF THE STRUCTURE OF THE SPINDLE, NUCLEUS AND CHROMOSOMES

Miguel Mota*

This investigation is carried on with the ultimate objective of obtaining more detailed information on the structure of the centromere and spindle and on their relationship, as a contribution to the study of the anaphase movement. The feasibility of the work is assumed on the basis of previous studies by Sedar and Wilson,(1) Nebel,(2) and others that show that the spindle at least can be studied with fair success under the electron microscope.

The work includes both plant and animal material. Vicia faba and Secale cereale root tips were pretreated with 0.002 M oxyquinoline solution to clear and render more visible the structure of the centromere, and fixed in Dalton fixative at pH 7.2. Embedding and sectioning followed the usual standard techniques. Mouse testis both from untreated and X-irradiated animals is also being studied by the same method using Dalton fixative at pH 6.5 and 7.2.

The ultimate problem as described requires, however, the observation of cells in a particular stage and sectioned through certain limited regions in the cell. A satisfactory technique has not yet been developed to concentrate the desired material in the grids, and consequently it has been necessary to observe relatively large amounts of material without the appropriate stages. For that reason it seemed desirable to use this material to study structures other than spindle and centromere.

In this respect two observations seem to be worth reporting. They concern the boundary between the nucleolus and the nucleus. In Secale cereale there is a diffuse region, apparently constituted by nucleolar material radiating from the nucleolus into the nucleus or, at least, into a clearer zone of nuclear material surrounding the nucleolus (Figure 18). There seems to be evidence enough to state that this is not caused by shrinkage of the material during fixation, embedding or sectioning.

In Vicia faba such a structure is not apparent or, at least, not as conspicuous as in Secale; the nucleolus appears to be surrounded by a large number of clear vesicles which are also seen spread over the entire nucleus (Figure 19).

These two aspects are believed to be relevant to the study of the relationship between nucleolus and nucleus and chromosomes.

---

*Resident Research Associate from Estação Agronómica Nacional, Sacavem, Portugal.

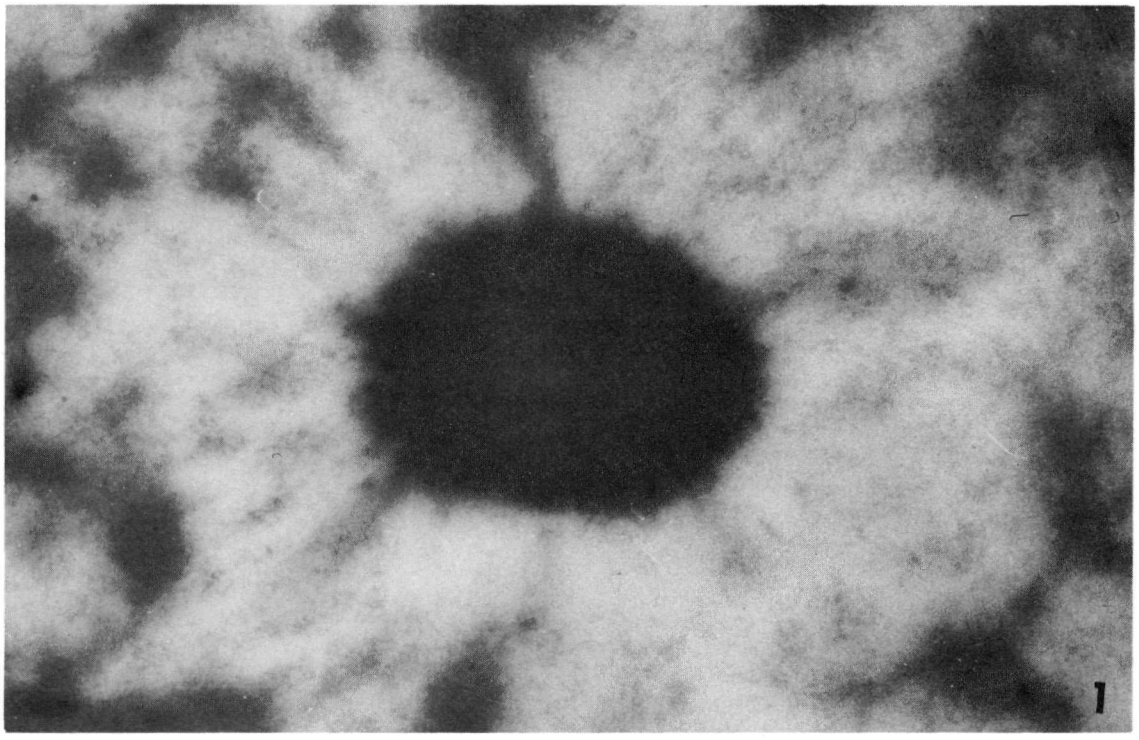

Figure 18. Nucleolus in Secale cereale root tip.

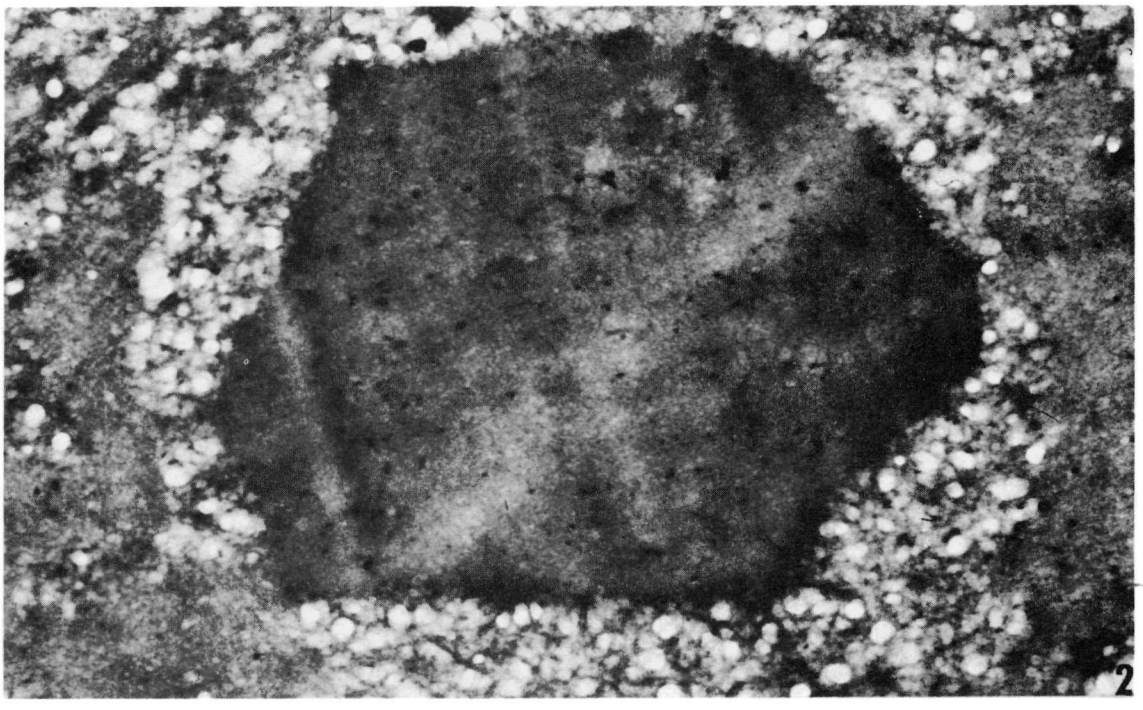

Figure 19. Nucleolus in Vicia faba root tip.

References

1. Sedar, A. W. and Wilson, D. F. Electron microscopic studies on the normal and colchicinized mitotic figures of the onion root tip (Allium cepa). Biol. Bull. 100:107-115 (1951).

2. Nebel, B. R. Unpublished observations.

SURVIVAL OF LAF_1 MICE UNDER DURATION-OF-LIFE EXPOSURE TO Co^{60} GAMMA RAYS AT RATES OF 24 TO 1650 r PER DAY

George A. Sacher, Douglas Grahn, and Joan M. Gurian

The exposure of various mouse strains and hybrids to daily dosages of Co^{60} γ-rays is one of the basic experimental procedures in the Gamma Ray Toxicity Program. One objective of this interrelated set of experiments is to determine the survival times at a number of closely spaced daily dosage levels and to correlate the mortality behavior with the histologic, hematologic and pathologic changes in samples from the irradiated groups. Another objective is to compare the responses of several mouse strains and hybrids exposed to a wide range of daily dosages. In the present report we present the mean after- survival times and standard deviations for male and female LAF_1 mice and examine the resulting dose-effect curves. Comparison of lethality data with hematologic and histologic responses will be made in subsequent reports.

Methods

The LAF_1 mice were received from Jackson Laboratories at about 7 weeks of age and held until they reached 100 days of age. The exposure groups were set up over a period of approximately 2 years, and each dosage level was built up from several replications. The number of replications is tabulated for each dose level in Table 17. In each replication, equal numbers of male and female mice were distributed into cylindrical plastic cages, 3 mice to a cage. The cages were positioned on aluminum racks in the Low-Level Gamma Exposure Room[1] and received exposure from a Co^{60} source which is raised into the room each night from a storage pit beneath the floor. The exposure period varies from 12 to 15 hr, exposure time is increased at regular intervals to compensate for the radioactive decay of Co^{60}, and the Co^{60} source is replaced as necessary to keep the exposure time within the limits of 12 to 15 hours.

Results

Table 17 gives for each sex and dose level the mean after-survival time (MAS), and standard deviation (SD), number of animals, number of replications and standard error of the MAS.

The survival data of Table 17 are presented in Figure 20 in terms of a quantity called the lethality cumulant, defined by

$$C_L = \frac{1}{I}\left(1 - \frac{t^*}{t_0}\right)$$

in which I is the daily dose in r/day, t* is the MAS at daily dose I, and t_0 is the MAS of control mice. A derivation of this relation has been given previously.[2,3] The cumulant curve, formed by plotting C_L versus t*, gives the presumptive time-course of lethal radiation injury, subject to certain assumptions that are discussed in the references cited above.

TABLE 17

Mean after-survivals (MAS), standard deviations (SD), standard errors (SE), number of individuals (N_i), and number of replications (N_r), for male and female LAF_1 mice exposed to γ-rays daily for the duration of life beginning at 100 days of age

I, r/day	Male		N_i	N_r	Female	
	MAS ± SE, days	SD, days			MAS ± SE, days	SD, days
0	471 ± 18	216	144	*	634 ± 13	158
6	462 ± 18	155	75	*	525 ± 14	122
12	371 ± 10	114	126	*	417 ± 10	115
24	251 ± 6.4	86.1	183	12	273 ± 6.5	87.7
32	206 ± 4.5	54.3	150	10	223 ± 4.4	53.5
43	149 ± 3.5	42.9	150	10	155 ± 3.1	38.2
49	127 ± 2.1	24.3	135	9	134 ± 2.3	26.2
56	102 ± 2.5	27.5	120	8	104 ± 2.1	23.6
64	80.6 ± 1.9	18.6	105	7	86.1 ± 2.0	20.2
74	64.5 ± 1.8	18.2	105	7	65.8 ± 1.3	13.6
85	51.8 ± 1.1	11.3	105	7	50.4 ± 1.0	10.1
97	41.4 ± 0.52	5.32	105	7	41.7 ± 0.61	6.24
125	33.9 ± 0.45	4.65	105	7	31.2 ± 0.52	5.31
145	29.6 ± 0.52	5.34	105	7	24.1 ± 0.38	3.90
170	22.0 ± 0.45	4.57	105	7	20.0 ± 0.25	2.55
220	16.5 ± 0.18	1.85	75	5	15.8 ± 0.18	1.88
270	14.3 ± 0.14	0.77	30	2	14.7 ± 0.18	1.01
330	13.3 ± 0.21	1.13	30	2	13.3 ± 0.18	1.00
410	12.2 ± 0.19	1.03	30	2	12.5 ± 0.23	1.27
500	11.0 ± 0.18	0.98	30	2	11.3 ± 0.20	1.08
610	9.33 ± 0.16	0.89	30	2	9.23 ± 0.19	1.07
750	7.23 ± 0.14	0.70	24	2	6.83 ± 0.11	0.55
1100	5.85 ± 0.08	0.40	24	2	5.48 ± 0.07	0.35
1650	5.40 ± 0.10	0.47	24	2	5.06 ± 0.08	0.40

*Incomplete

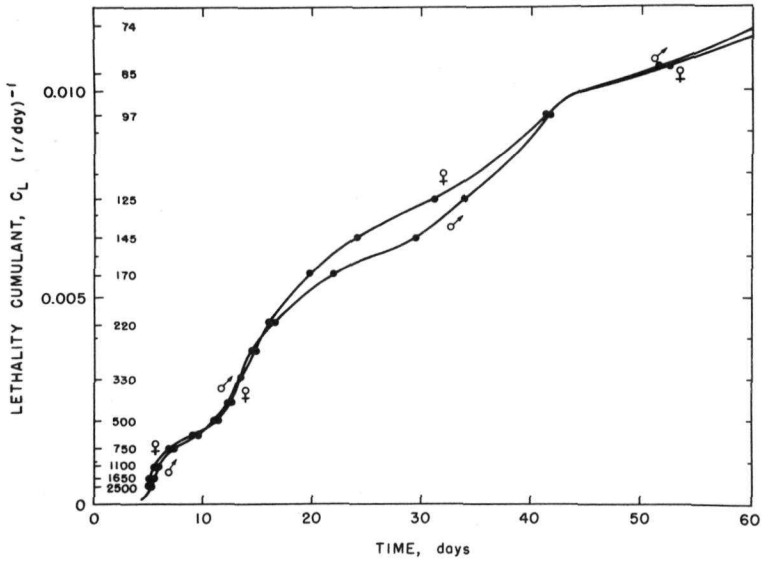

Figure 20. Cumulant functions for male and female LAF_1 mice exposed to Co^{60} γ-rays daily for the duration of life, beginning at 100 days of age. For most of the course of the function the curves for the two sexes run so close together that they cannot be resolved. We have therefore indicated, at each bend of the curve, which sex lies above and which below. Reversals occur only at 10.5, 15 and 45 days. Thus, even the small sex differences at early times are probably physiologically significant.

The cumulant curves for male and female LAF_1 mice for the first 60 days are shown in Figure 20. In view of the standard errors of the individual points, the three "waves" are significant deviations from a steady (uninflected) upward trend. These components reproduce, in location and in magnitude, the components observed in the original study on the ABC male mouse.(2) The form of the cumulant curve is a genetically determined characteristic, for genetically related lines have the strongest resemblances,(4) and the differences between species are greater than the strain differences within species.(3,4)

The difference between the sexes that is observed between the 15th and 40th days has not been described previously. In this period the female is significantly more sensitive than the male. At immediately preceding and succeeding times the differences between the sexes are not significant. At lower dose rates and much longer survival times (Table 17) a complex pattern of sex differences again appears. These will not be discussed here, because the data at 12, 6 and 0 r/day are not yet complete.

Discussion

The major characteristics of the design of the daily dose experiment, i.e., the provision of a large number of closely-spaced dose rates and of fairly large numbers of mice at each dose rate, were dictated by the nature of one of the hypotheses that we proposed to investigate. This hypothesis states, briefly, that the course of radiation mortality in homogeneous animal populations follows closely the average course of physiologic injury in the population. It is apparent to even casual observation that physiologic injury produced by ionizing radiations is of many kinds, and that each kind has its characteristic time-course of appearance and disappearance. If the above hypothesis is correct, the radiation dosage-survival curve should likewise be of a polyphasic nature; and furthermore, one should be able to relate each individual phase of lethality to a corresponding mode of physiologic injury. This hypothesis needs no further verification at the level of physiologic observation of the effects of single doses, for at least two distinct modes of death, the "intestinal" and the "hematopoietic," are universally recognized as being produced by appropriate single doses, and there is evidence also for still other modal death times associated with other pathology.

In spite of this consensus about the multicausal nature of radiation lethality, the most widely accepted mathematical treatment of the subject takes no account of these facts. The theory in question[5] states that "injury" appears immediately upon exposure and disappears, or recovers, exponentially. Sacher in 1950 presented data on survival under daily exposure[2] which rejected the hypothesis that radiation injury and recovery can be adequately described by means of a single exponential term. The subsequent history of the subject indicates that this implication was not properly appreciated.

The LAF_1 data presented here should be sufficient to dispose of the issue permanently. It is inescapably evident that the data of Table 17 cannot be fitted with a single exponential plus a constant term. The form of the cumulant curve in Figure 20 indicates that at least 7 parameters are needed to fit the cumulant curve for the first 100 days. The sex differences in LAF_1 mice and the nature of the strain and species differences referred to above further indicate that several, and probably all, of these parameters vary independently among species and strains. These observations are in perfect accord with the position that we have consistently maintained about the nature of mammalian radiation lethality.

In the ordinary case, the replacement of a two-parameter theory by a 7-parameter theory would be considered the inevitable historical development toward more complicated and sophisticated models. In the present instance, the introduction of a 7-parameter model is a real simplification, because there is every reason to believe that these parameters

will be identified with the parameters of physiologic injury processes. Lethality will thereby become an understandable and predictable consequence of physiologic injury. The gain in conceptual unification should more than compensate for the loss of a specious mathematical simplicity.

References

1. Sacher, G. A., D. Grahn, S. Lesher, and K. Hamilton. The gamma-ray toxicity program; calibration and equipment. Quarterly Report of the Biological and Medical Research Division, Argonne National Laboratory. ANL-5378, pp. 7-10 (1955).

2. Sacher, G. A. Survival of mice under duration-of-life exposure to X-rays at various rates. In Biological Effects of External X and Gamma Radiation, Part 2, R. E. Zirkle, ed. TID-5220, Washington,Dept. of Commerce, Office of Technical Services (1956).

3. Sacher, G. A. A comparative analysis of radiation lethality in mammals exposed at constant average intensity for the duration of life. J. Natl. Cancer Inst. 15: 1125-1144 (1955).

4. Grahn, D. The genetic factor in acute and chronic radiation toxicity. Proceedings Int. Conf. on Peaceful Uses of Atomic Energy, Geneva (1958). In press.

5. Blair, H. A. A formulation of the injury, life span, dose relations for ionizing radiations. I. Application to the mouse. University of Rochester Report UR-206 (1952). II. Application to the guinea pig, rat and dog. UR-207 (1952).

PROGRESS REPORT: DEUTERIUM OXIDE INTOXICATION IN RATS

I. Effect of D_2O *in vivo* and *in vitro* on the Uptake of p-Aminohippurate by Rat Kidney Slices

John F. Thomson and Florence J. Klipfel

We previously reported that both the glomerular filtration rate and the renal plasma flow were markedly reduced in rats drinking heavy water.(1) In view of the rapidity with which kidney function returned to normal after the drinking water was changed from D_2O back to H_2O, and since there was no evidence of changes in a number of enzyme systems of the kidneys of D_2O-treated animals, we felt that the change in physiologic function was not attributable to a specific kidney lesion, but was possibly the result of endocrine inbalance.

We have obtained additional confirmation of the lack of tubular damage in rats by the observation that the uptake of sodium p-aminohippurate (PAH) by slices of kidney is the same in rats drinking heavy water as in normal animals. However, D_2O in high concentration has an inhibitory effect *in vitro* on the uptake of PAH.

Methods

The method of Cross and Taggart,(2) modified by Mendelsohn,(3) was used for measuring the uptake of PAH. Between 150 and 250 mg of kidney slices, consisting principally of cortical tissue, were used in each Warburg flask. The flasks were incubated for 1 hr at 25°C, with oxygen as the gas phase, in the presence of D_2O in concentrations ranging from 0 to 100%. Acetate was used as the substrate.

For the study of the effects of D_2O *in vivo*, 6 rats were given drinking water containing 50% D_2O for 26 days. The average concentration of D_2O in the plasma at the time of sacrifice was 32%.* One rat died before it could be used, and the other five were obviously sick. The capacity of slices from the kidneys of these rats to concentrate PAH was measured in an incubation medium containing 27% D_2O as well as in the control medium (no D_2O).

Results

Figure 21 shows the effect of D_2O *in vitro* on the oxygen consumption and PAH uptake by kidney slices suspended in varying concentrations of

---

*The D_2O analyses were carried out by Dr. Henry Crespi of the Chemistry Division.

D_2O.* The rate of oxygen consumption decreased linearly with increasing concentration of D_2O, 100% D_2O producing 18% inhibition. The incorporation of PAH was markedly inhibited by high concentrations of D_2O, the ratio of concentration of PAH in the tissue slice to that in the medium (T/M) dropping to 37% of the control level in the presence of 100% D_2O.

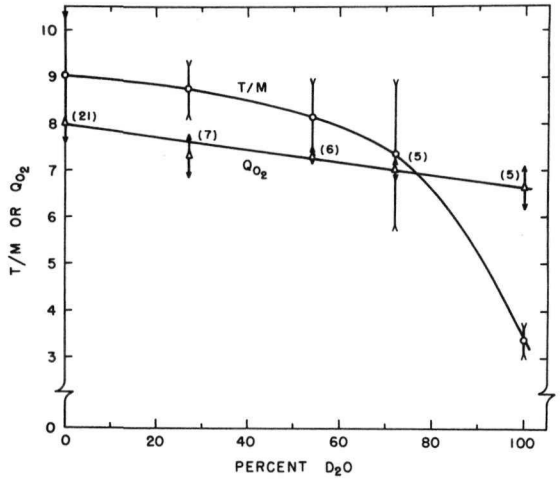

Figure 21

Effect of D_2O *in vitro* on oxygen consumption and PAH uptake by slices of rat kidney. Oxygen consumption is measured as μ1/hr/mg dry weight, PAH uptake as the ratio of concentration in the tissue slice (T) to that in the suspending medium (M) at the end of the 1-hr incubation period. Numbers in parentheses indicate the number of animals used at each point; vertical lines represent standard deviations.

The effects of D_2O *in vivo* on oxygen consumption and PAH uptake are shown in Table 18. The oxidation of acetate occurred equally rapidly in slices from both the normal and the D_2O-treated animals, both in D_2O and in 27% H_2O. The uptake of PAH was actually greater in the kidney slices from the treated rats, although the difference was not statistically significant. There seemed to be a positive correlation between the D_2O concentration in the plasma and the T/M ratio observed in the slices.

Table 18

Effect of D_2O *in vivo* on oxygen consumption and PAH uptake by slices of rat kidney

	Control	D_2O-treated
Days on D_2O	-	26
Final plasma D_2O, %	-	32.3 ± 1.8
Average weight change, g	+35.6	-8.4
Range	(+27 to +54)	(-18 to +5)
Kidney weight, g	1.47	1.44
Range	(1.25 - 1.77)	(1.24 - 1.66)
Q_{O_2} acetate (μ1/hr/mg dry weight)		
In H_2O	7.85 ± 0.29	7.90 ± 0.29
In 27% D_2O	7.18 ± 0.37	6.74 ± 0.55
T/M ratio		
In H_2O	9.73 ± 1.41	10.83 ± 2.32
In 27% D_2O	8.81 ± 1.01	10.04 ± 2.38

Five animals per group. Values presented are averages with standard deviations or ranges.

*The concentrations of D_2O are actually a few per cent lower than indicated, since no correction has been made for dilution by the exchangeable H in the tissue slices.

References

1. Thomson, J. F., and F. J. Klipfel. Changes in renal function in rats drinking heavy water. Proc. Soc. Exptl. Biol. Med. 97: 758-759 (1958).

2. Cross, R. J., and J. V. Taggart. Renal tubular transport: accumulation of p-aminohippurate by rabbit kidney slices. Am. J. Physiol. 161:181-190 (1950).

3. Mendelsohn, M. L. Response of PAH transport and oxygen consumption in the rabbit kidney slice to graded doses of X-ray and several metabolic inhibitors. Am. J. Physiol. 180:599-604 (1955).

PROGRESS REPORT: DEUTERIUM OXIDE INTOXICATION IN RATS

II. Arginase and Transaminase in Livers of D_2O-Treated Rats

John F. Thomson and Florence J. Klipfel

Certain observations have led us to suggest that one of the reasons for the toxicity of D_2O to rats is a disturbance in adrenal function.[1] The changes in concentrations of a number of components of blood, such as glucose, NPN, urea, and plasma protein, are similar to those seen in adrenalectomized animals. In addition, in D_2O-treated rats, the adrenals increase in size by as much as 50%. Furthermore, hypophysectomized rats, with atrophic adrenals, show toxic effects at much lower levels of D_2O than do normal rats.[2]

If the D_2O-treated rats actually behaved like adrenalectomized animals, one would expect that the concentrations of certain enzymes that are known to decrease after adrenalectomy, such as arginase[3] and transaminase,[4] would also be lowered by D_2O. That such a decrease does not take place is shown by the experiments reported here.

Methods

Rats were given 50% D_2O as drinking water, and were sacrificed when their plasma D_2O level was about 30%. Arginase was assayed by the method of Roberts.[5] Glutamic-alanine and glutamic-aspartic transaminases were measured according to the procedure of Brin et al.;[6] the former is assayed by determination of alanine formed from glutamate and pyruvate, the latter by estimation of oxalacetate formed from aspartate and α-ketoglutarate.

Results

The data on arginase activity are presented in Table 19. It is clear that there is a slight but not statistically significant increase in the arginase activity of rat liver. A similar change was observed with glutamic-aspartic transaminase (Table 20), although the activity of glutamic-alanine transaminase was decreased by 10%.

We had suggested earlier[1] that (a) the D_2O-treated rat may have a higher requirement for adrenal hormones than can be met even by a hyperplastic adrenal cortex; (b) the requirements may be unaltered but the production of adrenal hormones may be inhibited in deuterated tissues;

or (c) the metabolic processes of the rat may be so altered by deuteration that no additional amount of adrenal hormones would permit the animal to adapt to the change in internal environment produced by D_2O. It would seem that the second of these possibilities can be eliminated.

TABLE 19

Arginase activity in livers of D_2O-treated rats

	Control	D_2O-treated
Number of rats	6	5
Days on 50% D_2O	-	32
Final plasma D_2O, %	-	31.5
Range		(31.1 - 31.7)
Weight change, g	+27	-9
Range	(+25 to +30)	(-24 to +12)
Arginase activity*	461 ± 21	496 ± 75

*μM arginine destroyed per 10 min per mg N, averages and standard deviations.

TABLE 20

Transaminase activity in livers of D_2O-treated rats

	Control	D_2O-treated
Number of rats	9	7
Days on 50% D_2O	-	26
Final plasma D_2O, %	-	31.7
Range		(29.5 - 34.0)
Weight change, g	+42	+6
Range	(+22 to +61)	(-13 to +28)
Blood glucose, mg %	80	62
Range	(69 - 91)	(45 - 83)
Blood urea, mg %	18.9	44.3
Range	(13.8 - 21.4)	(28.7 - 58.0)
Transaminase*		
Alanine	24.9 ± 1.1	22.5 ± 1.8
Oxalacetate	67.8 ± 9.9	80.4 ± 9.6

*μM substrate produced per hour per g N, averages and standard deviations.

References

1. Thomson, J. F., and F. J. Klipfel. Changes in renal function in rats drinking heavy water. Proc. Soc. Exptl. Biol. Med. 97: 758-759 (1958).

2. Katz, J. J., H. L. Crespi, R. J. Hasterlik, J. F. Thomson, and A. J. Finkel. Some observations on biological effects of deuterium, with special reference to effects on neoplastic properties. J. Natl. Cancer Inst. 18: 641-659 (1957).

3. Thomson, J. F., and E. M. Moss. Effect of adrenalectomy on tryptophan peroxidase, adenosine deaminase, and arginase content of regenerating rat liver. Proc. Soc. Exptl. Biol. Med. 89: 230-233 (1955).

4. Brin, M., and R. M. McKee. Effects of X-irradiation, nitrogen mustard, fasting, cortisone, and adrenalectomy on transaminase activity in the rat. Arch. Biochem. Biophys. 61: 384-389 (1956).

5. Roberts, E. Estimation of arginase activity in homogenates. J. Biol. Chem. 176: 213-222 (1948).

6. Brin, M., R. E. Olson, and F. J. Stare. Metabolism of cardiac muscle. VIII. Pyridoxine deficiency. J. Biol. Chem. 210: 435-444 (1954).

EFFECT OF X-RADIATION ON THE INTRACELLULAR DISTRIBUTION OF CYTOCHROME OXIDASE IN THE RAT THYMUS

John F. Thomson and Florence J. Klipfel

After total-body irradiation in the LD_{50} range, there occurs in the thymus of rats extensive cellular destruction, which is reflected by a marked decrease in the concentration of deoxyribose nucleic acid; within 48 hr after exposure, the concentration on a dry weight basis is reduced to one-third of normal.(1) At the same time, however, the concentration of certain enzymes such as cytochrome oxidase and succinic dehydrogenase is unchanged,(1) while that of adenosine triphosphatase (ATPase) increases considerably.(2) It was thus of interest to see whether any changes took place in the intracellular distribution of these enzymes.

The use of gradients containing polyvinylpyrrolidone (PVP) and sucrose has enabled us to apply the technique of gradient centrifugation to the study of the thymus.(3)

Methods

The rats used in these studies were Sprague-Dawley females, 60 to 70 days old. They were exposed to 600 r X-radiation, delivered at a rate of 200 r/min. One, two, and three days after exposure the animals were killed and their thymuses homogenized in 8.5% sucrose containing 5% PVP. To obtain sufficient tissue it was necessary to pool two thymuses on the second day, and three or four on the third day. The homogenates of thymus were layered over PVP-sucrose gradients(3) and centrifuged in a Lourdes centrifuge with a swinging cup rotor, operated in a cold room at 1°C.

For the studies on cytochrome oxidase, the tubes were centrifuged for 1 hr at 10,000 rpm (14,900 g); under these conditions the majority of particles containing cytochrome oxidase (0.3 μ diameter) traveled halfway down the tube. Since the major portion of ATPase is associated with smaller particles (0.1 μ), the tubes used in the experiments with this enzyme were centrifuged for 3 hr at 12,000 rpm (21,500 g).

After centrifugation, successive layers of the solution in the tubes were removed and assayed for the enzymes in question. Distribution curves in terms of particle size were prepared as described elsewhere.(4)

Results

It is apparent from Figure 22 that the distribution of cytochrome oxidase was appreciably altered by radiation. The principal change took place within the first 24 hr after exposure, since the differences among the curves obtained 1, 2, and 3 days after irradiation are not significant. The shift in particle size associated with maximum activity from 0.32 μ to 0.28-0.30 μ after irradiation has been consistently observed.

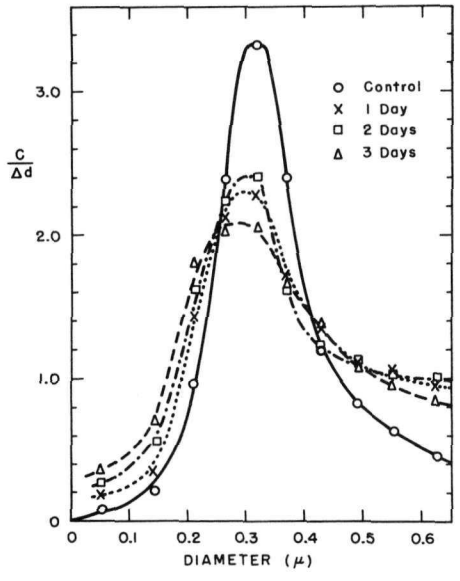

Figure 22

Intracellular distribution of cytochrome oxidase in normal and X-irradiated rats, 1, 2, and 3 days after exposure to 600 r total-body irradiation. The control curve represents the average of three experiments with one rat per experiment; the other curves are based on two experiments involving one, two, and three rats per experiment, respectively, for the 1-, 2-, and 3-day curves. $C/\Delta d$ represents the fraction of enzyme concentration found in a particular zone divided by the difference between extremes of particle sizes predicted for the zone.

The experiments with ATPase have been less extensive. Although the activity 2 days after irradiation was 3 times normal, the distribution curve appeared essentially unchanged. However, under the conditions of preparation (centrifugation for 3 hr at 12,000 rpm) an appreciable increase in temperature occurred which may have altered the distribution pattern of the enzyme in both irradiated and control tissues. It is hoped that more satisfactory arrangements can be made in the future for centrifugation under the conditions imposed by these experiments.

References

1. Thomson, J. F., W. W. Tourtellotte, and M. S. Carttar. Some observations on the effect of gamma radiation on the biochemistry of rat thymus. Proc. Soc. Exptl. Biol. Med. 80: 268-272 (1952).

2. DuBois, K. P., and D. F. Petersen. Adenosine triphosphatase and 5-nucleotidase activity of hematopoietic tissues of irradiated animals. Am. J. Physiol. 176: 282-286 (1954).

3. Thomson, J. F., and F. J. Klipfel. Fractionation of rat liver particulates using polyvinylpyrrolidone gradients. Exptl. Cell Research 14: 612-614 (1958).

4. Thomson, J. F., and E. T. Mikuta. Enzymatic activity of cytoplasmic particulates of rat liver isolated by gradient centrifugation. Arch. Biochem. Biophys. 51:487-498 (1954).

THE DEPENDENCE OF ACUTE AND SUBACUTE RADIOSENSITIVITY ON AGE IN THE LAF_1 MOUSE

George A. Sacher, Douglas Grahn and S. Lesher

The investigation of survival of mice under duration-of-life exposure to a wide range of daily dosages is reported elsewhere in this issue.[1] In that investigation, exposure was begun at a standard age of 100 days. The present report summarizes the results of an experiment in which 5 daily dosages, ranging from 170 to 43 r/day, were administered to LAF_1 mice at 8 different starting ages ranging from 100 to 850 days of age.

The experimental conditions were identical with those in the report cited above. Mean after-survivals (MAS) and standard deviations (SD) are tabulated in Table 21. The data at the highest ages are still not complete, and it will be another year before the requisite number of animals have reached the assigned starting ages. The data at 100 days of age are also part of the daily-dose survival study cited above.

Figure 23 represents one way of presenting the age-dependence relations. In this figure, the MAS for a given daily dose and starting age is expressed as a percentage of the MAS for that daily dose at 100 days of age. Data for the two sexes are combined. There is an age-dependence curve for each of the 5 daily dosages employed.

It is evident that the curves of relative resistance vs. age are quite different in form at the different daily dosages used. At 170 r/day, resistance increases markedly until 400 days of age, and then falls at a roughly constant rate. At 43 r/day, resistance decreases from the beginning, slowly at first and then more rapidly with increasing age. At all ages except 400 days, the relative resistance values for the 5 daily dosages are in the rank order of the daily dosages. In view of the sample sizes employed, the deviations from this consistent rank ordering at 400 days will probably not prove to be significant.

The age-dependence curve is also being determined for the single-dose 30-day LD_{50}. Data available thus far indicate that this curve resembles the age-dependence curve at 170 r/day.

Discussion

It would be premature to discuss at this time the reasons for the observed interaction between daily dose and starting age. At the lower daily dosages, the MAS of irradiated groups is an appreciable fraction of the after-expectation of controls, and especially so at the more advanced

TABLE 21

Mean after-survival (MAS) and standard deviations of survival time (SD) for male and female LAF_1 mice exposed to various dosages of Co^{60} gamma rays daily for the duration of life at starting ages ranging from 100 to 850 days

MALE			Starting age, days	FEMALE		
MAS, days	SD, days	n		MAS, days	SD, days	n
			170 r/day			
22.0	4.6	105	100	20.0	2.6	105
26.7	7.5	6	250	22.5	4.2	6
27.3	7.2	6	400	28.2	2.6	6
24.3	9.5	6	550	23.3	3.8	6
22.2	9.4	6	650	19.4	10.2	7
20.7	6.0	6	725	17.7	7.5	6
-	-	-	800	18.2	7.1	6
			125 r/day			
33.9	4.7	105	100	31.2	5.3	105
36.6	1.8	9	250	34.9	2.1	9
31.3	12.6	9	400	32.6	8.0	9
35.3	8.6	9	550	35.9	3.5	9
36.8	8.6	6	650	29.1	7.1	12
34.0	7.6	6	725	18.3	8.3	6
37.0	2.0	3	800	26.8	8.1	5
24.6	8.4	5	850	31.8	3.3	4
			97 r/day			
41.4	5.3	104	100	41.7	6.2	105
44.2	3.8	12	250	44.2	3.8	12
41.2	7.7	12	400	44.0	4.8	12
46.8	9.3	9	550	39.7	6.8	9
42.0	10.4	6	650	39.4	8.6	12
14.3	9.1	3	725	39.5	12.7	6
44.3	4.5	3	800	26.0	17.3	5
			74 r/day			
64.5	18.2	105	100	65.8	13.6	105
67.5	22.9	12	250	68.7	18.2	12
82.6	21.0	11	400	73.8	21.7	11
53.6	23.8	9	550	60.6	16.2	9
67.8	15.5	6	650	46.8	8.6	12
55.6	18.2	5	725	37.8	22.4	6
56.0	16.5	3	800	45.6	16.7	5
			43 r/day			
149.8	42.9	150	100	155.9	38.2	150
140.1	34.4	15	250	132.8	36.4	15
140.1	54.0	12	400	166.2	36.1	12
106.7	30.0	9	550	150.0	30.5	6
138.2	27.9	6	650	102.4	57.7	7
135.0	1.7	3	725	95.2	24.8	6
59.7	44.6	3	800	104.3	19.9	6
47.0	53.7	2	850	56.7	17.5	3

ages, and hence the observed curves are not pure measures of the change in resistance. However, the data at 170 r/day make it clear that resistance does not decrease as a linear function of age, even when the MAS is a negligible fraction of the after-expectation of controls. One certain conclusion we can draw now is that the prevailing views about the additivity of radiation damage and aging will require drastic revision as a consequence of the results reported here.

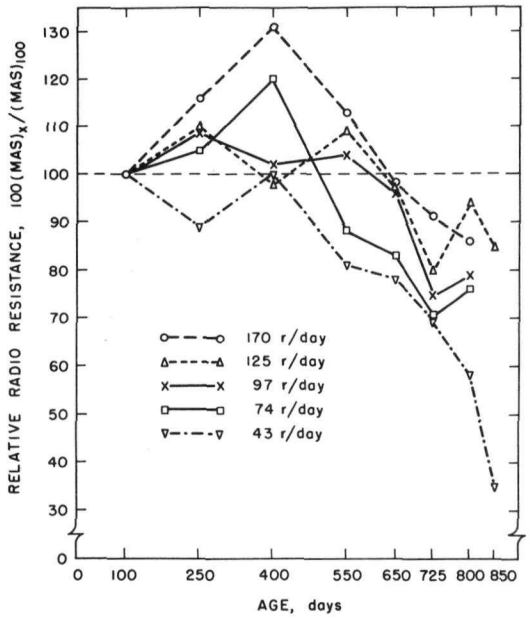

Figure 23

Radioresistance of LAF_1 mice (combined sexes) as a function of age, for duration-of-life exposure at 5 different daily dosages. At each daily dose level, the MAS at age x is expressed as a percentage of the MAS at 100 days of age.

The problem of age-dependence is also being investigated at the histological level, as described elsewhere in this issue.(2)

References

1. Sacher, G. A., D. Grahn, and J. M. Gurian. Survival of LAF_1 mice under duration-of-life exposure to Co^{60} gamma rays at rates of 24 to 1650 r per day. This report, p. 70.

2. Lesher, S., G. A. Sacher, D. Grahn, A. Sallese, and K. F. Hamilton. Influence of age on susceptibility of mice to the lethal effects of whole-body X-irradiation, with especial emphasis on intestinal damage. This report, p. 87.

INFLUENCE OF AGE ON SUSCEPTIBILITY OF MICE TO THE LETHAL EFFECTS OF WHOLE-BODY X-IRRADIATION, WITH ESPECIAL EMPHASIS ON INTESTINAL DAMAGE

S. Lesher, George A. Sacher, Douglas Grahn, Anthony Sallese, and Katherine F. Hamilton

The radioresistance of the mouse increases with increasing age from weaning up to mid-life span and declines thereafter.[1-5] Experiments have been designed to determine the degree of sensitivity at various ages ranging from 1 to 900 days and to investigate the role of critical organ systems at each age level. The preliminary phase reported here explores the relative sensitivity of the small intestine in 30- and 120-day-old mice.

A minimum of 20 BCF_1 hybrid mice at 30 and 100 days of age were given whole-body X-irradiation at 7 exposure levels: 750 r, 800 r, 900 r, 1000 r, 1200 r, 1500 r, and 2500 r. Mice were sacrificed at 2, 12, 24, 36, 48, 72, 84, and 96 hr, and frozen sections of the small intestine were cut and prepared for study. The cumulative mortality for each age group at each dose level was determined (Figure 24). It is obvious that the 100-day-old mouse is more resistant to X-irradiation at these levels. A histological examination of the small intestine shows that the damage is much greater in the 30-day-old mouse, and that the duodenum is completely denuded in a high percentage of cases at dose levels of 900 r and above. Approximately 60% of the young mice die as a result of intestinal damage after 900 r and 1000 r while none of the 100-day-old mice die from intestinal damage after 900 r and only 1 of 20 after 1000 r whole-body X-irradiation.

Damage and inhibition of mitosis increases with the dose in both groups; however, from the standpoint of mortality statistics the difference becomes less pronounced at higher doses. Nevertheless, at the cellular level there are definite differences in degree of damage and time of occurrence.

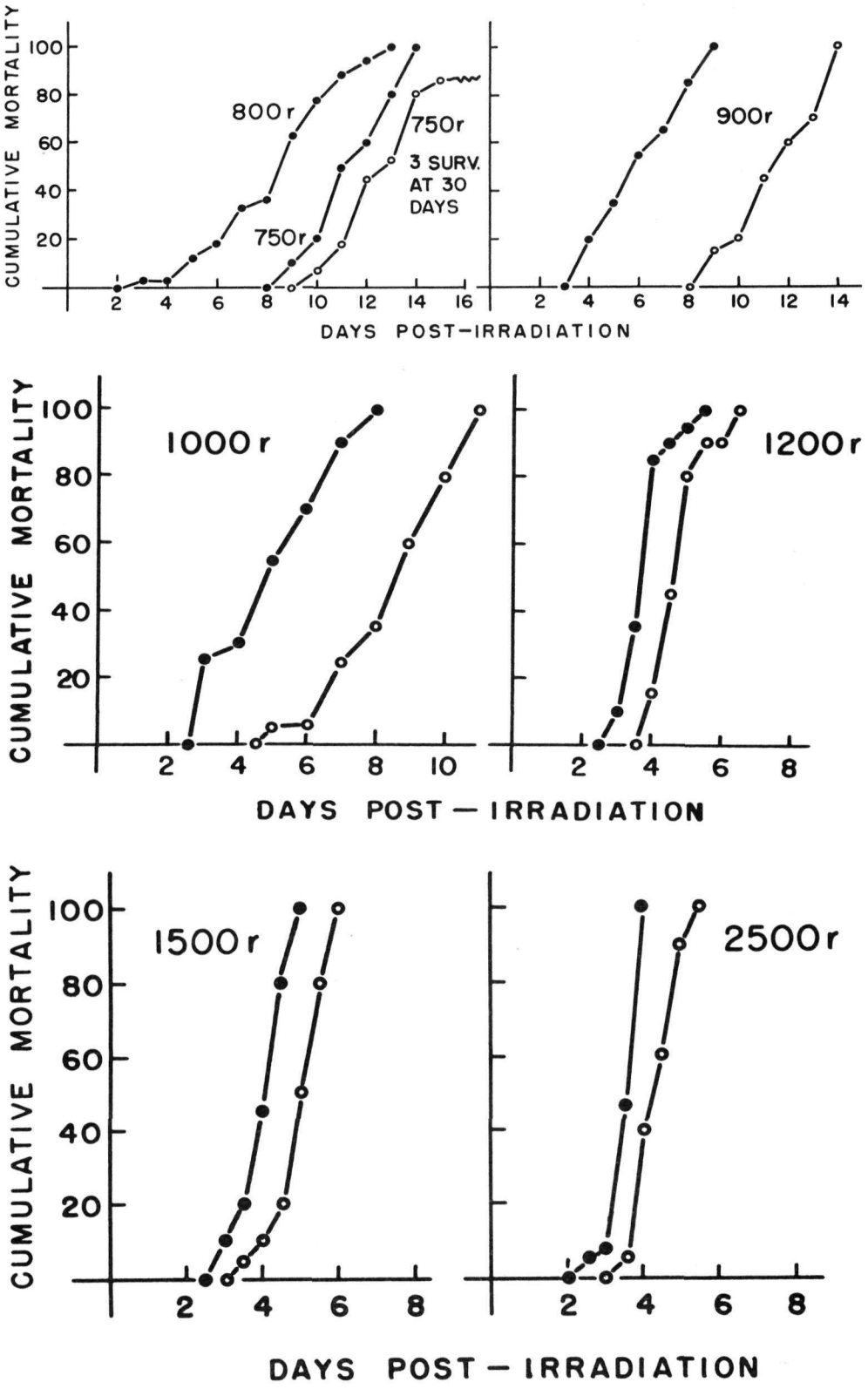

Figure 24. Cumulative mortality of mice of 2 age groups: 30-day-old (closed circles) and 100-day-old (open circles), after whole-body exposure to 7 dosage levels of X-irradiation.

References

1. Abrams, H. L. Influence of age, body weight, and sex on susceptibility of mice to the lethal effects of X-irradiation. Proc. Soc. Exptl. Biol. Med. 76: 729-732 (1951).

2. Sacher, G. A. Dependence of acute radiosensitivity on age in adult female mouse. Science 125: 1039-1040 (1957).

3. Quastler, H. Studies on roentgen death in mice. II. Body weight and sensitivity. Am. J. Roentgenol. 54: 457-461 (1945).

4. Quastler, H. Studies on roentgen death in mice. I. Survival time and dosage. Am. J. Roentgenol. 54: 449-456 (1945).

5. Kohn, H. I. and Kallman, R. F. Age, growth and the LD_{50} of X-rays. Science 124: 1078 (1956).

STUDIES ON THE NUCLEOLAR CHROMOSOMES

Arlene Longwell*

Although a nucleolus is present in almost all except a few specialized cell types, little is known about its origin and its function in the dividing and in the nondividing cell. Experiments with the plant aneuploids are being conducted to determine the effects of altered numbers of nucleolar chromosomes and alterations of the nucleolus-organizing regions of such chromosomes. Also differences in behavior during cell division of the micronuclei containing a nucleolus and the micronuclei without a nucleolus are being studied.

Estimates of the nucleolar and cytoplasmic ribonucleic acid in the sporocytes of the various wheat aneuploids are made by staining for RNA with the dye azure B, and measuring the dye content of the nucleolus and cytoplasm with the visible light microspectrophotometer.(1) Total nucleolar and cytoplasmic protein content is estimated by making dry mass determinations with the Cooke-Dyson interference microscope.(2)

Previous work has shown that hexaploid wheat (Triticum vulgare) contains four nucleolus-producing chromosomes, two of which are relatively inactive in all the tissues studied: in meiotic material, at the microspore divisions, in endosperm material, and in root tips.(3) Mid-pachytene sporocytes of hexaploid wheat tetrasomic for either of the two stronger nucleolar chromosomes show an approximately 100% increase in nucleolar RNA and a 50% increase in cytoplasmic RNA and protein. The same increase is found in the nullisomic-tetrasomics of this material when the nucleolar chromosome is tetrasomic and non-nucleolar chromosome pair is missing from the complement so that the total number of chromosomes remains 21 pairs as in normal material. Tetrasomics for the two weaker nucleolar chromosomes and for two of the non-nucleolar chromosomes show no differences from normal. The increases in RNA and protein, in the case of the two stronger nucleolar chromosomes, then, cannot be attributed to the simple nonspecific increase in chromosome number from 21 pairs to 22 pairs. A plant trisomic for one of the stronger nucleolar chromosomes showed no increase in either nucleolar or cytoplasmic RNA and protein. The absence of one pair of the nucleolar chromosomes, as in the case of the nullisomics, or one chromosome arm, as in the case of the isochromosomes and telocentrics of the nuclear chromosomes, results in no significant differences from normal. This is not surprising, since in the absence of one of the stronger pairs of nucleolar chromosomes, a third, weaker pair of organizing chromosomes becomes 13 times more active in the production of a nucleolus than in normal material. These results all agree with previous determinations of the mid-pachytene volume of wheat sporocytes and their nucleoli.

---

*Resident Research Associate.

Additional work is now in progress to complete the analysis of the various nucleolar chromosome nullisomics, tetrasomics, nullisomic-tetrasomics, isochromosomes and telocentrics of T. vulgare. Maize plants trisomic for the nucleolus-producing chromosome and plants trisomic for two non-nucleolar chromosomes will also be analyzed to determine if their nucleolar and cytoplasmic RNA and protein contents also differ from normal. Translocations of the nucleolar chromosome which result in one case in its shortened total length and in the other case in an increase in its length are also being studied. Since the content of nuclear but nonchromosomal protein may also be affected by nucleolar chromosome alterations, total nuclear mass will be determined.

Additional work has shown that wheat micronuclei produced at meiosis from lagging monosomes are viable in the maturing pollen grains. Those chromosomes which fail to produce a nucleolus in their microspore micronuclei do not form nucleoli at later stages. Nucleolus-producing chromosomes, on the other hand, show an increase in the per cent of their micronuclei containing a nucleolus until the time of the first microspore division when almost 100% of the micronuclei contain a nucleolus. No nucleolus-containing micronucleus has been observed at the time of the first and second microspore divisions. However, micronuclei with nucleoli are observed still persisting in an early prophase-like condition. Since the percentage of pollen grains with micronuclei also decreases during the microspore divisions, presumably the nucleolus-containing micronuclei form normal-appearing chromosomes undetectable from the complement of the large nucleus.

References

1. Swift, H. Cytochemical techniques for nucleic acids, Ch. 17 in The Nucleic Acids. Vol. II. Eds. E. Chargoff and J. N. Davidson. Academic Press, N.Y. (1955).

2. Davies, H. G. The determination of mass and concentration by microscope interferometry, in General Cytochemical Methods. Ed. J. F. Danielli. Academic Press, N.Y. (1958).

3. Crosby, A. R. Nucleolar activity of lagging chromosomes in wheat. Am. J. Bot. 44: 813-822 (1957).

RADIATION RECOVERY

IV. The Rate of Recovery from Radiation Injury (Fission Neutrons) as a Function of Injury

Howard H. Vogel, Jr. and Donn L. Jordan

This experiment was designed to test the hypothesis that the rate (or rates) of recovery from radiation injury is a function of the amount of injury present. A preliminary experiment has already been reported[1,2] in which mice were exposed to varying doses of Co^{60} γ-rays, and after an interval of 5 days, the amount of additional radiation necessary to kill a portion of the animals in 30 days was determined. A similar plan was carried out for the exposures to fission neutrons except that the interval between paired doses was doubled to 10 days to allow for the slower recovery rate after neutron radiation. Previous experiments[3] showed that when paired equal doses of radiation were delivered to mice, 50% of the first dose was residual (as judged by the 30-day acute mortality criterion used) when an interval of 5 days was allowed between γ-ray doses from Co^{60}. However, an interval of 10 days was necessary between equal paired doses of fission neutrons in order to achieve the same effect. It was therefore clear that recovery rates were different following these two radiations.

The first doses of fission neutrons were chosen to be approximately equivalent (when expressed as per cent of the $LD_{50/30}$ single exposure dose, Column 2 of Table 22) to those used in the preliminary γ-ray experiment.[1] In calculating the neutron doses necessary for some mortality within the 30-day period after the second neutron exposure, an exponential type of recovery was postulated (Column 3 of Table 22).

TABLE 22

Residual dose and rate of recovery after fission neutron irradiation

First neutron dose		Second neutron dose (after 10 days), rads	Number of mice dead in 30 days / number exposed	Observed 30-day mortality, %	Estimated single dose to produce observed mortality, rads	First dose residual (Column 6 - Column 3)	Fraction of first dose remaining at 10 days	Recovery rate constant per day
Rads	First dose expressed as % $LD_{50/30}$ (single exposure)							
Col. 1	Col. 2	Col. 3	Col. 4	Col. 5	Col. 6	Col. 7	Col. 8	Col. 9
85	26	318	15/32	47	325	7	0.08	0.25
169	51	320	30/32	94	360	40	0.24	0.14
228	69	267	20/32	62.5	335	68	0.30	0.12
274	83	164	3/31	10	300	136	0.50	0.069
300	91	96	5/32	15	305	209	0.70	0.035

The 5 groups of 159 animals (CF No. 1 young adult female mice) are listed in Table 22. If the second dose given is subtracted from a dose equivalent to that which would produce the observed mortality for single exposures, a measure of the residual injury present from the first dose can be obtained. This figure is listed in Column 7 of Table 22 for each group of mice. The unrecovered portion of the first dose (Column 8) and the daily recovery rate constants (Column 9) were also calculated.

Figure 25 is a plot of the injury remaining 10 days after the first neutron exposure as a function of the first dose. It is apparent that the higher this first neutron dose, the higher is the "unrecovered" portion of the first dose as judged by the criterion of 30-day mortality.

Figure 26 shows the relationship between the daily recovery constant and the injury, expressed as a fraction of the single dose $LD_{50/30}$, reported to be approximately 330 rads at the CP-5 Research Reactor.(2) There seems to be a linear relation between the two variables involved that indicates a progressive retardation of the recovery process as the neutron doses are increased.

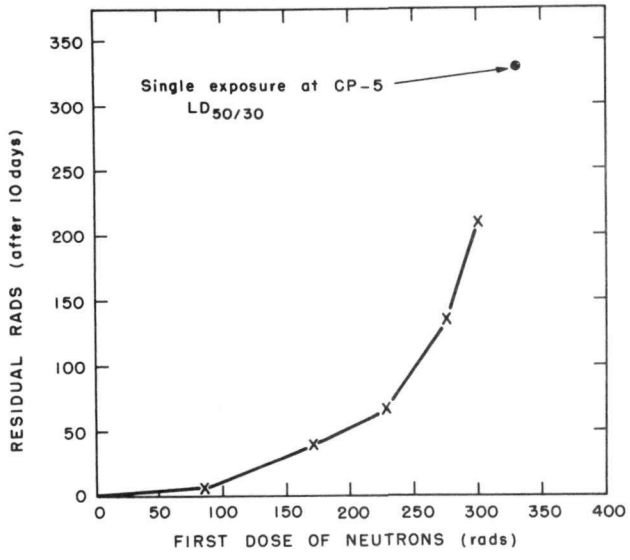

Figure 25. Injury remaining 10 days after a first exposure to fission neutrons, expressed as a function of the first neutron dose.

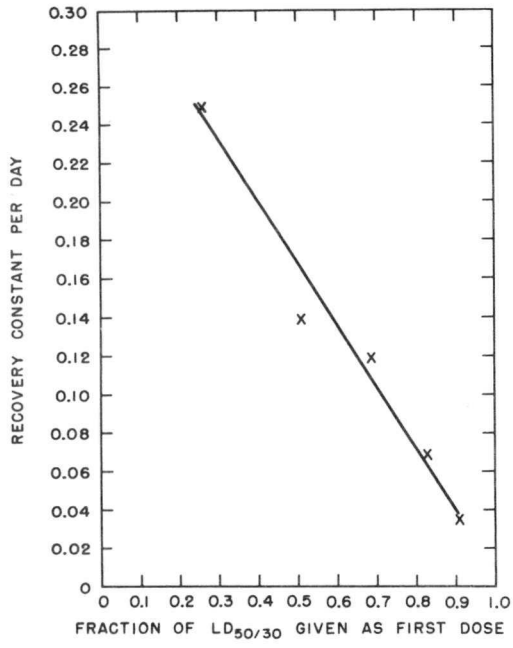

Figure 26. Relation between daily recovery rate constant and injury, expressed as a fraction of the $LD_{50/30}$ single exposure to fission neutrons.

It seems clear, therefore, that, according to the criteria selected in this experiment, recovery rate is dependent upon the size of the first neutron dose, or to the amount of injury inflicted.

References

1. Clark, J. W., D. L. Jordan and H. H. Vogel, Jr. Radiation recovery. III. The rate of recovery from radiation injury as a function of injury. Quarterly Report of Biological and Medical Research Division, Argonne National Laboratory. ANL-5655, pp. 99-101 (1956).

2. Vogel, H. H., Jr., J. W. Clark, and D. L. Jordan. Rate of recovery from γ-radiation injury as a function of the amount of injury. Federation Proc. 16:451 (1957).

3. Vogel, H. H., Jr., J. W. Clark, and D. L. Jordan. Recovery after fission neutrons: paired equal doses with varying time intervals. Radiation Research 7:458-459 (1957).

THE EFFECT UPON MOUSE LONGEVITY OF FRACTIONATION OF A DOSE OF FISSION NEUTRONS

Howard H. Vogel, Jr. and Donn L. Jordan

In October 1956, four groups of 36 CF No. 1 female mice, 7-8 weeks of age, were irradiated with fission neutrons at the CP-5 Research Reactor, operating at that time at approximately 1500 kw. The dose rate of the fission neutrons to the mice in the gamma-neutron radiation chamber was 6 rads/min. The first group was irradiated with a single, whole-body exposure of approximately 275 rads of fission neutrons, a dose planned as sublethal during the 30-day acute period. Actually 2 mice (5%) died during this interval. The other three groups of mice were irradiated with the same total neutron dose, but the exposures were divided into 3, 4, and 10 fractions respectively (see Table 23). In all these groups, the exposures were made on separate days. For example, the 10 fractional doses, each given in 4.8 minutes of daily exposure, were carried out within a period of two weeks.

TABLE 23

Irradiation data for neutron exposures

	Irradiation time, min	Number of mice	Estimated dose each exposure, rads	Mean after-survival time, days
Single exposure	48	36	275	262
Dose in 3 fractions	16*	36	96*	265
Dose in 4 fractions	12*	36	69*	235
Dose in 10 fractions	4.8*	36	27.5*	250

*Irradiation time for each fraction

At this time, approximately 600 days after exposure, only 2 irradiated mice and 5 control animals are still alive. The irradiation data and the mean survival time after irradiation are listed in Table 23.

Figure 27 compares the cumulative mortality (%) of the four irradiated groups with the control mice, for periods of 56 days after exposure. The single, "sublethal" neutron exposure decreased length of life by at least 50% as compared with control longevity. It seems clear from this graph and from the mean survival times after irradiation, that there is no significant difference between the mortality pattern following the single neutron exposure and those following fractionation of such a dose into 3, 4 or 10 separate daily exposures.

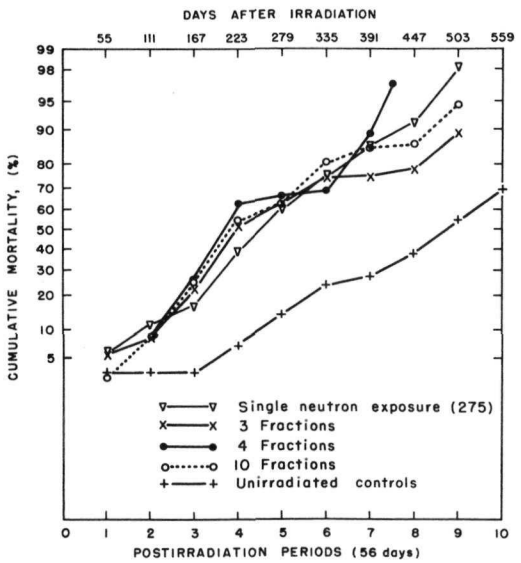

Figure 27

The effect of fractionation of the dose of fission neutrons on longevity of CF No. 1 female mice.

In Figure 28 the 4 irradiated groups have, therefore, been combined, and their mortality rates are compared with the similar rates for unirradiated control mice. The significant rise in the mortality rate of the irradiated mice during the 2nd to 4th periods (111-223 days) was correlated with a marked increase in reticular tumors; both thymic and "generalized lymphomas" were found at autopsy in all 4 irradiated groups.

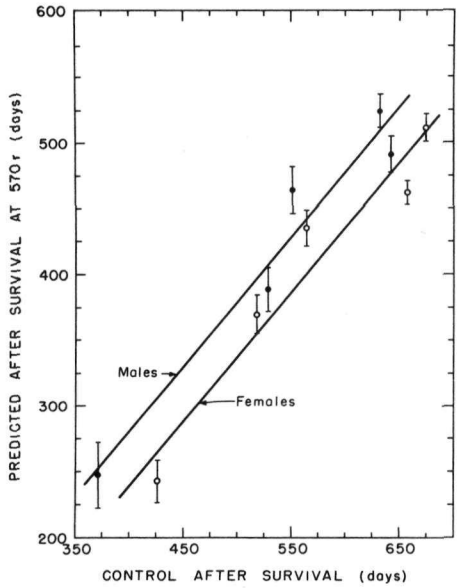

Figure 28

Comparative mortality rates of neutron-irradiated mice and unirradiated controls for 56-day periods after exposure. Mortality rate: number of mice dying during each 56-day period divided by number of mice alive at the beginning of each interval.

STUDIES OF RELATIVE BIOLOGICAL EFFECTIVENESS

Howard H. Vogel, Jr., Donn L. Jordan, and Norman A. Frigerio

The relative biological effectiveness (RBE) of two types of radiation may be defined as the ratio between doses of the two that produce equivalent specific biological changes. The study of RBE is important because the ratios presumably reflect differences in rate of dissipation of energy along the path of the two radiations in question. There is some reason for believing that these differences, if sufficiently great, may result in different basic mechanisms of radiation effect in biological systems. Hence such comparisons provide an experimental method for getting at the most difficult problem of radiobiology -- the means by which radiations produce biological effects. They also provide a basis for extrapolating existing information about radiation injury for one type of radiation to another type.

Fission neutrons and Co^{60} γ-rays have been chosen for study because of the wide range between the two with respect to spatial distribution of energy in tissue. Fission neutrons dissipate energy largely by recoil protons which lose energy at an average rate of about 30 kev per micron of path(approximately 1000 ion pairs per micron of tissue). On the other hand, γ-rays dissipate energy chiefly by means of recoil electrons, which lose energy at an average rate, for Co^{60}, of about 0.3 kev per micron of path (approximately 9 ion pairs per micron of tissue). Thus the linear energy transfer (LET) is 100-fold greater for neutrons than for γ-rays, and for equal doses, the total path length is 100th that for γ-rays. The resultant pattern for neutrons is one of short, heavily ionized tracks which are widely separated. In contrast, tracks from γ-rays are more sparsely ionized and much longer, and, therefore, less widely separated.

Over a period of several years, the exposures have been carried out in the same facility, a special γ-neutron radiation chamber utilizing fission neutrons from the thermal column of two of Argonne's reactors, CP-3' and CP-5. The γ-radiation was delivered from 18 sources of Co^{60} mounted on a turret on the radiation chamber. Material could be exposed either to one radiation alone or to mixtures of the two in varying proportions.

Table 24 summarizes the value for RBE for 15 different biological tests on a widely varying group of organisms, both animal and plants. In all but one test, fission neutrons were more efficient. Values ranged from 1.5 to 30, and even those for the mouse ranged from 3 to 7. This indicates that no simple relationship between LET and RBE can be derived on the basis of this information; other factors must be involved. It would not, of course, be surprising if the ratios were influenced not only by differences in LET but also by spatial, chemical, physical, or physiological characteristics of the biological target system as well.

TABLE 24

Summary of values for the relative biological effectiveness (RBE) of fission neutrons and Co^{60} γ-rays for 15 biological tests, all carried out in the same irradiation facility

Species utilized	Biological test system	Approximate doses (γ-rays/fission neutrons) necessary to produce given effect	RBE
"Giant" amoeba (Pelomyxa illinoisensis)	Single exposure necessary to kill half of the irradiated cells in a 10-day period.	17,000 rad / 11,000 rad (Dose rate: 25-30 rad/min)	1.5
Grasshopper (Melanoplus differentialis)	Single exposure necessary to destroy every egg in each grasshopper ovary with the exception of the most advanced or terminal egg.	420 r / 22.5 rep	19
Fruit flies (Drosophila melanogaster)	Genetic effects: chromosomal aberrations produced by single irradiation. 1.37-1.6% flies showing translocations in chromosomes (Bithorax method of E. B. Lewis).	3380 r / 400 rep	8.4
Seeds of red kidney beans (Phaseolus vulgaris)	Minimum dose to seeds necessary to produce pigment anomalies in chloroplasts of primary leaves (numerous scattered white areas at the ends of the smallest veins over entire blade, leading to a speckled appearance of leaf).	1500 r / 50 rep	30
4-Day chick embryo (Irradiated in ovo)	Dose necessary to kill 50% of the embryos, 6 hr after exposure; cessation of heart beat used as criterion.	1190 rad / 540 rad	2.2
4-Day chick embryo	Dose necessary to kill 50% of the embryos 6 days after irradiation.	894 rad / 317 rad	2.8
3-Day-old chicks	Single, whole-body dose necessary to kill half the irradiated birds in a 21-day period.	878 r / 236 rep	3.7
Rats (Female, Sprague-Dawley)	6-hr Fe^{59} uptake by bone marrow cells, 24, hr after single whole-body exposure.	Total doses from 40-150 rad	1
Mouse, CF No. 1 female	Cataract formation: minimal dose to produce a complete (Grade 4) cataract within 1 year after a single acute, whole-body exposure.	992 r / 170 rep	5.8
Mouse	Female sterility: single whole-body dose necessary to produce complete sterility 4-5 months after exposure.	60 rad / 15 rad	4.0
Mouse	Damage to blood-forming system as reflected by atrophy of the spleen: Dose necessary to reduce the splenic weight to 50% of control value, 5 days after single, whole-body exposure.	346 r / 78 rep	4.4
Mouse	Damage to digestive system: Dose necessary to reduce dry weight of small intestine to 75% of control value, 48 hr after single whole-body irradiation.	850 rad / 304 rad	2.8
Mouse	$LD_{50/30}$ (dose necessary to kill 50% of the animals in 30 days) in mice exposed to a single, 90-min whole-body irradiation at the CP-3' reactor.	930 r / 210 rep	4.4
Mouse	$LD_{50/30}$ in mice exposed to a single whole-body irradiation protracted over 24 hr (at CP-3' reactor).	1324 r / 210 rep	6.3
Mouse	$LD_{50/30}$ in mice exposed to a single, whole-body irradiation delivered in 45 min (at the CP-5 reactor).	900 rad / 330 rad	2.7

It is apparent that we need much more information about RBE's. The accumulation of such data is expensive and time-consuming. However, the concept of RBE has usefulness in calculating relative radiation hazards, and in postulating maximum permissible exposures for man for external radiations, particularly in the field of mixed radiations. Therefore, it is most important that we increase our understanding of what the RBE's are for those radiation-induced changes in mammals that have medical significance. The availability for more RBE data for all types of radiations and for all kinds of biological tests systems is highly desirable because of its applicability to these problems and to the problems of basic mechanisms.

THE PREDICTION OF LIFE SHORTENING IN MICE FOLLOWING ACUTELY LETHAL SINGLE DOSES OF X-IRRADIATION AND ITS POSSIBLE APPLICATION TO MAN

Douglas Grahn

The life-shortening effect of whole-body exposure to ionizing radiations is the subject of much discussion and review. Studies to date have demonstrated, in a reasonably consistent manner, the nature of the basic dose-effect relationship.(1) Nevertheless, the observed or predicted life-shortening effect of a given dose differs somewhat from one set of data to the next. The present study concerns one possible source of this variation, the genetic constitution. Since the data are limited to a narrow dose range around the $LD_{50/30}$ value (about 0.85 to 1.15 LD_{50} doses), direct prediction of life shortening at low levels of exposure cannot be made. However, the data do provide a means of estimating the extent of variability in life shortening that can be attributed to genetic factors.

Mice of both sexes from five inbred strains (Table 25) make up the data. These animals had been exposed to single doses of 200 kvp X-irradiation at the age of 60 to 110 days. All exposure doses were in the acute lethal range (5% to 95% mortality in the first 30 days). The results of the acute lethal response have been reported.(2)

TABLE 25

Mean after-survival (MAS) of control and irradiated mice measured from mean age at exposure of irradiated mice. Number of mice indicated in parentheses.

Strain	Mean age at Exposure	MAS ± SE (days)		$LD_{50/30}$ dose, r	Mean exp. dose, r*
		Control	Irradiated		
	days	Males			
BALB/c	89	371 ± 32 (33)	287 ± 16 (123)	493	470
A/Jax	89	529 ± 21 (33)	405 ± 16 (123)	555	531
A/He	96	552 ± 27 (43)	478 ± 17 (107)	559	536
$C3H_f$/He	85	633 ± 20 (36)	526 ± 12 (200)	588	569
C57BL/6	88	643 ± 15 (48)	478 ± 12 (202)	626	607
		Females			
BALB/c	89	427 ± 30 (33)	314 ± 10 (167)	513	473
A/Jax	88	518 ± 22 (40)	401 ± 14 (80)	538	527
A/He	93	564 ± 23 (32)	463 ± 13 (86)	549	534
$C3H_f$/He	86	658 ± 29 (27)	465 ± 9 (193)	597	567
C57BL/6	88	675 ± 19 (48)	489 ± 10 (164)	633	600

*Mean exposure dose of mice alive at 60 days after irradiation.

The survivors of the acute syndrome were kept for the duration of their life along with a nominal group of controls. The number of controls provides estimates of survival comparable in accuracy to about the largest group at any dose level among the irradiated animals. The data on the control and experimental populations were obtained concurrently under uniform environmental conditions in one animal room. It was necessary to cage the two sexes and all strains separately, and the controls were caged apart from the experimentals.

The chronic mortality data include only those deaths that occurred beyond 60 days after irradiation, although survival time is measured from the day of exposure. The small number of deaths that occurred between 30 and 60 days could generally be attributed to an extension of the acute mortality period (1-30 days).

Within each sex and strain there are 8 to 10 dose groups, each containing from about 3 to 40 mice. Doses that produced acute mortality above the level of 85% have not been included.

The data on the irradiated mice have been analyzed by means of a weighted covariance analysis in which dose is the independent variable and after-survival, S_X, is the dependent variable. This technique permits an analysis of variation in S_X that is independent of variation in dose. Details of the analysis and its results will not be given here. Briefly, strain differences in S_X are statistically significant. In addition, a significant sex by strain interaction is present. That is, the two sexes do not show a parallel response from strain to strain.

The covariance analysis also provides an estimate of the regression of S_X on dose for each sex and strain. Because of the narrow dose range, a linear regression adequately describes the relationship in these data. However, analysis of a separate experiment that involved a broader range of doses has shown that the over-all dose-effect curve is definitely nonlinear.(3) The magnitudes of the dose-effect slopes in the present data are consistent with the slope of the comparable segment of the nonlinear dose-effect equation.

There are no significant strain differences in the coefficient of regression of S_X on dose. However, the female has a significantly steeper regression than the male. The regression coefficients are: female: -0.737 ± 0.135 days/roentgen; male: -0.396 ± 0.192 days/roentgen. Table 25 provides the basic parameters of the survival data necessary to apply the slope values to any sex or strain for prediction purposes.

Table 26 gives the predicted after-survival values at a constant dose of 570 r for all strains (S_{X570}). This dose approximates an average LD_{50} value for the strains involved. The predictions are also given in terms of

days reduction of life and per cent reduction of life. In Table 27, the predicted after-survival at the LD_{50} dose are given (S_{xMLD}) along with the reduction of life in days and per cent. For both cases (at the constant dose and at the constant level of injury) strain differences are significant. This is true for any manner of expression of the data.

TABLE 26

Predicted after-survival, S_{x570}, days reduction of life and per cent reduction of life at 570 r.

Strain	Males	Reduction of life		Females	Reduction of life	
	$S_{x570} \pm SE^*$	Days	%	$S_{x570} \pm SE^*$	Days	%
BALB/c	247 ± 25	124	34	243 ± 16	184	43
A/Jax	390 ± 17	140	26	370 ± 15	149	29
A/He	465 ± 18	87	16	436 ± 14	128	23
$C3H_f$/He	526 ± 12	107	17	463 ± 9	195	30
C57BL/6	492 ± 14	151	23	512 ± 11	163	24
Average		122	22		164	29

*SE also applies to days reduction of life.

TABLE 27

Predicted after-survival, S_{xMLD}, days reduction of life and per cent reduction of life at the $LD_{50/30}$.

Strain	Males	Reduction of life		Females	Reduction of life	
	$S_{xMLD} \pm SE^*$	Days	%	$S_{xMLD} \pm SE^*$	Days	%
BALB/c	278 ± 16	94	25	285 ± 11	142	33
A/Jax	396 ± 16	134	25	393 ± 14	125	24
A/He	469 ± 17	83	15	452 ± 14	112	20
$C3H_f$/He	519 ± 13	114	18	443 ± 10	215	33
C57BL/6	470 ± 13	173	27	465 ± 11	210	31
Average		119	22		161	28

*SE also applies to days reduction of life.

Separate analyses of the days reduction of life and the per cent reduction of life have also been carried out. These analyses indicated a significant sex difference in the reduction of life. This was not clearly evident in the analysis of S_X, because the two sexes have very similar average S_X values. However, the female consistently has the greater control after-survival, S_O, and consequently shows significantly more life shortening. This greater sensitivity of the female to chronic injury has previously been indicated and discussed.(3)

Inspection and comparison of the data in Tables 25-27 reveal that, between strains, the LD_{50} values are positively related to the S_O values. The two sexes adhere to the one equation:

$$LD_{50/30} = 323 + 0.435\ S_O \qquad (1)$$

Standard error of slope: ± 0.078

The correlation between these two variables is +0.96. In other words, the LD_{50} dose for the young adult is a close measure of the normal viability of the strain, as determined by the S_O value.

Strains with higher S_O values also have the higher S_X values, and vice versa. Figure 29 presents the between-strain relationship of S_{X570} with S_O. While the two sexes can again be fitted by a common slope, they have significantly different intercepts. The equations are:

Females: $S_{X570} = -155.3 + 0.985S_O$ (2)

Males: $S_{X570} = -113.5 + 0.985S_O$ (3)

Standard error of slope: ± 0.094

The intercepts vary inversely with the dose at which S_X is predicted. The rate of change is -0.737 days/r for females and -0.396 days/r for males. The slope of 0.985 is the same for all doses in the acute lethal range. The correlation between S_{X570} and S_O is +0.97, which indicates that about 94% of the strain differences in S_X can be attributed to basic strain differences in normal viability.

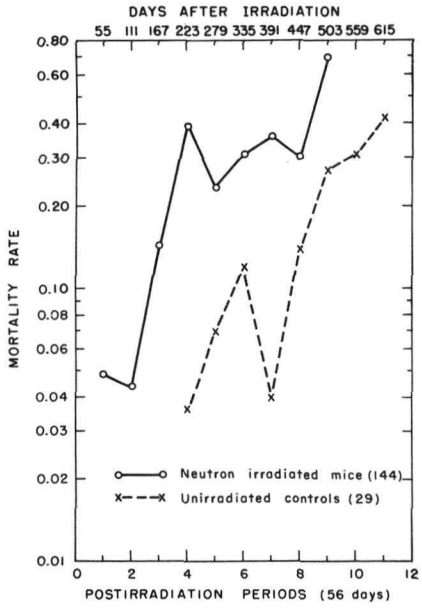

Figure 29 Between-strain regression of predicted after-survival at 570 r on control after-survival. Each strain value is bracketed by ± one standard error. Solid symbols: males; open symbols: females.

As a consequence of these close relationships, S_x can be predicted for any dose in the acute lethal range if one has knowledge of the control after-survival (S_o) or the LD_{50}. Figures 30 and 31 present the results of such predictions for an array of S_o values between 350 and 700 days. The predicted after-survivals have been re-expressed in terms of per cent reduction of life versus dose. Each S_o line represents a genetically determined level of normal survival.

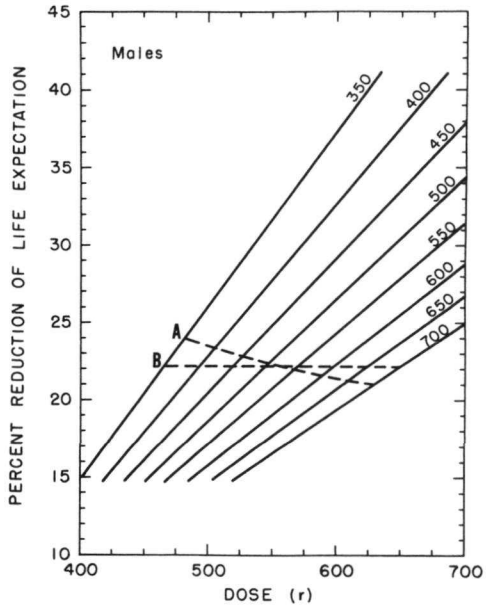

Figure 30 Prediction of per cent life shortening vs. dose for males. Each solid line represents a different genetically determined normal life expectancy (at 90 days of age). Broken lines (A and B) refer to predicted life shortening following exposure to an LD_{50} dose.

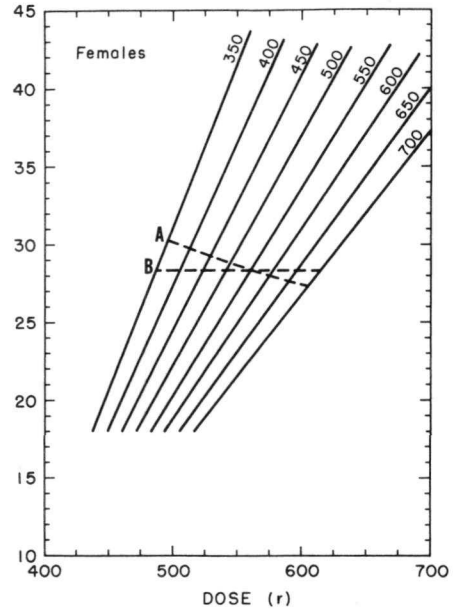

Figure 31 Prediction of per cent life shortening vs. dose for females. Each solid line represents a different genetically determined normal life expectancy (at 90 days of age). Broken lines (A and B) refer to predicted life shortening following exposure to an LD_{50} dose.

The S_{xMLD} values for the five strains (Table 27) are also linearly related to S_o. In this instance, the best fit is obtained with a log-log plot. The calculated slope is $+1.058 \pm 0.043$ ($r = +0.95$). The equations are:

$$\text{Females: } S_{xMLD} = 0.50 S_o^{1.058} \quad (4)$$

$$\text{Males: } S_{xMLD} = 0.54 S_o^{1.058} \quad (5)$$

Since the slope is slightly greater than 1.0, life shortening following an LD_{50} dose is a little lower in long-lived strains than in short-lived strains. This relation is depicted by line A in Figures 30 and 31. The straight line

B, is based on the assumption that S_{xMLD} is a constant multiple of S_o (a slope of 1.0). In this case, the equations become these:

$$\text{Females: } S_{xMLD} = 0.716S_o \quad (6)$$

$$\text{Males: } S_{xMLD} = 0.778S_o \quad (7)$$

These state that the life shortening caused by an LD_{50} dose is 28.4% for females and 22.2% for males, regardless of the normal expectation of life.

It should be emphasized here that all of these predictions are based upon animals that were exposed at about 90 days of age. The different S_o lines cannot be applied to any single strain at various stages of its life. The lines only refer to genetic differences in after-survival from young adulthood.

The between-strain regression of S_{x570} on S_o does not differ significantly from 1.0. A unit slope would indicate that a given single dose in the acute lethal range causes the after-expectation of life to be reduced by a constant number of days for all strains. The data permit the suggestion that there is one chronic injury parameter common to all mouse genotypes. Naturally, if the days loss of life is constant, the per cent reduction of life must increase as S_o decreases.

The slope of 1.058 that relates log S_{xMLD} to log S_o also cannot be statistically differentiated from a slope of 1.0. Here too there is evidence for a single injury parameter. As noted previously, this unit slope would indicate a constant proportion of life shortening for all genotypes at their respective LD_{50}'s.

The significant strain variation in the days reduction of life that is observed in these data may therefore be due to what might be called secondary genetic variation. In other words, this may be variation in characteristics whose genetic control is partially independent of, or only a small component of, the genetic complex controlling over-all viability.

Some evidence for this is present in a comparison of leukemic versus nonleukemic deaths. Most radiation-induced leukemias are manifested in an acute form within 300 days post exposure, so that high leukemic strains show a greater reduction of life than would be predicted. A preliminary analysis of the after-survival of only the nonleukemic mice of all strains indicates that, among males, strain differences in the days reduction of life are sharply reduced. This aspect of the data will be reported subsequently in more detail along with a more complete discussion of the chronic injury parameter.

In addition to the genetic variability in life shortening, there is a considerable amount of nongenetic variance. The present data indicate this variance to be approximately 21,000 for both sexes. The standard error of survival time for an individual animal is the square-root of 21,000; or ± 145 days. In terms of per cent life shortening, this term extends well beyound the limits of genetic differences indicated in Figures 30 and 31. Consequently, predictions of individual life shortening are not genetically discriminating, even when the LD_{50} or the normal life expectancy is known. With groups of 25 or more, the life-shortening effect of a single acutely lethal dose can be predicted to within about two standard errors ($\pm 145/\sqrt{25} = \pm 29$ days). If a population is of unknown genetic quality, the per cent reduction of life can be expected to fall within the limits set by the charts at the appropriate dose level.

With certain assumptions, the charts can also be applied to man. Initially, it must be recognized that any existing measure of human radiosensitivity, while extremely uncertain, is at best only an indication of the average level of sensitivity. If 350 r is assumed to be the human LD_{50}, it cannot be considered any more definitive than an assumption that the mouse LD_{50} is 570 r. The latter is an average value and varies with the genotype by at least ± 15%. It is reasonable to assume that a similar range of genetic variation in acute radiosensitivity can exist in man, since the human population is composed of genetically divergent racial groups that are known to differ for many morphological and physiological traits.(4) The extent of this variation may be approximated by the charts when several additional assumptions are made:

1. The per cent reduction of life in man is the same as observed in the mouse when both species are subject to doses that produce equal levels of acute physiological injury. Roughly, this dose equivalence should be the ratio of average LD_{50}'s: 350/570 or 0.6. The dose levels of Figures 30 and 31 should therefore be reduced by 40%.

2. Genetic variation in radioresistance in man is directly related to genetic variation in normal viability.

3. Normal viability in man varies by a factor of two, and the limiting values for the mouse are actuarially equivalent to limiting values for man.

4. Sex differences in radiosensitivity are similar for both species. (This assumption is highly unlikely as the female mouse is uniquely radiosensitive among mammals in terms of chronic injury. The female mouse at least may provide an upper limit to the expected life shortening.)

In addition, as for the mouse, the predictions are only to be applied to populations exposed during young adulthood.

With these assumptions, the prediction charts can be used to circumscribe the expectation of life shortening in man following exposure to single doses in the acutely lethal range. The life-shortening effect of the average LD_{50} (350 r) can vary among different human subpopulations from 17% to 34%. Should the human female be as sensitive as the female mouse to long-term injury, then the upper limit of life shortening could approach 45%.

The question of genetic variation in life shortening in man is pertinent to present studies on two different racial groups of irradiated humans: the Japanese and the Marshallese Islanders. Whatever life shortening may be observed (or projected from early results) can certainly test the general applicability of laboratory animal data to man. However, the possible existence of significant genetic variability among the races of man makes it difficult to assume that the average response of all humans can be approximated by either of these two groups. The results of the present study, together with an earlier study on acute lethality,[5] suggest that the genetic variance may make up as much as 50% of the total variance of response. An arbitrary doubling of the variance observed in genetically inbred laboratory populations can thus allow for the genetic variable among heterogeneous laboratory animals. As a first approximation, this factor of two could also be applied to the observed variance in any human data. In effect, this would increase the standard error by 41% ($\sqrt{2}$), and provide a reasonable allowance for differences due to genetic factors.

References

1. Hursh, J. B. The effect of ionizing radiation on longevity. Univ. of Rochester, Atomic Energy Proj. Report UR-506. (1957).

2. Grahn, D., and K. F. Hamilton. Genetic variation in the acute lethal response of four inbred mouse strains to whole body X-irradiation. Genetics 42: 189-198 (1957).

3. Sacher, G. A. On the statistical nature of mortality, with especial reference to chronic radiation mortality. Radiology 67: 250-257 (1956).

4. Boyd, W. C. Genetics and the Races of Man. D. C. Heath and Co., Boston. (1950).

5. Grahn, D. Acute radiation response of mice from a cross between radiosensitive and radioresistant strains. Gnetics, in press.

PENICILLAMINE AND PLUTONIUM METABOLISM

Asher J. Finkel and Dorice M. Czajka

Recent reports on the efficacy of oral penicillamine (β,β-dimethylcysteine) as a chelating agent in the treatment of human diseases involving excess accumulations of copper, lead, and iron[1] prompted a test of its effect on plutonium metabolism and distribution.

Young adult female CF No. 1 mice were used in these studies. In a preliminary experiment 15.0 mg of penicillamine injected intraperitoneally produced fatal convulsions in each of 5 mice. Similar injections of 7.5 mg led to 1 death among 5 mice in 24 hr while 0.75 mg produced no adverse effect. The latter amount is roughly equivalent to 2.0 g per 70-kg man.

In the first experiment 0.17 μc of $Pu(NO_3)_4$ was injected intravenously into each of 24 mice. One hour later 3.0 mg of penicillamine was injected intraperitoneally into 12 of these mice. Mice in groups of three were sacrificed in the experimental and control groups 1, 3, 5, and 24 hr after the penicillamine was administered. Liver, kidney, spleen, femur, lung, a sample of heart blood, and the residual carcass were analyzed for plutonium. Pooled urine and feces were also collected and analyzed for each group of mice. These analyses revealed no significant differences between the treated and the control groups.

In a second experiment, each of 36 mice was injected intravenously with 2.72 μc $Pu(NO_3)_4$. One hour later 3.0 mg penicillamine was injected intraperitoneally into 18 of these mice; this injection was repeated daily for the next 4 days and again on the 7th day. Three treated and 3 control animals were sacrificed 4 hr after each penicillamine injection, and the liver, femur, and residual carcass were analyzed for plutonium. Analysis of the data again revealed no constant difference between treated and control groups.

Apparently, intraperitoneally administered penicillamine is without effect on the metabolism and distribution of intravenously introduced plutonium in mice.

Reference

1. Boulding, J. E. and R. A. Baker. The treatment of metal poisoning with penicillamine. Lancet 273: 985 (1957).

MULTIPLE RADIOISOTOPE INJECTION IN MICE (Ce^{144}, Cs^{137}, AND Zn^{65})

Analysis of Retention at Tracer and Toxic Dose Levels by NaI-Tl Crystal Spectrometry in vivo

Finn Devik* and Austin M. Brues

The use of radioactive tracers in general, and of double tracing techniques (e.g. Fe^{55}, Fe^{59}, and Cr^{51}, Ca^{45} and Sr^{89}) in particular, is based on the well-founded assumption that radioactive tracers do not interfere with metabolic processes from a practical point of view. Experimental evidence also tends to support the assumption that when two or more radioistopes are present in tracer amounts in a living organism there is no mutual interference in the pattern of distribution, retention and excretion. At radiotoxic levels this may not necessarily be so, because radiotoxic effects as manifested by pathological and physiological changes may be expected to change the factors that govern the pathways of each specific radioisotope in such a way that distribution, retention, and excretion would be affected. The possibility of mutual chemical interaction between radioelements with resultant change in behavior naturally would increase when the amounts are increased, although for carrier-free radioisotopes the amount of element present (by weight) may still be so low as to make a difference less likely with respect to tracer doses. The ingestion of a number of different radioisotopes at acute toxic levels may be conceived as a possibility if exposure to substantial concentrations of fission products were to take place.

Few experiments on the effects of a mixture of radioisotopes in living organisms have been reported, and these have mainly involved administration of mixed fission products of known age, with recording of total activities. Since sensitive techniques are now available for the analysis of the amounts of single components of a mixture of β- or γ-ray emitters, a series of experiments was carried out with three γ-emitters to test if the distribution and retention pattern at radiotoxic dose levels would differ from that at the tracer dose levels.

Materials and Methods

Female CF No. 1 mice 6 weeks old weighing about 25 g were used for the experiments.

---

*World Health Organization Fellow from State Laboratory of Radiation Hygiene, Rikshospitalet, Oslo, Norway.

Ce^{144}-Pr^{144}, Cs^{137}-Ba^{137} and Zn^{65} were chosen because they are γ-emitters with γ-ray energies sufficiently different to be easily separated in the energy spectrum, the main peaks being at 0.134, 0.6612 and 1.114 Mev respectively. The radioisotopes were procured from Oak Ridge National Laboratory. Cerium and cesium were carrier-free fission products, purity better than 99% (exclusive of Ce^{141}). Zn^{65} had been produced by the $Zn^{64}(n,\gamma)$ Zn^{65} reaction; the specific activity was stated to be more than 75 mc per gram of zinc.

The elements were administered separately as $CeCl_3$, CsCl and $ZnCl_2$. The original hydrochloric acid solutions were diluted with saline, and pH was adjusted to about 3; the volume injected of each solution was 0.1 - 0.2 ml per mouse. $CeCl_3$ was injected intravenously, and the more soluble chlorides of cesium and zinc were injected intraperitoneally.

To count the γ activity in the mice in vivo, a $2\frac{3}{4}$ in. x 2 in. NaI-Tl crystal was used in connection with a photomultiplier tube. The impulses were led to a linear amplifier and counted in three different parts of the spectral range of a pulse-height analyzer. These parts were selected empirically so that the pulse height and channel width of each corresponded to the optimum counting yield below and including the main γ-peak of each element. For counting, each mouse was placed in a perforated $1\frac{1}{4}$ in. plastic centrifuge tube in a holder over the crystal, to ensure a fixed geometry. The distance from crystal to mouse was approximately 2 in. in the tracer dose series, and 12 in. when radiotoxic doses had been administered.

Results

The results of the tracer dose experiments are summarized in Table 28 and Figure 32.

Preliminary experiments indicated that it was impractical to adminster all three radioactive elements in radiotoxic or near-radiotoxic amounts. Therefore, one of the three radioisotopes was given in radiotoxic amounts, the other two in tracer amounts (Figure 33). In small animals such as mice the main radiotoxic effect is accounted for by the absorption of β-rays. The absorption of γ-rays may be regarded as relatively insignificant in determining toxicity.

Available information on rats, calculation of the dose from β-ray absorption, and preliminary tests indicated that the $LD_{50/30}$ for Ce^{144}-Pr^{144} was 2-3 $\mu c/g$, and that for Cs^{137}-Ba^{137} somewhat more than 30 $\mu c/g$ body weight in the mice.

Zn^{65} is a weak β-emitter. Besides, a dose of 100 μc/mouse had a toxic effect which killed most mice the first day after injection. This effect was ascribed to the presence of zinc and impurities in amounts which had a chemical toxic effect at this dose level.

TABLE 28

Retention of radioelements in four groups of mice after injection of 2 μc Ce^{144}, 1 μc Cs^{137} and 1 μc Zn^{65} respectively, combined and single. Figures in parentheses give the ranges of variation between single animals

Number of mice	Isotope	Retention, % of counts 1 day after injection				
		Days after injection				
		1	2	3	6	14
6	Ce^{144}	100	96 (92-103)	92 (89-103)	81 (75-88)	59 (52-63)
	Cs^{137}	100	72 (68- 87)	55 (50- 68)	28 (23-35)	7 (5- 9)
	Zn^{65}	100	89 (81- 93)	79 (73- 82)	59 (54-65)	36 (32-40)
4	Ce^{144}	100	100 (93-111)	92- (87-108)	81 (70-101)	58 (45-78)
4	Cs^{137}	100	72 (68- 79)	55 (52- 63)	30 (25-35)	8 (5-11)
4	Zn^{65}	100	86 (85- 88)	79 (77- 80)	63 (63-64)	38 (37-39)

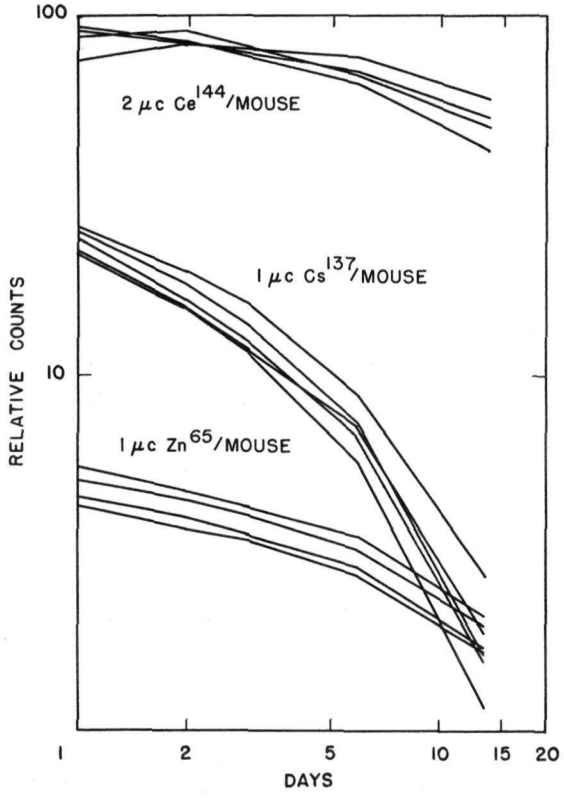

Fig. 32 Retention after tracer amounts.

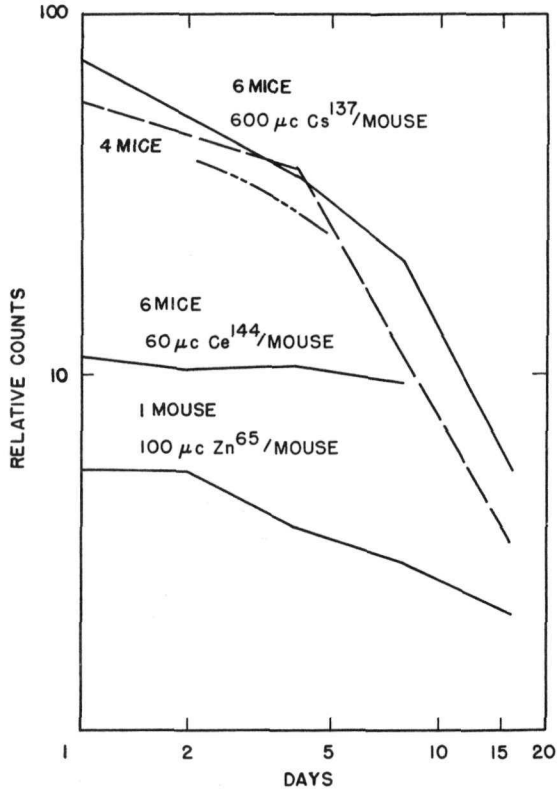

Fig. 33 Retention after radiotoxic amounts.

EFFECTS OF ULTRAVIOLET RADIATION ON AMOEBAE

Edward W. Daniels

The sensitivity of the giant amoeba Pelomyxa illinoisensis to UV radiation has been investigated in order to extend a comparative study of the effects of different kinds of radiation on this relatively radiosensitive species of amoeba. Survival and cell division data have previously been obtained following exposures to X-rays,[1] γ-rays and fission neutrons.[2] This information was then used in experiments designed to determine whether or not unirradiated protoplasm will bring about recovery after its injection into supralethally ultraviolet-irradiated amoebae, and also to determine whether protoplasm from supralethally ultraviolet-irradiated organisms will prevent death in supralethally X-irradiated amoebae. Since the primary physical action of ultraviolet radiation differs from that of ionizing radiation, it appeared possible that differently irradiated systems of this type might be mutually helpful.

Procedure

The source of ultraviolet (UV) radiation was a General Electric 15-watt germicidal mercury vapor lamp with a peak emission at 2537 A. A Latarjet dosimeter (selenium block layer photocell covered with a fluorescent layer with proper filters) was used to determine the output before each exposure. The calibration of this device had a 5% error. At a target distance of 53 cm, 50 organisms at a time were exposed in about 1 ml of phosphate buffer,[3] pH 6.9 - 7.0. They were spread out on the bottom of glass vials 6 mm high which were open at the top to permit free transmission of the UV radiation. The temperature was kept between 22.5 and 23.5°C during and after exposure. The cells were removed and isolated in fresh buffer medium about 15 min after irradiation. All except those in photoreactivation studies were kept either in the dark or in red light. Although it was only necessary to keep the experimental cells for 10 to 15 days after exposure to ionizing radiation, those exposed to UV radiation were studied for 45 days, since some of the cells lived about this long before either mass culture formation or death occurred.

Results

Effect of ultraviolet radiation. The sensitivity of this amoeba to UV radiation is shown in Table 29 and Figure 34. The lethal dose was obtained after 5.5 - 6 min exposure or about 5000 ergs mm^{-2}. Although insufficient data are available to differentiate between a linear and a sigmoid curve, the linear type of curve is more closely approximated after UV radiation than after any of the ionizing radiations which have been used.

TABLE 29

Sensitivity of Pelomyxa illinoisensis to different radiations

	X-rays, 4 kr/min	γ-rays, 25 r/min	Fission neutrons, 31 rep/min	Ultraviolet (2537A) 14.3 ergs sec^{-1} mm^{-2}
Approximate maximum dose producing no mortality	7 kr	9 kr	8 krep	<500 ergs mm^{-2}
Approximate dose producing 50% mortality*	11 kr	17 kr	11 krep	2150 ergs mm^{-2}
Minimum single dose which killed all cells (LD_{100})*	14 kr	25 kr	15 krep	5000 ergs mm^{-2}
Mean time of death in days after above dose (LD_{100})**	4.9 ± 0.2 (63)	4.2 ± 0.4 (25)	4.4 ± 0.1 (25)	14.7 ± 1.1 (50)
Supralethal dose*	24 kr	40 kr	30 krep	13000 ergs mm^{-2}
Mean time of death in days after supralethal dose**	4.6 ± 0.1 (164)	4.1 ± 0.2 (25)	4.2 ± 0.1 (158)	5.0 ± 0.2 (20)

*Period of observation was 10 days after ionizing radiation exposures and 45 days after ultraviolet irradiation.

**The values represent means, plus or minus Standard Error. Numbers in parentheses represent numbers of cells observed.

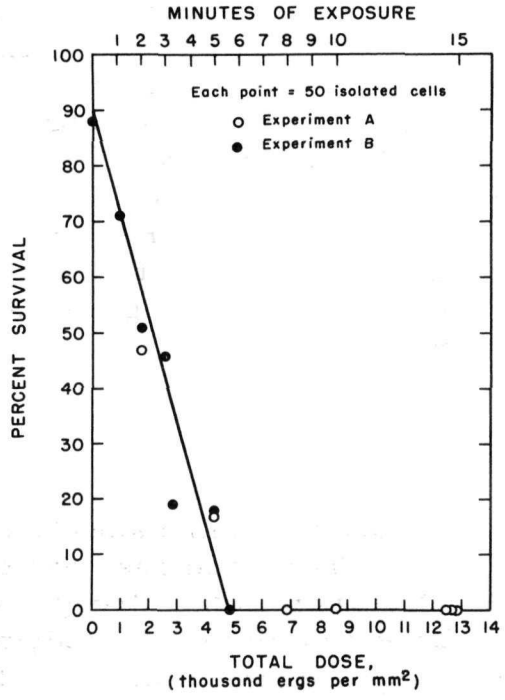

Figure 34

Survival curve of Pelomyxa illinoisensis after exposure to ultraviolet radiation (2537 A). Exposure rate, 14.3 ergs sec^{-1} mm^{-2}.

The mean survival time of amoebae exposed to supralethal doses of UV radiation is 5 days or about the same as that after a killing dose of ionizing radiation (Table 29). These data are supported by studies of 200 amoebae kept in mass cultures until death after a single continuous dose of 13,000 ergs mm^{-2}, and also by death time measurements of fifty isolated amoebae after a dose of 8600 ergs mm^{-2} at the rate shown in Table 29. On the other hand, after a dose of UV radiation just sufficient to kill all cells, the amoebae survive some 15 days, or about 3 times longer than those given supralethal doses of UV radiation, or any of the doses of ionizing radiations sufficient to cause some cells to die (Table 29). Amoebae that die following UV doses near the LD_{50} also live about 15 days or about 3 times as long as those given supralethal doses of the same radiation. On the other hand, the cells that die after exposure to doses of ionizing radiation near the LD_{50} die in about 5 days.

Cells lethally irradiated by UV frequently became gradually smaller in size until, at the time of death several days after irradiation, they were greatly reduced in size. These changes were not seen in cells dying after exposure to lethal doses of ionizing radiation. The lethally UV-irradiated amoebae fed poorly if at all on other protozoa, in contrast to amoebae exposed to lethal doses of ionizing radiations.

Amoebae exposed to a lethal or supralethal dose of UV radiation seldom underwent a cell division. If exposed to lower doses near the LD_{50}, 11% of the single cell isolates that eventually died, divided at least once, and among those that divided, 33% had daughter cells which underwent one or more cell divisions. On the other hand, amoebae that underwent a second cell division (division of the daughter cell) after exposure to ionizing radiation almost always produced mass cultures. Among the survivors the mean time lapse between UV exposure and the first cell division was as long as or longer, but in no case shorter, than the mean time lapse between the first and second cell divisions. Four dose levels (955, 1715, 2568, and 4290 ergs mm^{-2}) were studied (Figure 34). The actual time required for the first and second divisions was about twice that for the respective nonirradiated controls. The mean time between the second and third divisions in the irradiated amoebae was only slightly delayed.

Photoreactivation. In a study of photorecovery in P. illinoisensis, an LD_{50} dose (1715 ergs mm^{-2}) of far UV light was used to irradiate two groups of amoebae at the same time under similar conditions. One group (53 cells) was put in the dark after exposure and examined under red light thereafter to minimize photoreactivation. The other group (51 cells) was immediately exposed to white light continuously for 6 hr at constant room temperature. This light, emitted by a 100-W, 120-V, 60-cycle bulb in a microscope lamp (open diaphragm), was reflected by the ground glass mirror of the microscope into the amoebae that were on the microscope stage. The distance of the light path was 12 cm. Both groups of amoebae

were transferred to fresh media and isolated at approximately the same time. They were then subcultured daily until death or formation of mass cultures, which required 45 days in a few cases. Survival in the group that was not exposed to light was 51% while that in the group exposed to white light was 65%; according to the chi-square analysis, this difference is not significant.

Microtransfer of nonirradiated protoplasm. Pelomyxae were given a supralethal dose of UV radiation (2.5 x minimum dose which killed all of 50 exposed cells in 45 days) and then fused with nonirradiated amoebae, or with portions cut from them. A total of 21 fusions was made in which protoplasmic transfer was directly observed. Of these fused protoplasts, 76% survived and produced mass cultures. Evidence from stained specimens indicates that both irradiated and nonirradiated nuclei divided synchronously at the first mitosis following UV exposure and fusion; only young nuclei were present in the daughter cells fixed a few minutes after mitosis. Cell division was not significantly delayed in these fused organisms. The mean time and standard error of the first cell division after the isolation of 50 nonirradiated control cells was 3.0 ± 0.2 days while in the fused organisms (irradiated plus nonirradiated) the equivalent time was 3.7 ± 0.4 days. The mean time lapse between first and second divisions in the controls was 2.6 ± 0.1 days while the equivalent time in the daughter cells of the fused organisms was 2.5 ± 0.3 days. Fusion alone does not delay division.(3)

Fusion of differently irradiated cellular systems. As would be expected, the fusion of one supralethally X-irradiated amoeba with another does not prevent death or extend the time of death, as shown by 42 fusions which were made combining pairs of amoebae each of which had been given a lethal dose of X-rays.(4) However, it is theoretically possible that the therapeutic component(s) in nonirradiated protoplasm that prevent death in supralethally X-irradiated amoebae might not be damaged in cells given supralethal doses of certain other types of radiation. This concept was directly tested for two radiations other than X-rays.

Supralethally neutron-irradiated amoebae were combined with portions cut from supralethally X-irradiated amoebae(5) so that the fused protoplasts each contained both types of irradiated protoplasm. The average ratio of X-irradiated to neutron-irradiated protoplasm was approximately 1 to 8. The data from a total of 21 fusions show clearly that these systems are not mutually helpful and survival does not follow this type of union.

As an extension of this idea, supralethally X-irradiated cells were fused with supralethally UV-irradiated amoebae. A total of 21 fusions were made, and the protoplasts, each containing X-irradiated and UV-irradiated protoplasm, were isolated and fed. All of these organisms died, most between the 4th and 6th day after exposure. Only a single division occurred, and both daughter cells died.

Discussion and Conclusions

If a lethal dose of radiation or other toxic agent critically damages only certain kinds of intracellular components essential to the life of the cell, it should be possible specifically to replace or repair the damaged units. In connection with this hypothesis, a major problem is to find which units are critically damaged by radiation and to discover a means of helping the cell to overcome the damage. This can be done by introducing a whole new spectrum of ingredients necessary to a living cell, namely whole protoplasm from the same species. The major knowledge that this approach has so far given is that radiation death can be prevented in single cells by the injection of whole protoplasm, and that irradiated and nonirradiated nuclei continue to undergo mitosis in an apparently normal manner in the same cell.

If one type of radiation (X-rays) does not incapacitate the same vital components in a cell that another type of radiation (fission-neutrons or UV) does, then two of these protoplasmic systems might be mutually beneficial following fusion. This is of theoretical interest particularly since the initial physical action of these radiations is different. X-rays bring about ionization by the production of recoil electrons, whereas fast neutrons produce it by recoil protons. In addition to this, the ionization tracks are different. On the other hand, ultraviolet radiation causes excitation and is differentially adsorbed at specific wavelengths. At the wavelength used (2537 A) the nucleic acids absorb heavily.[6] However, as shown in this paper, there were no mutually beneficial effects after the fusion of cells exposed to different radiations and then combined in the manner described. This indicates that fission neutrons as well as UV photons incapacitate the therapeutic component required for survival in supralethelly X-irradiated amoebae. As far as this therapeutic aspect of radiation injury is concerned, these three different radiations appear to act either on the same substances, or on different substances localized on the same organelle. In other words, each of these radiations probably affects a number of different intracellular units but the protective component(s) of special interest in the present work seem to be directly or indirectly damaged by each type of radiation which was used. If the fine particulates are the target organelles, several pathways all leading to their inactivation can be imagined: energy dissipation at any one of several lower (biochemical) organizational levels might result in the inactivation of a fine particle as far as its therapeutic effect is concerned.

The greatest delay in cell division among survivors of various doses of UV radiation (Figure 34) occurred before the first division according to mean values of control and experimental groups; the time between divisions was from two to three times that of the nonirradiated control. The mean time lapse between the first and second cell divisions

was nearly as great—about twice that of the corresponding nonirradiated controls. The third division means, however, showed only slight delay, and mass cultures of 20 or more cells were produced in the single cell clones within a few days after the third division occurred. Thus, the greatest delay occurs prior to the first and second cell divisions after UV irradiation as it does after sublethal exposure to ionizing radiations (X-rays, gamma rays and fission neutrons).

In Paramecium, X-rays, as well as nitrogen mustard (HN_2), cause delay in cell division that is greatest before the first division and gradually decreases between successive divisions[7] as in Pelomyxa carolinensis[8] and P. illinoisensis.[1] However, in the latter organism the greatest delay sometimes occurs after the first division although not later than this. It is interesting that in X-irradiated P. carolinensis the block in cell division occurs before the first division, but after HN_2 treatment it occurs after the first division.[9] If well-fed, rapidly-dividing paramecia are exposed to UV, they show a major division delay period after some 2 or 3 divisions, which is followed by recovery in sublethally irradiated organisms.[10] However, less rapidly dividing or starved paramecia exposed to UV might be expected to show the lag in cell division earlier, before the first division or immediately afterward. A special study of this nutritional aspect has not been made on Pelomyxa. Up to the present time very little use has been made of starved or poorly-fed amoebae in this laboratory. Wilber and Slane[11] exposed starved Pelomyxa carolinensis amoebae to 2537-A UV radiation, but the organisms were not fed again after irradiation. Mazia and Hirshfield[12] have shown that well-fed Amoeba proteus, which is at least 10 times more resistant to X-rays than P. illinoisensis[1,13] has an ultraviolet sensitivity almost identical to that of P. illinoisensis. Furthermore, delay in cell division in UV-exposed A. proteus[12] is essentially complete after one or two postirradiation divisions.

References

1. Daniels, E. W. X-irradiation of the giant amoeba, Pelomyxa illinoisensis. I. Survival and cell division following exposure. Therapeutic effects of whole protoplasm. J. Exptl. Zool. 130: 183-197 (1955).

2. Daniels, E. W. and H. H. Vogel, Jr. Survival of giant amoebae after single exposures to Co^{60} gamma rays and fission neutrons. Semiannual Report of Biological and Medical Research Division, Argonne National Laboratory. ANL-5732, pp. 123-127 (1957).

3. Daniels, E. W. Cell division in the giant amoeba, Pelomyxa carolinensis, following X-irradiation. II. Analysis of therapeutic effects after fusion with nonirradiated cell portions. J. Exptl. Zool. 127: 427-462 (1954).

4. Daniels, E. W. X-irradiation of the giant amoeba, Pelomyxa illinoisensis. II. Further studies on recovery following supralethal exposure. J. Exptl. Zool. In press.

5. Daniels, E. W., and H. H. Vogel, Jr. Recovery following injection of nonirradiated protoplasm into amoebae irradiated with fission neutrons. II. Protective effect of centrifuged cell portions. Semiannuel Report of Biological and Medical Research Division, Argonne National Laboratory. ANL-5841, pp. 139-143 (1958).

6. Giese, A. C. Protozoa in photobiological research. Physiol. Zool. 26: 1-22 (1953).

7. Powers, E. L. Radiation effects in Paramecium. N. Y. Acad. Sci. 59: 619-636 (1955).

8. Daniels, E. W. Studies on the effect of X-irradiation upon Pelomyxa carolinensis with special reference to nuclear division and plasmotomy. J. Exptl. Zool. 117: 189-210 (1951).

9. Daniels, E. W. Some effects on cell division in Pelomyxa carolinensis following X-irradiation, treatment with bis-(β-chloroethyl)-methyl amine and experimental plasmogamy (fusion). J. Exptl. Zool. 120: 509-523 (1952).

10. Kimball, R. F., and N. Gaither. Influence of light upon the action of ultraviolet on Paramecium aurelia. J. Cell. and Comp. Physiol. 37: 211-233 (1951).

11. Wilber, C. G. and G. M. Slane. The effect of ultraviolet light on the protoplasm in Pelomyxa carolinensis. Trans. Am. Microscop. Soc. 70: 265-271 (1951).

12. Mazia, D. and H. I. Hirshfield. Nucleus-cytoplasm relationships in the action of ultraviolet radiation on Amoeba proteus. Exptl. Cell Res. 2: 58-72 (1951).

13. Ord, M. J., and J. F. Danielli. The site of damage in amoebae exposed to X-rays. Quart. J. Microscop. Sci. 97: 29-37 (1956).

PROGRESS REPORT: GRANULOCYTE LIFE CYCLE

Harvey M. Patt and Mary A. Maloney

Preliminary studies of the granulocyte life cycle as revealed by radioautographic analyses of marrow and blood from dogs receiving tritiated thymidine were reported previously.(1,2) We wish at this time to present data relating to the disappearance from peripheral blood of neutrophils labeled with tritiated thymidine.

Information concerning the normal pathways for neutrophil utilization and removal is incomplete. Many neutrophils are apparently destroyed in discharging their functions of removing cellular debris and helping to maintain the sterility of the internal environment. Large numbers of cells are probably also lost in various secretions and excretions. Thus, it seems reasonable to assume that the peripheral time span to neutrophils may be somewhat less dependent upon age than that of erythrocytes. The disappearance of labeled neutrophils from the peripheral blood of a dog, shown in Figure 35, is suggestive of a random utilization. Although the data indicate that the half-time for disappearance of all labeled cells from blood is about 2 days, a half-time of 12 to 24 hours is apparent when consideration is given to more homogeneous classes of labeled cells as revealed by grain count. Thus, we may note the sharp difference in the initial decay of the 4-9 and 10-19 grain classes. Cells with 4 to 9 grains, which are derived mainly from progenitors with 10 to 19 grains apparently continue to be released for several days after labeled cells first appear in the blood. This is consistent with the finding that labeled myelocytes are detectable in marrow for several days after injection of tritiated thymidine, though with decreasing grain concentration. Since the more homogeneous classes of labeled cells disappear with a half-time of the order of 12-24 hours, the peripheral pool of neutrophils may not be nearly as large as has been inferred. Perhaps only 5 to 10 times as many cells may reside in the periphery as in obvious circulation in contrast to previous estimates of some 50 times.(3-5)

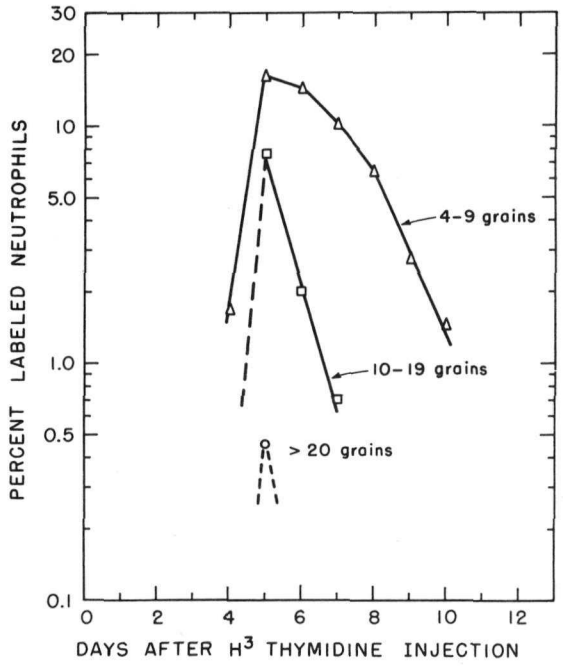

Figure 35 Disappearance of labeled neutrophils from blood. (Each point is based on enumeration of 2000 neutrophils.)

References

1. Maloney, M. A. and H. M. Patt. Progress report: Granulocyte life cycle. Semiannual Report of Biological and Medical Research Division, Argonne National Laboratory. ANL-5841, pp. 144-146 (1958).

2. Maloney, M. A., and H. M. Patt. Granulocyte life cycle. Federation Proc. 17: 103 (1958).

3. Osgood, E. E. Number and distribution of human hemic cells. Blood 9: 1141-1154 (1954).

4. Patt, H. M. A consideration of myeloid-erythroid balance in man. Blood 12: 777-787 (1957).

5. Patt, H. M., and M. A. Maloney. Control of granulocyte formation, in Symposium on Hemostatic Mechanisms, Brookhaven Symposia in Biology Series, in press.

PROGRESS REPORT: PLUTONIUM REMOVAL

I. Treatment of Plutonium Poisoning with New Chelating Agents

Jack Schubert, Joan F. Fried, William M. Westfall,
Elizabeth S. Moretti and E. H. Graul*

Until now, the most effective chelating agent for the treatment of plutonium poisoning has been ethylenediaminetetraacetic acid (EDTA). Two new chelating agents, diethylaminetriaminepentaacetic acid (DTPA) and bis(2-aminoethyl ether)tetraacetic acid (BAETA), both related to EDTA, have become available. The formulas for these two agents and EDTA are shown below:

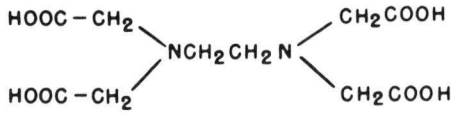

EDTA

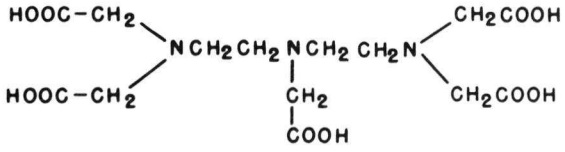

DTPA

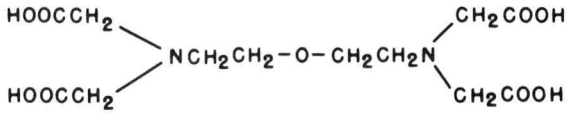

BAETA

Since these two new chelating agents were expected to form stronger chelates with plutonium than EDTA, the following experiment was set up. Four different groups of rats were injected with a mixture of Pu^{239} and Sr^{85} intravenously. Treatment was begun 6 days after injection and repeated at about weekly intervals. Group I received only saline, Group II received DTPA, Group III received BAETA, and Group IV received EDTA. Identical amounts of the respective chelating agents, ~0.8 mM/kg, were administered in all the groups. All animals were sacrificed at 27 days after injection for tissue analyses.

Preliminary results show, in a striking way, that the new chelating agents are far superior to EDTA. For example, at the 6-day treatment period, the excretion of Pu in DTPA- and BAETA-treated animals was increased five to six times over than that observed in EDTA-treated animals.

As was expected from theoretical considerations, none of the chelating agents had any effect on the excretion of radiostrontium.

---

*Resident Research Associate from University of Marburg/Lahn, W. Germany.

DYNAMICS OF THE RELEASE OF HISTAMINE FROM THE TISSUE MAST CELL

Douglas E. Smith

It is generally acknowledged that the tissue mast cell contains histamine and heparin.[1] This note is concerned with a series of cytological changes that we have observed in living mast cells treated with histamine liberators. Our findings extend those previously reported[2,3] in living mast cells treated similarly. Microscopic observations and cinephotomicrographic recordings were made of the mast cells of the transilluminated mesentery of the intact, anesthetized Sprague-Dawley rat. Bright-field illumination and magnifications of 400-900 X were employed. The experiments consisted of supplanting the oxygenated Tyrode's solution normally bathing the preparation with Tyrode's solution containing one of the following test substances: Compound 48/80,* 1:100,000; stilbamidine, 1:80 to 1:8000; protamine sulfate, 1:5000 to 1:100,000; or toluidine blue, 1:5000 to 1:200,000. All of these compounds bring about the release of histamine from the mast cell.[4,5]

Prior to treatment the mast cells of the mesentery are round or spindle-shaped and densely packed with dark granules. Shortly after introducing any of the above test solutions there occurs a marked change in the refractile properties of the granules: they suddenly lose their dark appearance and become almost invisible. First one granule and then another reacts until all have become involved, and the cell is barely discernible. Correlated with these events there is a gradual swelling of the cell to about $1\frac{1}{3}$ times its original diameter.

After toluidine-blue treatment the nucleus of the mast cell takes on a blue color when about 50-80% of the granules have lost their dark appearance. When most or all of the granules are scarcely visible, metachromatic staining of the faded granules begins. At first a few granules stain purple, then more and more, until apparently all are so stained. As the staining of the granules proceeds, the mast cell shrinks toward its normal size. At this stage, those living cells stained with toluidine blue resemble closely mast cells in mesenteries fixed in alcohol and then stained with toluidine blue. The details of the late events following the other test substances will be described at a later time.

We consider the present findings to be indicative of significant chemical changes in the mast cell. We interpret the changes in refractile properties of the granules to be a manifestation of the freeing of some material from binding either within or on the surface of the granule where it is osmotically inactive. Once free, the material is osmotically active;

*A polymer of N-methylhomoanisylamine and formaldehyde supplied through the courtesy of Dr. Edwin J. de Beer of the Wellcome Research Laboratories.

water enters the cell and swelling results. We consider it likely that the material liberated is histamine which is freed from its known binding with heparin.(6) The cytological changes that we have noted here are common to a variety of treatments that cause release of histamine from the mast cell, and the time course of the changes is the same as that for histamine release resulting from such treatments.(4,5) We suggest that histamine is freed from its binding with heparin because the histamine liberators have a stronger affinity for heparin than does histamine. The sequence of changes in the experiments with toluidine blue is consistent with such an interpretation; toluidine blue does not stain the granules until binding sites are made available on molecules of heparin. When the molecules of toluidine blue bind heparin they become osmotically inactive and the cell loses water and becomes smaller in size. The movement of histamine out of the cell at this time also contributes to the loss of water and shrinking of the cell. According to the present interpretation heparin is not lost from the mast cell treated with histamine liberators.

References

1. Fulton, G. P., F. I. Maynard, J. F. Riley, and G. B. West. Humoral aspects of tissue mast cells. Physiol. Rev. 37: 221-232 (1957).

2. Zollinger, H. U. Gewebsmastzellen und Heparin. Experientia 6: 384-386 (1950).

3. Mota, I., W. T. Beraldo, and L. C. U. Junqueira. Protamine-like property of compound 48/80 and stilbamidine and their action on mast cells. Proc. Soc. Exptl. Biol. Med. 83: 455-457 (1953).

4. Smith, D. E. The nature of the secretory activity of tissue mast cell. Abstracts of Communications, XXth International Physiological Congress, Brussels, p. 835 (1956).

5. Smith, D. E. Nature of the secretory activity of the mast cell. Am. J. Physiol. 193: 573-575 (1958)

6. Wehrle, E., and R. Amann. Zur Physiologie der Mastzellen als Träger des Heparins und Histamins. Klin. Wchnschr. 23: 624-630 (1956).

THE EFFECT OF REPEATED PARACENTESIS ON THE GROWTH OF EHRLICH ASCITES TUMORS

Robert L. Straube

The total number of ascites tumor cells that accumulate in the peritoneal cavity of the mouse is dependent upon the characteristics of the tumor species inoculated. It has been demonstrated[1] that the hypertetraploid Ehrlich, with double the cell volume of its diploid counterpart, reaches an asymptote at one-half the total cell number of the latter. It is assumed that maximal tumor growth is limited by the total protoplasmic tumor mass that the host can support. Exceptions may occur in ascitic tumors with early, widespread metastases because of infiltration in vital organs. This factor, however, is not critical in the development of the slower metastasizing, common ascitic carcinomas. Since the growth asymptote of the Ehrlich diploid is about 1×10^9 tumor cells, we wished to determine whether this value could be exceeded by periodically depleting the host of the cells and fluid that accumulate during the growth of the ascites tumor.

Mice were injected intraperitoneally with 20×10^6 ascites tumor cells and subsequently tapped to remove cells and fluid on the 3rd, 6th and 9th days after inoculation. An initial sample, followed by injection of Evans Blue[2] prior to removal of cells and fluid permitted repeated determinations of total cell number and fluid volume in the peritoneal cavity of the same host.

As can be seen from Figure 36, the total number of tumor cells accumulated does not exceed that normally found in Ehrlich ascites tumor growth.

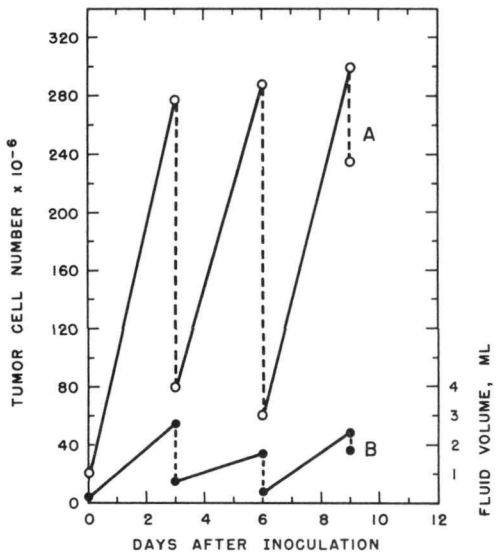

Figure 36

The effect of repeated paracentesis on the growth of Ehrlich ascites tumor (diploid) in CF No. 1 female mice. Abscissa: days after intraperitoneal inoculation with 20×10^6 Ehrlich ascites tumor cells. Ordinate: A, total number of free tumor cells present in the peritoneal cavity (left) and B, total ascitic fluid volume (right). Dotted lines indicate the number of cells and volume of fluid removed.

However, the rate of increase from the 6th to the 9th day parallels that of the 1st to 3rd day whereas in the normal growth curve the rate is approaching an asymptote at this period. Similar results were obtained in six of seven animals studied. Since, therefore, the Ehrlich ascites tumor can be maintained in the log phase of growth by repeated removal of cells and fluid, the rate of tumor cell synthesis does not appear to be a direct function of host exhaustion or of the total protoplasmic mass of tumor formed.

References

1. Hauschka, T. S., and S. Grinnell. Comparison of the growth curves of a diploid mouse ascites tumor and a tetraploid subline of the same tumor. Proc. Am. Assoc. Cancer Research, 2: 22 (1955)

2. Patt, H. M., M. E. Blackford and J. L. Drallmeier. Growth characteristics of the Krebs ascites tumor. Proc. Soc. Exptl. Biol. Med. 83: 520-524 (1953).

STUDIES ON EFFECTS OF DEUTERIUM OXIDE

VII. Effect of Deuterium on Pregnancy and on Viability of Newborn Mice

Dorice M. Czajka and Asher J. Finkel

Previous work has shown that deuterium is effective in retarding the growth of a rapidly growing ascites tumor in mice.(1) In view of this finding we decided to investigate the effect of deuterium on the pregnant female mouse and on the viability of the newborn. In a pilot study a litter of 2 males and 5 females was given 25 atom % deuterium in the drinking water beginning at 7 weeks of age. After 3 months the 5 females had had 2 pregnancies each, but all of the young were destroyed within a few hours. It was impossible to ascertain whether the young were viable at birth and destroyed later, or whether they were born dead. These observations suggested the value of a systematic experiment in which deuteration of female mice was instituted at various times before and during pregnancy.

Six groups of female mice were given 25% deuterium oxide in the drinking water according to the following schedule: A, control, no deuterium ; B, 7 days prior to mating; C, the day mating was begun; D, 1 week after mating was begun; E, 2 weeks after mating was begun; F, 3 weeks after mating was begun. The groups were each composed of 10 3-month-old CF No. 1 females. The males were allowed to remain in the breeding cages for one week. The male used in Group B was placed on deuterium for one week before he was transferred into the breeding cage. After $2\frac{1}{2}$ weeks the pregnant females were isolated in confinement cages. Three weeks after mating was begun the nonpregnant females were regrouped and rebred. Those from Group C, having been on deuterium for three weeks, were transferred to Group G, and kept on D_2O. Those from Group D, having been deuterated for two weeks, were transferred to Group H. The nonpregnant mice from Group E were added to Group B because they had been on deuterium for one week. The nonpregnant animals from Group F were added to Group C, which was started on deuterium on the same day that the male was introduced.

Because of the low incidence of pregnancies in the first series, a second series was started with fresh animals according to the same plan. After three weeks the nonpregnant mice in this series were also regrouped according to the above arrangements with two exceptions: in Groups G and H the males used in the second series were deuterated for the same length of time as the females, and the nonpregnant animals in Group F were kept in the same group without deuteration because only 2 of the 10 were pregnant.

After two breeding periods, administration of deuterium was terminated in the females from Groups, C, D, E, and F after 49 days and they were rebred. In this way administration of deuterium was terminated in Group C females on the first day of mating; in Group D 7 days later; in Group E 14 days later, and in Group F 21 days later. The second series of mice were removed from deuterium drinking water after 42 days and are being rebred at the present time.

Table 30 gives the incidence of pregnancies as a result of this breeding program. Columns 4 and 5 refer only to those animals that were definitely believed to be pregnant. These mice showed a rapid weight gain during the week prior to expected delivery and had palpable fetuses during this period. Several questionable pregnancies were not included. The animals that were presumed to have delivered because of weight loss showed an overnight drop of from 6 to 12 grams. Since all of the animals of one litter of Group C were seen to be alive on the day of delivery, it is presumed that at least some of the animals from each of the groups deuterated for shorter lengths of time were alive.

TABLE 30

Incidence of pregnancies among deuterated female mice

Group	Number of days on D_2O before delivery	Number of mice	Pregnancies		Method of noting delivery			Pregnancies with nonviable litters,%
			Number	Per cent	Sudden weight loss	Observations		
						One or more viable	All dead	
A	-	24	16	66.7	1	14	1	12.5
B	25-28	24*	3	12.5	2	0	1	100
C	18-21	27*	10	37.0	7	1	2	90
D	11-14	20**	8	40.0	8	0	0	100
E	4-7	20**	11	55.0	9	2	0	81.8
F	0-3	33**	12	36.4	1	10	1	16.7
G	42-45	7**	2	28.6	2	0	0	100
		3*	0	0.0	0	0	0	-
H	35-38	8**	3	37.5	2	0	1	100
		2*	0	0.0	0	0	0	-

*Males deuterated.

**Males not deuterated.

In general, the incidence of pregnancies increases with decreasing length of time on deuterated drinking water. A noteworthy exception is Group F, which might be expected to approximate the control group. It is possible that the institution of deuteration altered the thirst pattern of the mice so that they destroyed the newborn in an effort to satisfy this need. Observations on the effect of deuteration on fertility are complicated by

the relatively small numbers of animals in each group in the studies and the variability between replicated series. Furthermore, there is the possibility that the regimen led to the resorption of fetuses before weight gain was sufficient to make the pregnancies apparent.

Table 31 shows the number of living animals per litter at 1, 2, and 3 weeks post partum. It can be seen that most of the deuterated animals died within 1 week of birth. One animal of each deuterated litter plus a control animal were sacrificed on the 14th day of life for histological examination. The results in Table 31 are consistent with those recently published by Haggqvist[2] who reported on the effects of deuteration on the pregnancies of 5 mice. One of these was put on 25% D_2O 6 days before delivery of 10 normal-sized young that were eaten by the mother after several days, and a second female, having been on 25% D_2O for 8 days, delivered 6 newborn that were apparently dead at birth.

TABLE 31

Viability of newborn mice from deuterated mothers

Group	Number of days on D_2O before delivery	No. of pregnant mice with observed newborn	Total number newborn	Mean number per litter	Living offspring					
					At 6-8 days		At 13-14 days		At 20-21 days	
					No.	%	No.	%	No.	%
A	0	15	111	7.4	95	85.6	80	72.1	79*	71.2
B	25-28	1	1	-	0	0.0	0	0.0	0	0.0
C	18-21	3	9	3.0	0	0.0	0	0.0	0	0.0
D	11-14	0	0	-	-	-	-	-	-	-
E	4-7	2	19	9.5	6	31.6	4	21.1	3*	16.7
F	0-3	11	69	6.3	37	53.6	29	42.0	28*	40.6
G	42-45	0	0	-	-	-	-	-	-	-
H	35-38	1	4	4.0	0	0.0	0	0.0	0	0.0

*One 14-day-old mouse sacrificed and not included in this column.

The results shown in Tables 30 and 31 indicate that deuteration of mice with 25% D_2O in the drinking water leads to decrease in the number of detectable pregnancies and an increase in the percentage of nonviable litters. Whether this increase in nonviability is attributable to toxic effects on embryological development or to behavior changes in the parturient female is not distinguishable from our observations. The viable newborn in these experiments are being kept on 25% D_2O in the drinking water and their growth curves are being followed.

References

1. Finkel, A. J., and D. Czajka. Studies on effects of deuterium oxide. III. The effects of deuteration on ascites tumors in mice. Quarterly Report of Biological and Medical Research Division, Argonne National Laboratory. ANL-5696, pp. 74-76 (1956).

2. Haggqvist, G. Über die Einwirkung vom schwerem Wasser auf die embryonale Entwicklung. Acta Anat. 30: 326-338 (1957).

A STUDY OF THE RADIOACTIVITY FOUND IN GRASS GROWN ON THORIUM-BEARING (MONAZITE) SAND

Philip F. Gustafson and Austin M. Brues

Through the generosity of Father F. X. Roser of the Catholic University of Rio de Janeiro, some grass was made available, collected from a region in Brazil known to be rich in monazite sand. A sample of the ashed grass was analyzed by γ-ray spectroscopy starting some four months after harvest. Spectra were taken, using a 5" x 4" NaI crystal and a 256-channel analyzer, of a thorotrast solution of known age and therefore of known state of radioactive equilibrium; a thorium ore sample from the New Brunswick Laboratory of the Atomic Energy Commission, assumed to be in radioactive equilibrium; and the ashed grass. Use of the 5" x 4" crystal produces a relatively large photofraction (i.e., ratio of the intensity in the photopeak to the total intensity) for the 2.62 Mev gamma from ThC".

Comparison of the intensity of this line with that of the 0.96 Mev line from Ac^{228} ($MsTh_2$) serves to establish the degree of radioactive equilibrium reached by the activity in the specimen. The intensity at 0.96 Mev was corrected for the component due to ThC" in this region.

Table 32 indicates the values of this ratio for thorotrast, NBL ore sample, and grass on three different dates. The NBL sample and thorotrast ratios were essentially constant over the period of three months during which the measurements were made, and thus serve to standardize the procedure.

TABLE 32

The use of the ratio of ThC" intensity to Ac^{228} intensity as a measure of radioactive equilibrium of the Thorium series

Sample	Date (1958)		
	March 13	May 12	June 19
NBL ore sample	1.000	1.000	1.000
Thorotrast solution	0.929	0.917	0.922
Grass	0.395	0.457	0.492

The rate of equilibration of the grass activity is consistent with the supposition that the radioactivity originally taken up by the grass was Ra^{228}($MsTh_1$). Furthermore, the data fit the calculated equilibration curve

quite closely if the assumption is made that incorporation of radium took place some 8 months before the material was first counted. This restriction is in keeping with knowledge concerning the actual growth of the grass itself.

These results indicate that radium is preferentially taken up by the grass during growth. This is probably equally true of Ra^{224} (ThX) as well as Ra^{228}; however, due to the short half-life of Ra^{224} and its daughter products, any evidence of their presence initially and not as a result of growth from Ra^{228} is lost.

THE MEASUREMENT OF PROTEIN TURNOVER IN RAT LIVER

V. The Effect of Endocrine Status

Robert W. Swick and Rita A. Martin

There have been numerous attempts to relate different states of hormonal balance to the turnover of various proteins by determining the uptake of a single tracer dose. The correct interpretation of data in this manner may possibly be obscured by any of the following factors. The shape of the turnover curve may be altered by the change in conditions, the metabolism of different proteins in the same tissue may be affected differently, and the distribution of the tracer between various tissues may be altered by the hormonal imbalance. The data to be presented may suffer from the second of these faults. Since the exposure period used was only two days, the data are largely derived from those proteins which are being metabolized most actively. However, since normally about 40% of the liver protein is replaced during this period, the data represent the incorporation of isotope into an appreciable fraction of the liver proteins.

Adult female rats were continuously exposed as described previously.(1) The hormonal status was altered from 1-6 weeks prior to the administration of isotope, depending on the sensitivity of the animal to the aberration. The results of these experiments are shown in Table 33. That alteration of the thyroid balance changed the renewal rates was to be expected. Excess thyroid caused the turnover rate to increase by 15% while removal of the gland depressed the rate by 27%. The apparent acceleration of the turnover rate in adrenalectomized animals was not foreseen. Here the rate was 120% of the normal rate. In hypophysectomized rats, the average renewal rate of liver protein decreased to about 57% of the normal value. Ulrich et al.(2) reported that hypophysectomy decreased the turnover rate of plasma albumin to 53% of the normal value; while these workers observed a restoration of the turnover rate by administration of growth hormone to hypophysectomized rats, no such effect was observed in the present experiments.

The similarity of the effects of hypophysectomy on the replacement rates of liver proteins and plasma albumin suggests a relationship between the two. Preliminary examination of the renewal rates of plasma albumin obtained from our animals indicates an almost identical rate for total liver proteins and for albumin under conditions of normal and high protein intake. Under conditions of protein deprivation, the renewal rate of albumin is lowered while that of the total liver proteins is accelerated.

TABLE 33

Effect of hormonal status on protein turnover

Treatment	Renewal rate, fraction replaced per day*
Normal	0.26, 0.27, 0.25, 0.27
Thyroidectomy	0.16, 0.18, 0.22, 0.21, 0.20
Desiccated thyroid ($1\frac{1}{4}$ - $1\frac{1}{2}$%)	0.28, 0.32, 0.30, 0.30
Hypophysectomy	0.14, 0.15, 0.15, 0.16
Beef growth hormone, 5 mg/day intramuscularly	0.27, 0.24, 0.23, 0.24
Hypophysectomy plus growth hormone	0.15, 0.19
Adrenalectomy	0.24, 0.32, 0.38, 0.32
Ovariectomy	0.22, 0.22, 0.24, 0.26

*Each value represents data obtained from one animal.

References

1. Swick, R. W. Measurement of protein turnover in rat liver. J. Biol. Chem. 231: 751-764 (1958).

2. Ulrich, F., H. Tarver, and C. H. Li. Effect of growth and adrenalcorticotropic hormones on the metabolism of albumin in hypophysectomized rats. J. Biol. Chem. 209: 117-125 (1954).

FURTHER STUDIES UPON AN ADENOSINETRIPHOSPHATASE INHIBITOR DERIVED FROM EPINEPHRINE

Mario A. Inchiosa, Jr.

Demonstration of the formation of an adenosinetriphosphatase (ATPase) inhibitor during the oxidation of epinephrine has been described in earlier reports.[1,2] This work has been continued, and attempts have been made to isolate the inhibitory substance and to gain information as to its identity.

As in the earlier work,[1,2] the ATPase activity of a contractile protein extract from bovine uterine muscle was used for tests of inhibitory activity. It has been found that uterine extracts of this type catalyze the oxidation of epinephrine at about 8 to 9 times the rate of autoxidation. During this oxidation the reaction mixtures turn a pink color which was assumed to be due to formation of adrenochrome. To answer the question of the actual formation of adrenochrome during the oxidation of epinephrine in the presence of the uterine preparation, the reaction was followed with an automatically recording spectrophotometer. After approximately 20 min incubation of epinephrine with the uterine preparation an analysis of the solution demonstrated the characteristic absorption spectrum for adrenochrome. The adrenochrome was not stable under these conditions, however, and the absorption spectrum soon changed.

Attention was next turned to the nature of the inhibitory substance. Adrenochrome was prepared in crystalline form from epinephrine,[3] and crystalline adrenolutine, an isomeric rearrangement product of adrenochrome, was prepared from adrenochrome.[4] The structures of these substances are presented below.

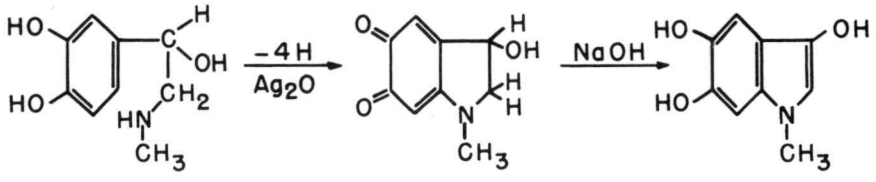

EPINEPHRINE ADRENOCHROME ADRENOLUTINE

The epinephrine derivatives were identified conclusively by their characteristic absorption spectra. The spectra for the materials we prepared are presented in Figure 37. Lund[5] has described the absorption spectra for these substances. Neither adrenochrome nor adrenolutine was found to inhibit ATPase activity, but the inhibitor could be formed by incubating dilute solutions of adrenochrome (4.8 μg/ml to 24 μg/ml) anaerobically overnight at slightly alkaline pH and 38°C. Anaerobic conditions were

obtained either by gassing adrenochrome solutions with purified commercial gas mixtures of N_2 and CO_2 or by evacuation of solutions. The extent of anaerobiosis has not been determined. These results, which are considered of a preliminary nature, are presented in Figure 38.

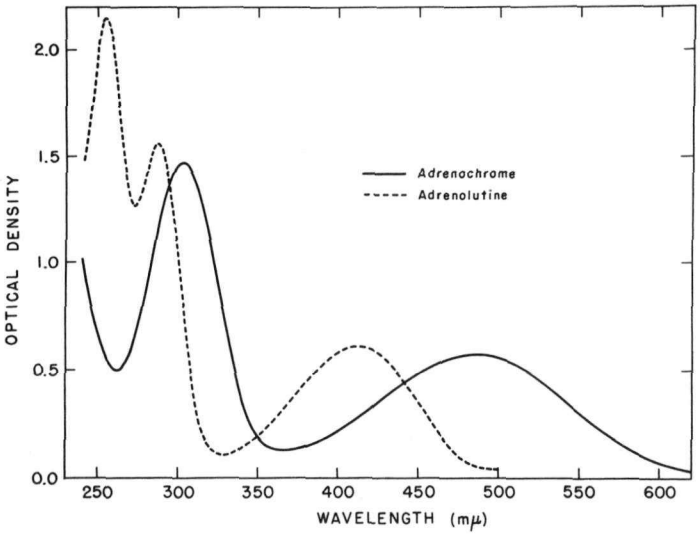

Figure 37 Absorption spectra for adrenochrome and adrenolutine. Approximate concentration, 24 μg/ml; 1-cm light path.

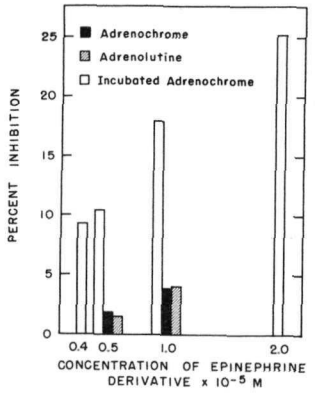

Figure 38 Effect of epinephrine derivatives upon ATPase activity of uterine muscle preparation.

A third epinephrine derivative has been prepared by reduction of a concentrated solution of adrenochrome to form a zwitterionic product described by Harley-Mason.[3] Harley-Mason has postulated the following structure for this substance.

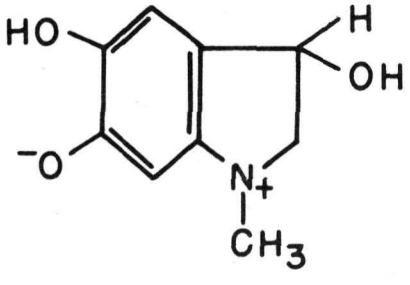

The zwitterion is currently being studied for an effect upon ATPase activity.

In an attempt to isolate the inhibitory substance, incubated adrenochrome solutions have been successfully chromatographed on paper using butanol-acetic acid-water (4:1:5) as a solvent. When the developed chromatograms are viewed under ultraviolet light, one clearly defined fluorescent spot is detectable. On some chromatograms, a second spot of slightly higher R_f than the main fluorescent area was barely detectable with ultraviolet light. An eluate from the fluorescent area has been found to inhibit ATPase activity. The results for eluates from one complete chromatogram are presented in Figure 39. The identity of the inhibitory substance is still unknown.

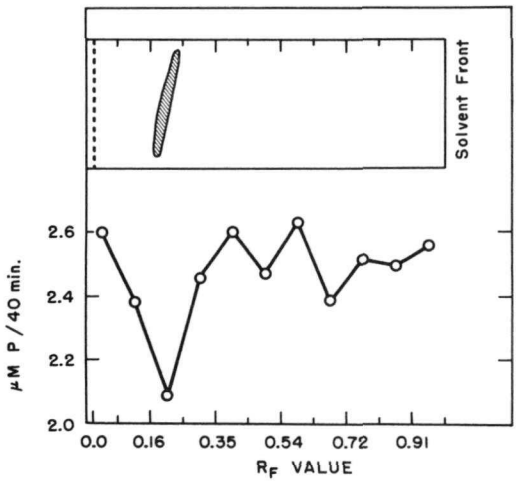

Figure 39 Demonstration of an ATPase inhibitor isolated by paper chromatography. ATPase activity was assayed by measurements of the μM of phosphorus released enzymatically from ATP during a 40-min period.

References

1. Inchiosa, M. A., Jr., and N. L. VanDemark. Influence of oxidation products of epinephrine upon adenosine-triphosphatase activity of uterine muscle preparation. Proc. Soc. Exptl. Biol. Med. 97: 595-597 (1958).

2. Inchiosa, M. A., Jr. Metabolic involvements of epinephrine in uterine muscle extracts. Federation Proc. 17: 77 (1958).

3. Harley-Mason, J. The chemistry of adrenochrome and its derivatives. J. Chem. Soc. 1950: 1276-1282.

4. Fischer, P. Sur la substance responsable de la fluorescence de l'adrenaline. Bull. soc. chim. Belg. 58: 205-209 (1949).

5. Lund, A. Fluorimetric determination of adrenaline in blood. II. The chemical constitution of adrenolutine (the fluorescent oxidation product of adrenaline). Acta Pharmocol. 5: 121-128 (1949).

PROGRESS REPORT: THE PREPARATION OF TRITIUM-LABELED FATTY ACIDS

I. cis-7, 8-Tetradecenoic Acid

William M. O'Leary

Studies in lipide metabolism are often hampered by the lack of isotopically labeled fatty acids and related compounds. In many cases such material can be obtained, if at all, only by laborious and time-consuming radiochemical synthesis. Since randomly labeled compounds are quite satisfactory for many purposes, it was thought that the relatively simple Wilzbach tritium labeling technique as modified by Kisieleski and Smetana[1] might find application here. cis-7, 8-Tetradecenoic acid was selected for the initial attempt at labeling an unsaturated fatty acid by this method primarily because of its usefulness in the author's present program of research.

Tetradecenoic acid was synthesized by the appropriate modification of the method described by Ahmad et al.[2] 500 mg of the acid were converted into the sodium salt by the addition of an equivalent amount of sodium hydroxide. 468 mg of the dried powdered salt were exposed to 9 curies of tritium gas at room temperature for 2 days.[1] The free fatty acid was then recovered by acidification and ether extraction of an aqueous solution of the tritiated sodium salt.

The acid obtained from evaporation of the ethereal extract was subjected to fractional recrystallization from three successive solvents: petroleum ether (30-60°C), acetone, and ethanol. The material from the last recrystallization was then further purified by the column chromatographic technique of Boldingh.[3] A portion of the chromatographically purified acid was chromatographed a second time by the same technique. At each step in the purification procedure specific activities of the acid were determined using a Tri-Carb scintillation counter. These activites appear in Table 34. A total of 217 mg of purified material was recovered.

Characteristics of the recovered acid compared favorably with those established for cis-7, 8-tetradecenoic acid (Table 35). Of special significance is the biotin activity (i.e., the ability to replace biotin, expressed as the number of mμg of biotin equivalent to 1.0 mg of acid, as determined by microbiological assay using Lactobacillus arabinosus) since this value is quite sensitive to both isomeric differences and the presence of saturated fatty acids.

The above data indicate that tritium labeling can be successfully applied, at least to this unsaturated fatty acid, and suggest that the technique may be applicable to a variety of similar compounds. If so, this method would be a useful tool for the study of lipide metabolism.

TABLE 34

Specific activities of tritium-labeled fatty acid after successive purification steps

Material	Activity, mc/g
Sodium salt after irradiation	390
Acid from ether extract	137
Acid from petroleum ether recrystallization	88
Acid from acetone recrystallization	58
Acid from ethanol recrystallization	43
Acid from chromatography	42
Acid from chromatography (second)	42

TABLE 35

Comparison of the characteristics of the tritiated compound with those of cis-7, 8-tetradecenoic acid

Acid	Melting range, °C	Neutral equivalent	Iodine number	Biotin activity
cis-7, 8-Tetradecenoic	4.0-5.0	226.4	111.8	5.1
Tritiated compound	3.0-4.0	224.2	110.9	5.0

The author is indebted to W. Kisieleski and F. Smetana who performed the tritium irradiation and who offered valuable advice regarding the purification procedure.

References

1. Kisieleski, W. E., and F. Smetana. Tritium labeling of organic compounds by self-irradiation. Semiannual Report of Biological and Medical Research Division, Argonne National Laboratory. ANL-5732, pp. 172-174 (1957).

2. Ahmad, K., and F. M. Strong. The synthesis of unsaturated fatty acids. J. Am. Chem. Soc. 70: 1699-1700 (1948).

3. Boldingh, J. The separation of fatty acids by chromatography. International Conference on Biochemical Problems of Lipids, Brussels, pp. 64-81 (1953).

UNSATURATED FATTY ACIDS AND CHOLESTEROL METABOLISM

V. Dietary cholesterol and the formation of arachidonic acid in rat liver

Peter D. Klein

In the previous report[1] it was established that feeding rats a diet containing 0.5% cholesterol resulted in a decrease in the liver cholesterol ester content of the polyunsaturated fatty acids (PUFA) and a marked change in the composition of the plasma cholesterol esters. In the latter, there was a profound decrease in the content of tetraenoic acid, presumed to be arachidonic acid. This report deals with further considerations of these changes and with studies of formation of arachidonic acid from linoleic acid.

Materials and Methods

Animals. Male Holtzmann rats weighing 350-400 g were fed either a stock diet or a 5% corn oil diet[2] containing 2% cholesterol. The latter has been reported by Morris et al.[3] to produce an inhibition of hepatic cholesterol synthesis within 2 to 4 weeks.

Procedures. Most of the determinations were made using methods already described in earlier reports.[4] Tracer studies were carried out on pairs of control, 2-week cholesterol-fed, and 4-week cholesterol-fed animals by the injection of 250 μc of C^{14} carboxyl-labeled sodium acetate intraperitoneally. Four hours later the animals were sacrificed by heart puncture and exsanguination. The livers were removed and the lipides extracted. An aliquot of each lipide extract was saponified, the nonsaponifiable fraction was extracted with ether, and the free fatty acids were extracted from the acidified aqueous layer. The ether extract of fatty acids was dried, evaporated to dryness and dissolved in absolute methanol. The saturated fatty acids were precipitated by the lead-salt method[5] and the last traces of saturated fatty acids "washed out" with two 10-mg portions of palmitic acid. The soluble lead salts were decomposed with acid and extracted from the aqueous layer with ether and the ether solution dried. After the ether solution was evaporated to dryness, the free unsaturated fatty acids were again dissolved in ether and brominated at 0°.[6] The "octabromide" fraction which precipitated from the ethereal solution was removed by centrifugation and washed several times with cold ether, after which it was extracted with hot benzene[7] to remove traces of lower polybromides. The "octabromide" fraction was dried, weighed, combusted to CO_2, and counted in a proportional gas counter.[8]

Results and Discussion

In the previous report in this series, we suggested that the effect of dietary cholesterol in changing the composition of the liver and plasma cholesterol esters might be the result of inhibition of the formation of arachidonic acid. This stemmed from the consideration that the formation of arachidonic acid from linoleic involved the incorporation of a two-carbon fragment and might be affected in a fashion similar to the incorporation of acetate into cholesterol which is inhibited in these circumstances. The data presented below appear to support this concept.

Table 36 has been calculated from data given in previous reports. In it are shown the concentrations of cholesterol ester in liver as diene, triene, tetraene and pentaene under normal conditions, and after feeding 0.5% cholesterol in the diet. It is evident that at all levels of deitary fat, the addition of cholesterol results in an increased concentration of diene and triene ester in liver; there is however, no increase in the tetraene or pentaene ester. While the content of a component in liver does not directly reflect the turnover or renewal rate, it would appear that when cholesterol is fed, the newly laid-down ester is devoid of tetraenoic acid.

TABLE 36

Concentrations of polyunsaturated fatty acids as cholesterol esters in livers of normal and cholesterol-fed rats

Values are in milligrams per 100 g liver

	FF*		5H		5U		30H		30U	
Added dietary cholesterol	-	+	-	+	-	+	-	+	-	+
Ester:										
Dienoic	5.00	10.36	2.65	18.12	14.44	112.13	14.61	29.47	63.05	262.20
Trienoic	1.65	2.07	0.64	5.86	1.62	10.19	1.42	8.42	3.30	10.53
Tetraenoic	0.24	0.0	0.49	0.53	1.21	1.70	2.83	2.53	2.33	3.16
Pentaenoic	0.24	0.0	0.0	1.07	0.20	0.0	0.22	0.84	1.55	1.05

*The following abbreviations are used: FF, fat free; 5H, 5% Crisco; 5U, 5% corn oil; 30H, 30% Crisco; 30U, 30% corn oil.

Table 37 presents the values for free and ester cholesterol in the livers of the normal, 2-week cholesterol-fed and 4-week cholesterol-fed animals, as well as the total PUFA content of these organs. As was anticipated, there was an increase in the amount of cholesterol ester as a result of the cholesterol feeding. The dienoic content of the liver rose gradually in the first two weeks and had almost doubled by the end of the fourth week.

In contrast, the tetraenoic and pentaenoic acid levels dropped at first but rose to slightly below normal again. However, there was a steady decrease in the proportion of tetraene to diene in these livers, and the decreased ratio over this period of time again supports the concept that the conversion of dienoic to tetraenoic acid is being impaired.

TABLE 37

Liver cholesterol and polyunsaturated fatty acid content in rats fed normal and 2% cholesterol diets

Animal number	3	4	5	6	7	8
Diet	Normal		2 Week 2% cholesterol		4 Week 2% cholesterol	
Free cholesterol, mg %	206	185	167	174	174	217
Ester cholesterol, mg %	107	57	300	139	446	763
PUFA, mg/g liver						
Diene	6.28	7.36	7.65	6.77	11.42	15.18
Triene	0.70	1.06	1.35	0.90	1.48	1.62
Tetraene	7.09	7.55	5.00	5.42	6.59	6.71
Pentaene	1.56	1.98	1.02	1.09	1.47	1.51
Average	6.82		7.21		13.30	
	0.88		1.21		1.55	
	7.32		5.21		6.65	
	1.77		1.06		1.49	
Tetraene/diene	1.07		0.72		0.50	

Table 38 lists the specific activities of the "octabromide" fractions isolated from these animals, together with the total incorporation rate of these fractions (i.e., the total counts incorporated into tetraenoic plus pentaenoic acids per gram liver). The 2-week animals showed a higher specific activity than the controls, but since the size of the pool was decreased (Table 37), the total incorporation was only slightly higher. On the other hand, at the end of four weeks, this fraction showed a marked decrease in both specific activity and total incorporation.

In the orginal demonstration of incorporation of acetate into linoleic acid to form arachidonic acid, Mead and co-workers[7] called attention to the fact that the so-called "octabromide fraction" was in actuality not a pure fraction, but consisted of tetraenoic and pentaenoic polybromides. In order to ascertain with precision that acetate was indeed introduced into the arachidonate molecule, they further purified this fraction by debromination, hydrogenation and reverse-phase chromatography of the arachidic acid formed. In light of the amount of material available, as well as the

TABLE 38

Incorporation of C^{14} acetate into "octabromide" fraction of rat liver

Animal number	3	4	5	6	7	8
"Octabromide" isolated from standard aliquot, mg	14.9	13.2	9.7	4.4	(1.5)*	
Specific activity, cpm/mM carbon	12,600	15,960	22,600	24,380	2,570	
Total incorporation cpm/g liver, as tetraene + pentaene	102,100		115,710		16,371	

*Octabromide yield very small; samples pooled for analysis.

number of such determinations which it was necessary to carry out, purification beyond the polybromide stage was omitted. It is pertinent, therefore, to consider what errors if any this might introduce into the values obtained and into their subsequent interpretation. The two chief types of contaminants are the polybromides of the less unsaturated and of the more unsaturated fatty acids. Extraction with hot benzene is reported to remove the lower polybromides,[7] but the possibility of traces of these in the fraction cannot be ruled out. That these would not contribute significantly to any error, can, however, be surmised from the fact that they are not synthesized by the animal organism and hence would not incorporate acetate. If present, they would serve only to dilute the "octabromides" in proportion to their concentration. On the other hand, the presence of polybromides of the more highly unsaturated fatty acids is quite likely, and it is safe to assume that these will amount to as much as 20% of the "octabromide" fraction. Yet this, in itself, does not serve to invalidate the values, since Mead's group has also shown that these fatty acids arise by processes analogous to those leading to arachidonic acid, i.e. incorporation of acetate and further desaturation. Thus, chain-lengthening processes of the same type are involved, and with respect to the effect of cholesterol feeding they would be expected to respond similarly. Therefore, while the presence of more highly unsaturated fatty acids in this fraction prevents us from localizing the defect in the arachidonic acid formation processes, it appears none the less valid to state that, as a class, the tetraene and pentaene acids incorporate less acetate when cholesterol is fed. It would be desirable, of course, to have a definitive answer to this problem, but this will not be possible until a gas-density balance becomes available which will enable us to isolate arachidonic acid directly.

The evidence presented here, however, supports the proposed mechanism by which cholesterol feeding alters cholesterol metabolism: by inducing a derangement of arachidonate synthesis. It is perhaps sufficient to point out that such interference with the synthesis of this essential fatty acid may lead also to significant changes in the animal organism not directly related to cholesterol metabolism.

References

1. Klein, P. D. Unsaturated fatty acids and cholesterol metabolism. IV. Effect of dietary cholesterol on cholesterol composition in liver and plasma of rats. Semiannual Report of Biological and Medical Research Division, Argonne National Laboratory. ANL-5841, pp. 188-191 (1958).

2. Klein, P. D. Unsaturated fatty acids and cholesterol metabolism. II. Influence of linoleic acid in diet on the unsaturated fatty acid content of cholesterol esters in liver and plasma of rats. Semiannual Report of Biological and Medical Research Division, Argonne National Laboratory. ANL-5732, pp. 185-188 (1957).

3. Morris, M. D., E. L. Chaikoff, J. M. Felts, S. Abraham, and N. O. Fansah. The origin of serum cholesterol in the rat: Diet versus synthesis. J. Biol. Chem. 224: 1039-1045 (1957).

4. Klein, P. D. Polyunsaturated fatty acid composition of cholesterol esters in rat liver and plasma. Arch. Biochem. Biophys. 72: 238-239 (1957).

5. Schoenheimer, R., and D. Rittenberg. Deuterium as an indicator in the study of intermediary metabolism. V. The desaturation of fatty acids in the organism. J. Biol. Chem. 113: 505-510 (1936).

6. Ault, W. D., and J. B. Brown. The fatty acids of the phosphatides of beef suprarenals. J. Biol. Chem. 107: 607-614 (1934).

7. Mead, J. F., G. Steinberg, and D. R. Howton. Metabolism of essential fatty acids. Incorporation of acetate into arachidonic acid. J. Biol. Chem. 205: 683-689 (1953).

8. Buchanan, D. L. and A. Nakao. A method for simultaneous determination of carbon-14 and total carbon. J. Am. Chem. Soc. 74: 2389-2395. (1952).

PROGRESS REPORT: SCINTILLATION SPECTROSCOPY OF THE X-RAY BEAM FROM A GENERAL ELECTRIC MAXITRON-250

Sarmukh S. Brar, Philip F. Gustafson, Joseph E. Trier

A knowledge of the photon spectrum emitted by an X-ray machine is desirable in various biological experiments. The determinations reported here were made using a 2" x 2" NaI(Tl) crystal mounted on a Dumont photo-tube in conjunction with a 256-channel analyzer.

The work was performed at 100 cm from the target to the face of the crystal which was covered with 1 mm beryllium window for light shielding. The particular X-ray machine used has an inherent filtration of 4.75 mm beryllium. The crystal and its associated preamplifier were shielded from stray radiation by enclosing them in a lead pig lined with 3.2 mm brass. The port end of the X-ray machine had a collimating hole 2.2 cm in diameter. Approximately 5 cm from the crystal was placed a piece of lead 3 cm in diameter and 1.38 cm thick with a hole 0.4 mm in diameter in the center through which the beam was allowed to reach the crystal.

Since the photon flux was found to be too great for the measuring equipment to handle without pile-up of pulses for the range of currents used, it was decided to obtain as much information as possible for an over-all survey of the problem for future experimentation. By the use of thick absorbers, it was established that the shape of the spectrum does not change appreciably from 100 μa to 30 ma of current. This was done with graphite, aluminum, copper and lead absorbers. Figure 40 shows some of the results using 1.7 cm lead and 1-, 15-, and 30-ma currents.

Figure 41 shows the result of the work done with 100 μa of current and various thicknesses of aluminum. Even at this low current (the lowest at which this machine can be operated without major changes in its control cirucits), it is seen from Figure 41 that pile-up of pulses has complicated the problem by giving a long tail on the spectrum. That this is due to pile-ups was confirmed by the use of a single-line isotope, Cr^{51}.

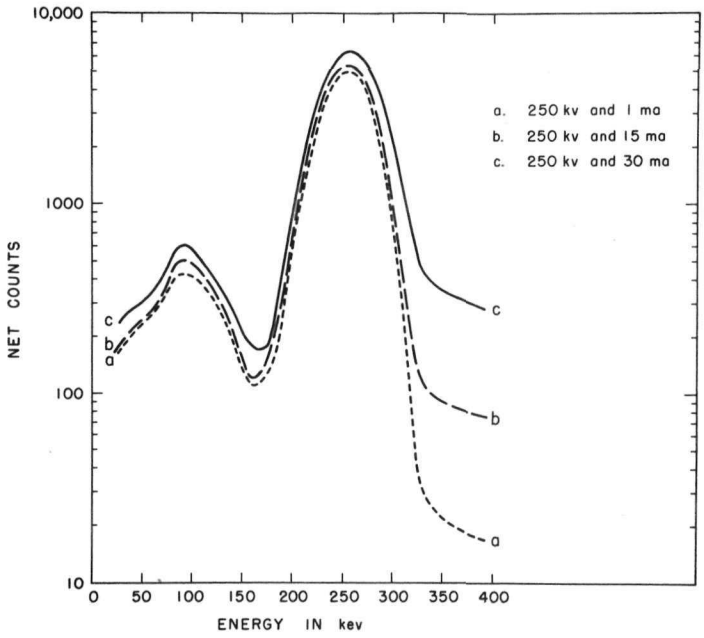

Figure 40

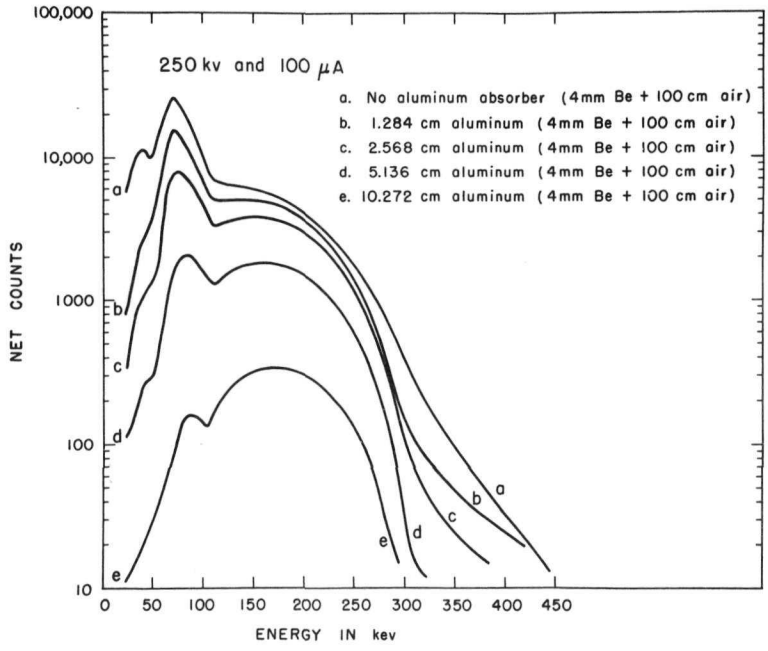

Figure 41

These two graphs represent raw spectra minus backgrounds which were obtained by replacing the collimating lead with a piece which was solid but equivalent in thickness.

PROGRESS REPORT: THE BACTERIAL METABOLISM OF UNSATURATED FATTY ACIDS

I. The Utilization of cis-Vaccenic Acid by Lactobacillus arabinosus

William M. O'Leary

The ability of long-chain unsaturated fatty acids to replace biotin in the nutrition of various lactobacilli and other microorganisms is well known; however, the explanation of this phenomenon is a matter of considerable controversy. Indirect evidence has led many workers to believe that in such organisms biotin may be involved in the biosynthesis of indispensable unsaturated fatty acids, and that when such acids are supplied preformed, the biotin requirement is minimized.

Careful analysis has shown that the major unsaturated fatty acid constituent in lactobacilli is cis-vaccenic (cis-11, 12-octadecenoic) acid, a compound which exhibits a high biotin-replacing activity. An acid of similar structure and biotin-replacing activity found in these bacteria is lactobacillic (cis-11, 12-methylene-octadecanoic) acid. Recent work of the author as well as others has suggested that cis-vaccenic acid may be the precursor of lactobacillic acid.(1,2)

The purpose of the present investigation was to determine whether or not cis-vaccenic acid is actually incorporated in bacterial lipides when supplied in lieu of biotin, and, if so, whether it is retained as such or is converted into other lipide materials.

Materials and Methods

Synthesis of cis-vaccenic-1 C^{14}. 1-Chloro-10-heptadecyne was prepared by the method of Ahmad et al.(3) and carbonated by the method described by Calvin et al.(4) using $BaC^{14}O_3$. The 11, 12-octadecenoic acid so obtained was purified by fractional recrystallization and partially hydrogenated using palladium on charcoal catalyst in ethanol containing 20% pyridine. The resulting cis-vaccenic acid was purified by fractional recrystallization followed by chromatography.(5)

Cultivation of microorganisms. Thirteen liters of semisynthetic medium containing 405 mg of cis-vaccenic acid (93,700 cpm/μM) were inoculated with Lactobacillus arabinosus 17-5, ATCC 8014, and incubated at 30°C for 36 hr. The cells were recovered by centrifugation, washed and lyophilized.

Microbiological assays of the medium before and after growth showed that 105 mg (0.374 mM) of cis-vaccenic acid had been removed from the medium.

Extraction and analysis of cellular fatty acids. The dried cells (7 g) were hydrolyzed by autoclaving with 2 N sulfuric acid for $1\frac{1}{2}$ hr. The lipides were extracted from the hydrolysate with ether and subjected to the usual saponification procedure to obtain the constituent fatty acids (165.9 mg).

After converting the unsaturated fatty acids to their chromatographically separable dihydroxy derivatives, aliquots of the fatty acid mixture were subjected to reversed-phase rubber column chromatography.(6) The eluate fractions were monitored by titration with 0.01 N sodium hydroxide.

The acids present in each chromatographic peak were recovered by acidification and ether extraction, and their specific activities were determined using a Tri-Carb scintillation counter.

Results and Discussion

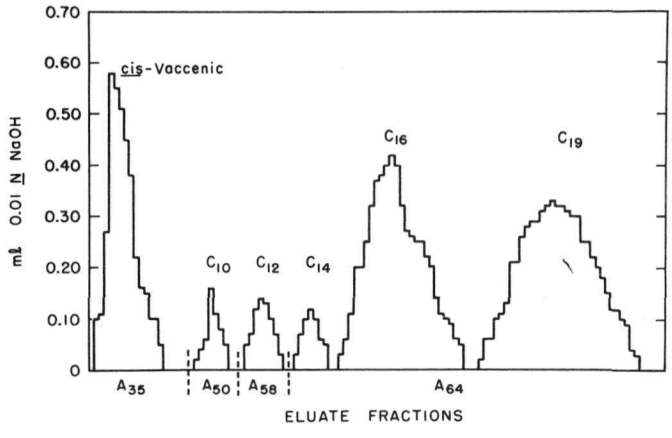

Figure 42 Chromatographic pattern of the fatty acids of L. arabinosus grown on cis-vaccenic-1-C^{14} acid (48.3-mg sample). Acetone-water elution solvent A_{35}, A_{50}, A_{58}, and A_{64} contained 35, 50, 58, and 64% acetone respectively.

The pattern of a typical chromatographic analysis is shown in Figure 42.

The data in Table 39 show that 94.6% of the cis-vaccenic acid removed from the medium during growth can be accounted for by the combined cellular contents of cis-vaccenic and lactobacillic acids. The remaining 5.4% may represent degraded acid or lactobacillic acid that has in turn been metabolized to some non-lipoidal material. The metabolic function of lactobacillic acid is as yet unknown.

It was also found that the specific activities of both cis-vaccenic and lactobacillic acids from the cells were approximately 95% that of the acid supplied in the medium which suggests that a low level of de novo synthesis may be taking place.

TABLE 39

Analysis of L. arabinosus fatty acids

Acid	Percentage of total fatty acids	Specific activity, cpm/μM	Total in cells, mM
cis-Vaccenic	22.4	89,100	0.132
Capric	1.9	-	-
Lauric	3.0	-	-
Myristic	2.6	-	-
Palmitic	29.8	930	-
Lactobacillic	39.6	88,900	0.222
Totals	99.3		0.354

It appears evident from the above data that cis-vaccenic acid supplied to L. arabinosus in lieu of biotin is indeed taken into the bacterial cell as such, and that it is in turn converted into lactobacillic acid.

The author is indebted to Dr. John H. Pomeroy for his helpful advice regarding the synthesis of cis-vaccenic-1-C^{14} acid.

References

1. Hofmann, K., D. B. Henis, and C. Panos. Fatty acid interconversions in lactobacilli. J. Biol. Chem. 228: 349-355 (1957).

2. O'Leary, W. M. Bacterial metabolism of unsaturated fatty acids. Thesis, University of Pittsburgh (1957).

3. Ahmad, K., F. M. Bumpus, and F. M. Strong. A synthesis of cis-11-octadecenoic and trans-11-octadecenoic (vaccenic) acids. J. Am. Chem. Soc. 70: 3391-3394 (1948).

4. Calvin, M., C. Heidelberger, J. C. Reid, B. M. Tolbert, and P. F. Yankwich. Isotopic Carbon, John Wiley and Sons, New York, pp. 178-179 (1949).

5. Boldingh, J. The separation of fatty acids by chromatography. In International Conference on Biochemical Problems of Lipids, Brussels, pp. 64-81 (1953).

6. Hofmann, K., C. Y. Hsiao, D. B. Henis, and C. Panos. The estimation of the fatty acid composition of bacterial lipides. J. Biol. Chem. 217: 49-60 (1955).

NEUTRON IRRADIATION OF VARIOUS PHOSPHATES IN VACUO

Takuya R. Sato and Harold H. Strain*

Our studies of the neutron activation process have shown that the neutron irradiation of phosphorus compounds is a very complex and variable phenomenon. It is influenced by a great variety of conditions, including the presence or absence of oxygen, the presence or absence of moisture, the nature of the containers for the samples, the neutron flux, the intensity of the γ-irradiation, and the duration of the exposure. The effects of some of these conditions upon the nature of the irradiation products have already been reported.(1) The neutron (plus γ) irradiation of phosphorus compounds at high neutron flux yielded much of the radioactive phosphorus in the same chemical species that were irradiated. With sodium hypophosphite, sodium phosphite, and phosphine, which readily undergo dismutation reactions, the γ-rays accompanying the neutrons produced significant yields of secondary disruption products. But with phosphate, which does not undergo dismutation reactions, there was little alteration by the γ-rays, and nearly all the radioactive phosphorus atoms were found in the form of phosphate. It is unlikely that these results with phosphate can be due to shortcomings of the analytical techniques, because our differential migration methods of analysis were so selective that disruption products formed as radioactive species only (i.e., without carrier) would have been separated from the phosphate.

These observations on the neutron activation of phosphorus compounds, particularly phosphate, may be interpreted in two ways. Either the activation of the phosphorus atoms did not disrupt the molecule into small fragments, or it did disrupt the molecule but the fragments recombined to form the original phosphorus compounds. At the present stage of our knowledge of phosphorus compounds, it seems unlikely that many small fragments would recombine to form primarily the starting material; hence, one must consider the possibility of activation without extensive disruption of the molecule, particularly with phosphate.

To obtain further information about the neutron activation process, we have extended our studies to various phosphorus compounds, all with the oxidation state of phosphate. In these experiments, we have now irradiated monobasic, dibasic, and tribasic salts of phosphoric acid at high neutron flux. We have also prepared anhydrous crystalline phosphoric acid and irradiated it at temperatures above its melting point. In all these experiments with liquid phosphoric acid and its crystalline salts, virtually all of the radioactive phosphorus was found in the form of phosphate. When salts of pyrophosphate were irradiated, all the activity was found in the form of pyrophosphate.

---

*Chemistry Division

We have irradiated salts of the cyclic trimetaphosphate and have found all the activity in the form of trimetaphosphate. In this molecule two-fifths or 40% of the P - O bonds form links in the cyclic structure. Rupture of any one of these would destroy the ring by converting it into the linear tripolyphosphate.

From the neutron binding energy, we have calculated the recoil energy for $P^{31} \longrightarrow P^{32}$, assuming this energy to be released in the phosphate group, $P^{32}O_4$, molecular weight 96. With all the energy liberated as a single γ-ray, the recoil energy would be many times the heat of formation of phosphate from the elements. With less energetic γ-rays, the recoil energy would be smaller. And for other emission mechanisms, as a cascade or opposed rays, the recoil energy would be very much less than the energy for the emission of a single γ-ray. The n-capture gamma spectrum indicates, however, that most of the neutron-binding energy of phosphorus is dissipated in the range of 3 to 7 Mev.(2) Each of the 20 γ-rays in this energy range would provide enough energy to break the chemical bonds about the phosphorus atom.

With some of the neutron-binding energy liberated as heat about the activated phosphorus compound, one might expect to find the activated species in the form of condensation products such as pyrophosphate, which is formed rapidly from Na_2HPO_4 at temperatures above 200°. Yet none was found.

We believe that our results provide strong support for the view that neutron activation of phosphate and of its condensation products (pyrophosphate and trimetaphosphate) does not disrupt the molecules into small fragments, as might be obtained by rupture of all the chemical bonds.

At high neutron flux, the neutron activation products of phosphate and its condensation products may be affected by the high temperature produced by the reaction of neutrons with the containers. To minimize this effect, the irradiation of phosphorus compounds at low neutron flux is now being studied.

References

1. Sellers, P. A., T. R. Sato, and H. H. Strain. Neutron irradiation of some crystalline salts of phosphoric, phosphorous, and hypophosphorous acids in vacuum. J. Inorg. Nucl. Chem. 5: 31-47 (1957).

2. Kinsey, B. B., G. A. Bartholomew, and W. H. Walker. Neutron capture γ-rays from phosphorus, sulfur, chlorine, potassium, and calcium. Phys. Rev. 85: 1012 (1952).

MORTALITY EXPERIENCE AT ARGONNE NATIONAL LABORATORY

II. Analysis of causes of death

Asher J. Finkel* and Harry Auerbach

In the period from January 1951 through December 1955 there occurred 43 deaths among the employed population of Argonne National Laboratory. Of this number, one death was in the category of occupationally related trauma.

Table 40 gives the distribution of deaths by sex and comparison with the expected deaths in the ANL population on the basis of several sets of age- and sex-specific death rates. The U.S. rates were used as a general background for comparison, and the Illinois rates were selected because they presumably reflect the death rates prevalent in the geographic area in which ANL is located. A further comparison was made to evaluate the possible effects of differences in socio-economic factors. For this purpose, appropriate death rates from a high per capita income state (Connecticut) and a low per capita income state (Mississippi) were also applied to the ANL population in the calculation of expected deaths. For further comparison, the death rates for Industrial Policyholders of the Metropolitan Life Insurance Company for 1951-1955 were used to match the selection of the ANL employed population.

TABLE 40

Expected and observed deaths in ANL population by age and sex, 1951-1955

	Male	Female	Total
Observed:			
ANL, 1951-1955	40	3	43
Expected:			
Comparison population			
U.S.A., 1949-1951	58.9	7.6	66.5
Illinois, 1949-1951	61.5	7.7	69.2
Connecticut, 1949-1951	52.8	6.9	59.7
Mississippi, 1949-1951	58.4	7.3	65.7
Industrial policyholders, Metropolitan Life Insurance Company, 1951-1955	59.7	5.9	65.6
Mean of comparison populations	58.4	7.2	65.6
ANL/Mean of comparisons, %	68.5	41.7	65.5

*Health Division, ANL

It is noteworthy that the ANL deaths are about two-thirds of the expected number by comparison with any of the reference populations. The probable reasons for this decrease in the expected number of deaths can be seen by an examination of Table 41. This table presents an analysis of the expected and observed ANL deaths by sex and by broad disease categories. The expected deaths were calculated by applying the U.S. 1949-1951 age-, sex-, and disease-specific death rates to the ANL population.

TABLE 41

Expected and observed deaths, ANL population, 1951-1955 by sex and by broad disease categories

Disease group	Male		Female		Total	
	Exp.	Obs.	Exp.	Obs.	Exp.	Obs.
Cardiovascular (410-443)*	20.1	20	1.8	1	21.9	21
Neoplasms (140-205)*	7.9	11	1.8	1	9.7	12
Accidents (E800-E962)*	8.6	7	1.3	1	9.9	8
All other	22.3	2	2.7	0	25.0	2
Total	58.9	40	7.6	3	66.5	43

*Categories as listed in International Lists of Diseases and Causes of Death, 6th Revision. World Health Organization, Geneva, Switzerland (1949).

When the three major causes of death are considered, there is a striking correspondence between the expected and the observed numbers of deaths. On the other hand, there is marked discrepancy in deaths in all other categories, which include infective and parasitic diseases, and those of the nervous system and sense organs, and diseases of the respiratory, digestive, and genito-urinary systems. The almost complete absence of deaths in these categories among ANL employees accounts for the significant decrease in the total number of deaths. Disease of the cardiovascular system, neoplasms, and accidental deaths away from work are evidently not greatly affected by an occupational health program or by provisions for a medical-surgical and hospital-insurance program. It is not surprising then that these diseases occur in a small population with the expected frequencies. Selection of personnel and such medical supervision as is afforded by periodic recheck examinations probably

serve to reduce the numbers of deaths in categories other than those that are responsible for the major numbers of deaths in the U.S.A. at the present time.

Further data are being collected to test these conclusions and should be available at the close of the 1956-1960 period.